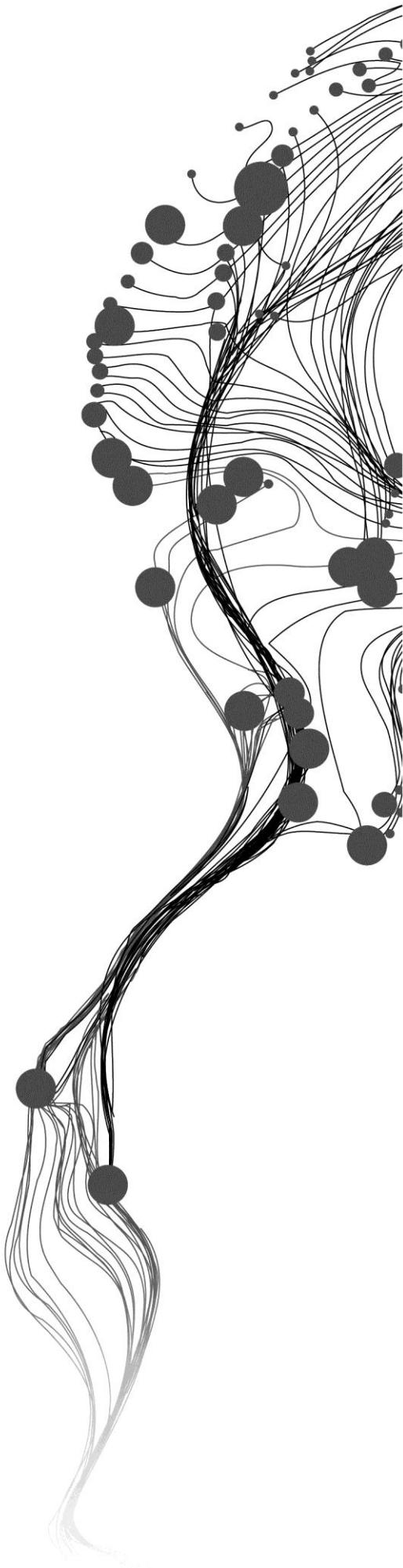


**Effects of soil depth and saturated
hydraulic conductivity spatial
variation on runoff simulation by
the Limburg Soil Erosion Model
(LISEM), a case study in Faucon
catchment, France**

POOYAN RAHIMY
February, 2011

SUPERVISORS:
Dr. D. G. Rossiter
Prof. Dr. V. G. Jetten



**Effects of soil depth and saturated
hydraulic conductivity spatial
variation on runoff simulation by
the Limburg Soil Erosion Model
(LISEM), a case study in Faucon
catchment, France**

POOYAN RAHIMY

Enschede, The Netherlands, February, 2011

Thesis submitted to the Faculty of Geo-Information Science and Earth
Observation of the University of Twente in partial fulfilment of the
requirements for the degree of Master of Science in Geo-information Science
and Earth Observation.

Specialization: Applied Earth Sciences-Geohazards

SUPERVISORS:

Dr. D. G. Rossiter

Prof. Dr. V. G. Jetten

THESIS ASSESSMENT BOARD:

Dr. C. J. van Westen (Chair)

Dr. L.P.H. van Beek (External Examiner, Department of Physical Geography,
University of Utrecht)

DISCLAIMER

This document describes work undertaken as part of a programme of study at the Faculty of Geo-Information Science and Earth Observation of the University of Twente. All views and opinions expressed therein remain the sole responsibility of the author, and do not necessarily represent those of the Faculty.

ABSTRACT

Soil depth (thickness) and saturated hydraulic conductivity (K_s) are important parameters for models of surface runoff. Distributed models require not only accurate estimates but also their spatial distribution. The objective of this study was to use terrain and environmental variables to map these parameters, comparing different spatial prediction methods by their effect on simulated runoff hydrographs. The study area is called Faucon, located in south east of the French Alps. From amongst variables of “land cover class”, “lithologic units”, “elevation”, “LS factor”, “slope”, “aspect”, “wetness index”, “Overland flow distance to channel network”, “plan- profile curvature” and “convergence”, the “land cover class” was the best explanatory variable for soil thickness. None of the variables were good predictors for K_s . Also, An additive linear model of “land cover class” and “overland flow distance to channel network” best predicted soil thickness. Regression Kriging (RK) using this model and local spatial correlation of the residuals gave better accuracy than Ordinary Kriging (OK). These methods failed for K_s , so it was mapped by Thiessen polygons. The parameter maps, including conditional simulations of soil thickness, were exported to the hydrologic model of LISEM, where three synthetic rainfall scenarios were used. The hydrographs produced by RK and OK were significantly different at rainfall of low intensity or short duration but at rain events of longer duration or higher intensity, the hydrographs had no significant differences. The same results were obtained when simulated fields of soil thickness were applied in modelling. As a whole, the study revealed that RK of soil thickness represents better spatial variations than the OK. Also, various spatial patterns of soil thickness significantly influence simulated runoff at only rainfalls of low intensity and/or short duration.

Keywords. LISEM, soil thickness, saturated hydraulic conductivity, Kriging, conditional simulation, Faucon, hydrograph.

ACKNOWLEDGEMENTS

Herewith I'd like to highly appreciate my supervisors, Prof. Dr. Victor Jetten and Dr. David Rossiter, for their great support and guidance during this research. I am really proud and thankful for having a chance to work with such great scientists.

I gratefully thank Dr. Jean-Philip Malet, Dr. Dinand Alkema, Dr. Cees Van Westen, Dr. Menno Straatsma, Ms. Azadeh Ramesh and Mr. Byron Quan Luna who helped me in data acquisition.

I express gratitude to Drs. Boudewijn de Smeth for allowing me to work at Laboratory and helping me find proper tools and methods during soil samples analysis.

I also greatly thank Drs. Nannette Kingma. She accompanied me in field work for one week and kindly looked after me when I'd caught a hard illness.

I send my hearty appreciations to Mr. Andre Kooiman, Drs. Tom Loran, Ms. Angelique Holtkamp and Ms. Monique Romarck who granted me such an opportunity to study at the Earth System Analysis Department.

I am happy for getting to know Dr. Abbas Farshad who did all his best to comfort and guide me through rough times.

I acknowledge the Faculty of Geo Information science and Earth observations (ITC) administration which provided me with such a wide scientific environment where I learnt a lot and could see new horizons ahead.

In the end, I wholeheartedly send gratitude to my family with which support I could continue up until now. I hope to be able to continue this way.

Pooyan Rahimy,
Enschede, February 2011.

TABLE OF CONTENTS

1. INTRODUCTION	1
1.1. RESEARCH PROBLEM	2
1.2. OBJECTIVES.....	2
1.3. RESEARCH QUESTIONS.....	2
1.4. RESEARCH HYPOTHESIS.....	3
2. STUDY AREA	5
3. LITERATURE REVIEW.....	9
3.1. STATISTICS TECHNIQUES FOR SOIL PROPERTIES SPATIAL PREDICTION	9
3.1.1. <i>Introduction to Geostatistical interpolations</i>	9
3.1.2. <i>Conditional simulation</i>	10
3.1.3. <i>Using environmental variables in soil properties prediction</i>	11
3.2. HYDROLOGIC MODELLING	12
3.2.1. <i>Introduction to the Limburg Soil Erosion Model (LISEM)</i>	12
3.2.2. <i>Application of the LISEM model, in runoff simulation</i>	12
3.2.3. <i>Theoretical basis of the LISEM</i>	12
4. METHODS AND MATERIALS	15
4.1. DATA ACQUISITION.....	15
4.2. SAMPLING DESIGN	15
4.3. FIELD OBSERVATIONS	16
4.3.1. <i>Soil texture classification</i>	16
4.3.2. <i>Saturated hydraulic conductivity (Ks) measurement</i>	16
4.3.3. <i>The soil thickness measurement</i>	18
4.3.4. <i>Soil surface stoniness</i>	18
4.3.5. <i>Measurement of plants height and ground fraction covered by plant</i>	19
4.3.6. <i>Roads width measurement</i>	19
4.4. LABORATORY WORK.....	19
4.4.1. <i>Field capacity and porosity measurement</i>	19
4.4.2. <i>Soil Bulk Density</i>	19
4.5. ANALYSIS OF THE CATCHMENT HYDROLOGY	19
4.6. COMPUTING THE ENVIRONMENTAL VARIABLES	21
4.6.1. <i>Land cover and lithologic data</i>	21
4.6.2. <i>The terrain parameters</i>	22
4.7. STATISTICAL MODELLING APPROACH	22
4.7.1. <i>Study on the environmental variables as predictors of the soil properties</i>	22
4.7.2. <i>Kriging of the soil thickness and Ks</i>	22
4.7.3. <i>The conditional simulation of the soil thickness and Ks</i>	23
4.7.4. <i>Mapping other soil surface properties</i>	23
4.7.5. <i>Mapping of plants height, ground fraction covered by plants and the Leaf Area Index (LAI)</i>	24
4.8. HYDROLOGIC MODELING	24
4.8.1. <i>Preparing the LISEM input maps</i>	24
4.8.2. <i>Preparing rainfall intensity input for the LISEM</i>	25
4.8.3. <i>Run of the LISEM</i>	25
5. RESULTS AND DISCUSSION	27

5.1.	STATISTICAL ANALYSIS ON DATA.....	27
5.1.1.	<i>The Ks and soil depth (thickness) frequency distribution.....</i>	27
5.1.2.	<i>Exploratory graphics: target vs. environmental variables.....</i>	29
5.1.3.	<i>The linear model analysis between the soil parameters and the environmental factors.....</i>	31
5.1.4.	<i>The Ordinary Kriging (OK) of the soil depth (thickness) and Ks.....</i>	33
5.1.5.	<i>The Ks data transformation and Ks mapping.....</i>	36
5.1.6.	<i>The Regression Kriging (RK) of the soil depth (thickness).....</i>	38
5.1.7.	<i>Conditional simulation.....</i>	40
5.2.	MAPPING OF THE SURFACE STONINESS AND OTHER SOIL PROPERTIES.....	42
5.3.	THE LISEM OUTPUT ANALYSIS.....	46
5.3.1.	<i>The effect of different soil thickness interpolation methods on hydrograph.....</i>	46
5.3.2.	<i>The effect of different simulated fields on the resultant hydrographs.....</i>	48
5.3.3.	<i>Comparison of RK, OK and simulated fields in hydrograph modelling.....</i>	50
6.	CONCLUSIONS.....	51
	LIST OF REFERENCES.....	54
	APPENDIX I : TABLES OF APPLIED DATA.....	58
	1. <i>Table of the field observation records.....</i>	58
	2. <i>Example of one the Infiltration measurement sheets.....</i>	59
	3. <i>Table of measured Ks (the results of the present and previous study).....</i>	60
	4. <i>Average soil thickness and variances.....</i>	61
	5. <i>Soil data after laboratory analysis (x and y are UTM coordinates of sampled points in meters).....</i>	62
	6. <i>Table of the environmental variables used in linear modelling.....</i>	63
	APPENDIX II: SCATTER PLOTS.....	69
	APPENDIX III : THE R SCRIPT.....	73
	APPENDIX IV: THE PCRASTER SCRIPT.....	83
	APPENDIX V: THE LISEM PART.....	85

LIST OF FIGURES

Figure 1. The Faucon Sub basin	5
Figure 2. Geologic map of the Faucon sub basin	6
Figure 3. Geomorphie map of the Faucon sub basin.....	6
Figure 4. Land cover map of the Faucon sub basin	7
Figure 5. The Seasonal average rainfall of Barcelonnnette.....	8
Figure 6. The sampling points	16
Figure 7. The Cumulative infiltration against Cumulative time (plot for one of the samples)	17
Figure 8. The Reynolds and Elrick's graph for G factor	18
Figure 9. The Canal shape at the outlet.....	20
Figure 10. The temporal variations of the torrent discharge.....	20
Figure 11. The rainfall intensity variation of the first peak	21
Figure 12. The main basin mask map derived from the sub basins map.....	25
Figure 13. Comparison of previous and present studies data by box plots	27
Figure 14. The frequency distribution of K_s and soil thickness	28
Figure 15. The post plot of the K_s field measurements	29
Figure 16. The post plot of soil depth.....	29
Figure 17. Box plots of the soil thickness and K_s against the Lithologic and land cover units	30
Figure 18. Scatter plots of soil depth (thickness) and K_s against slope and convergence variables.....	31
Figure 19. Diagnostic plots of the K_s model by convergence variable	32
Figure 20. The diagnostic plots of soil depth modelled by land cover and overland flow distance to channel network.....	33
Figure 21. The empirical variograms for K_s and soil depth.....	34
Figure 22. The sample variogram of the K_s data without the previous research points.....	34
Figure 23. The map of soil depth (thickness) made by the Ordinary Kriging.....	35
Figure 24. The soil thickness ordinary kriging variance.....	35
Figure 25. The Ordinary Kriging residuals histogram	36
Figure 26. The normalized K_s distribution	36
Figure 27. The normalized K_s variogram	37
Figure 28. The ordinary kriging of normalized K_s and the kriging variance	37
Figure 29. The normalized K_s kriging residuals histogram.....	38
Figure 30. K_s map produced by Thiessen polygons method.....	38
Figure 31. The variogram of soil depth model residuals	39
Figure 32. The Regression Kriging of the soil depth and the Kriging variance.....	39
Figure 33. The RK residuals histogram.....	39
Figure 34. Four simulated fields of soil depth (thickness) map by OK.....	40
Figure 35. Four simulated fields of soil depth (thickness) created by the RK	41
Figure 36. The histograms of Kriged and simulated values	42
Figure 37. The soil porosity variogram and map produced by the OK.....	43
Figure 38. The surface stoniness variogram and map produced by OK.....	43
Figure 39. The Soil Field Capacity variogram and map produced by the OK.....	44
Figure 40. The soil Bulk Density variogram and map produced by the OK	44
Figure 41. variogram of the soil matric potential	45
Figure 42. Hydrographs resulted from application of soil thickness OK and RK at 3 rainfall scenarios	46
Figure 43. Comparison of the two soil depth maps total soil volume	48
Figure 44. Hydrographs resulted from application of soil depth RK simulations.....	49

Figure 45. Total soil volumes of the simulated fields.....50

LIST OF TABLES

<i>Table 1. The rainfall return periods of the study area</i>	8
<i>Table 2. The list of data used for the LISEM model</i>	15
<i>Table 3. The Manning and Random Roughness values of land cover units</i>	23
<i>Table 4. The synthetic rain scenarios used in the LISEM modelling</i>	25
<i>Table 5. The soil properties linear models validity</i>	31
<i>Table 6. Hydrographs characteristics resulted from different interpolation methods at different rainfall scenarios</i>	47
<i>Table 7. Hydrographs characteristics resulted from simulated fields of soil thickness at three rainfall scenarios</i>	48
<i>Table 8. Comparison of hydrographs resulted from RK, OK and simulated fields</i>	50

1. INTRODUCTION

The surface runoff has always been a problem for agriculture land uses in mountainous areas (De Roo 1996a), because it is the cause of erosion, gullies and flash floods. The urgency to control these hazards pushed people to build dams or use lands in a way to reduce the runoff generation. As they developed in science, hydrologic statistics and simulation were applied to the approach so that prior to any conservative measure; there should be a good runoff and hydrologic simulation for which spatio-temporal information of hydrologic processes in study site is necessary.

The hydrologic processes in a watershed are influenced by soil characteristics, land cover, land use, topography and geology (Grayson 2001; Herbst, Diekkrüger et al. 2006). Soil characteristics such as depth (thickness) and saturated hydraulic conductivity (K_s) are very important in soil-water processes and strongly affect water infiltration and accordingly runoff generation (Neitsch 2002; Herbst, Diekkrüger et al. 2006). This was first explained by the Green-Ampt model (Neitsch 2002) in which surface water infiltration rate is directly proportional to the soil saturated hydraulic conductivity (K_s) and inversely proportional to cumulative infiltration, i.e. infiltration depth (Jetten 2002). The cumulative infiltration is determined by soil thickness, porosity and initial soil moisture (Kutilek 1994).

In mountainous areas and catchments, soil characteristics vary significantly in space, as results of different studies found that the saturated hydraulic conductivity's coefficient of variation ranges from 90 to 190 percent (Warrick and Nielsen D.R. 1980; Merz 1998). Also, the soil thickness covaries spatially with soil type, land use, land cover, topography and climate (Dietrich 1995; Minasny 1999; Kuriakose 2009). This fact, largely affects the hydrologic behaviour in different parts of such areas. Upper reaches of catchments where soil is shallow, soil thickness is determinative in making the saturation overland flow, while in lower reaches where soil is deep, saturated hydraulic conductivity (K_s) role in causing the Hortonian overland flow is highlighted.

For hydrologic modelling, having detailed soil information from many parts of catchments is impossible due to inaccessibility of those parts. In conventional soil survey, the unapproachable areas were either assumed to be the same as closest soil units or extrapolated by other information. In such resulted maps, soil spatial variations are generalized into discrete spatial units with no spatially-explicit internal variability (Zhu and Mackay 2001), so that using them in hydrologic models may cause unrealistic estimation. Best-predictor maps of soil properties give the best prediction at each location, but as a whole they do not realistically represent the spatial variation (Kuriakose 2010). For this, the conditional simulation of the soil properties, will result in better soil spatial variations representation (Webster 2007). The conditional simulation gives the very detailed spatial realizations of the soil properties.

The study area has experienced flash floods since 1850 (OMIV-EOST 2010), for which many check dams have been built but half of them are no more efficient. For the check dams' reconstruction, having a good runoff prediction of the worst case scenario is necessary. This requires accurate estimates and realistic spatial variation of the soil properties.

1.1. Research problem

The Faucon study area is a catchment prone to flash flood hazard (OMIV-EOST 2010). Important factors that determine flash floods simulation are (1) rainfall variability and relation to elevation (Singh 1997; Goovaerts 2000), for which there is no information in the area, (2) infiltration capacity of soil. The latter mostly depends on saturated hydraulic conductivity (Ks) and storage capacity of soil which is effect of soil depth (thickness), porosity and initial soil moisture.

If rainfall intensity is larger than Ks, most of the rain will produce runoff, else all the rain will infiltrate. Also, if soil has no enough storage capacity because of being shallow and/or having high initial moisture, most of the rain will contribute to runoff generation. Since in mountainous areas, there are a wide variety of soils with different depths (thicknesses) and saturated hydraulic conductivities, both processes may play important role in runoff generation. Hence, there is no clue on how runoff is generated, unless the Ks and soil depth (thickness) spatial variations effect on runoff simulation is known. On the other hand, it is important to know how sensitive runoff behaviour is to various spatial patterns of soil thickness and Ks.

No enough information of the soil properties spatial distribution has been obtained in recent studies of the area (Remaitre 2005; Hosein 2010; Mountain Risks 2010). Thus, the soil properties, specifically Ks and soil thickness were to be prepared and mapped. Having more realistic spatial variations of the soil properties result in better hydrologic simulation. In order to attain this goal, intensive soil survey is inevitable. Considering difficulty and expense of accessing detailed soil information in a mountainous area, the question arises that how far having general or very detailed spatial variations of the Ks and soil thickness, affects the hydrologic modelling results. The answer to this question will guide researchers to plan optimally for future studies on flash floods modelling.

1.2. Objectives

The objective of the research is to examine the effect of soil thickness and saturated hydraulic conductivity spatial variations, on runoff modelling, in Faucon catchment. In order to accomplish this, a secondary objective is to make sufficiently detailed maps of the soil properties spatial pattern in the study area.

1.3. Research questions

Based on the objectives, the following questions are to be answered:

- 1- How well can the land cover classes, lithologic units and the terrain parameters (including elevation, LS factor, slope, aspect, wetness index, Overland flow distance to channel network , plan- profile curvature and convergence) or their combinations, predict the soil thickness and saturated hydraulic conductivity? i.e., which of the factors are the best predictors?
- 2- Is a regression kriging with one or more of the above –mentioned environmental covariables, able to satisfactorily predict spatial variation in soil thickness and hydraulic conductivity?
- 3- How does the modelled hydrologic response to a rainfall event at the catchment outlet, change with different interpolation methods of soil thickness and Ks?

- 4- How much do conditionally simulated fields of the Ks and soil thickness, vary in their runoff predictions?

1.4. Research hypothesis

- 1- Since, land cover types, lithologic units as well as the terrain parameters of the elevation, LS factor, slope, wetness index, aspect, overland flow distance to channel network, plan-profile curvature and convergence can influence processes occurring on soil (Milevski 2007), they may have significant correlation with the soil thickness and saturated hydraulic conductivity variations.
- 2- Various soil thickness and Ks maps, produced by different interpolation methods, do make significant differences in the simulated runoff characteristics.
- 3- Various conditionally simulated fields of soil thickness and Ks make significant differences in runoff prediction.

2. STUDY AREA

The study area of Faucon, is a sub basin of Barcelonnette Watershed, located in the southern French Alps, centred on $44^{\circ}25'N$, $6^{\circ}40'E$ (Hosein 2010), has a stream which is a tributary of the Ubaye river. The Faucon stream which is approximately 5.5 km in length, starts from the headwater and ends to a 2 km² alluvial fan. Base flow of the torrent is ground water which gushes out of flysch/sandstone outcrops and superficial formations (Remaitre 2005).

Altitude ranges between 1000 and 3000 meters. The catchment area is 9.8 km². Figure 1 shows the Faucon sub basin geographic location. Since, the aim of the study was to model the runoff and discharge at the outlet of the watershed (i.e. the hydrometric station), areas lower than the hydrometric station including the alluvial fan, were excluded from the study area.

Along the basin stream, there is abundant sediment accumulation resulted from past flood events (OMIV-EOST 2010). Boulder deposits in the main stream are also evidence of the debris flows. According to the French Forest Office reports, fourteen debris flows have occurred in the area since last century, which caused lot of damage to buildings and people. The most recent of them happened in August 2003. The area has also experienced flash floods so as to control them, check- dams have been built on the torrent (OMIV-EOST 2010).

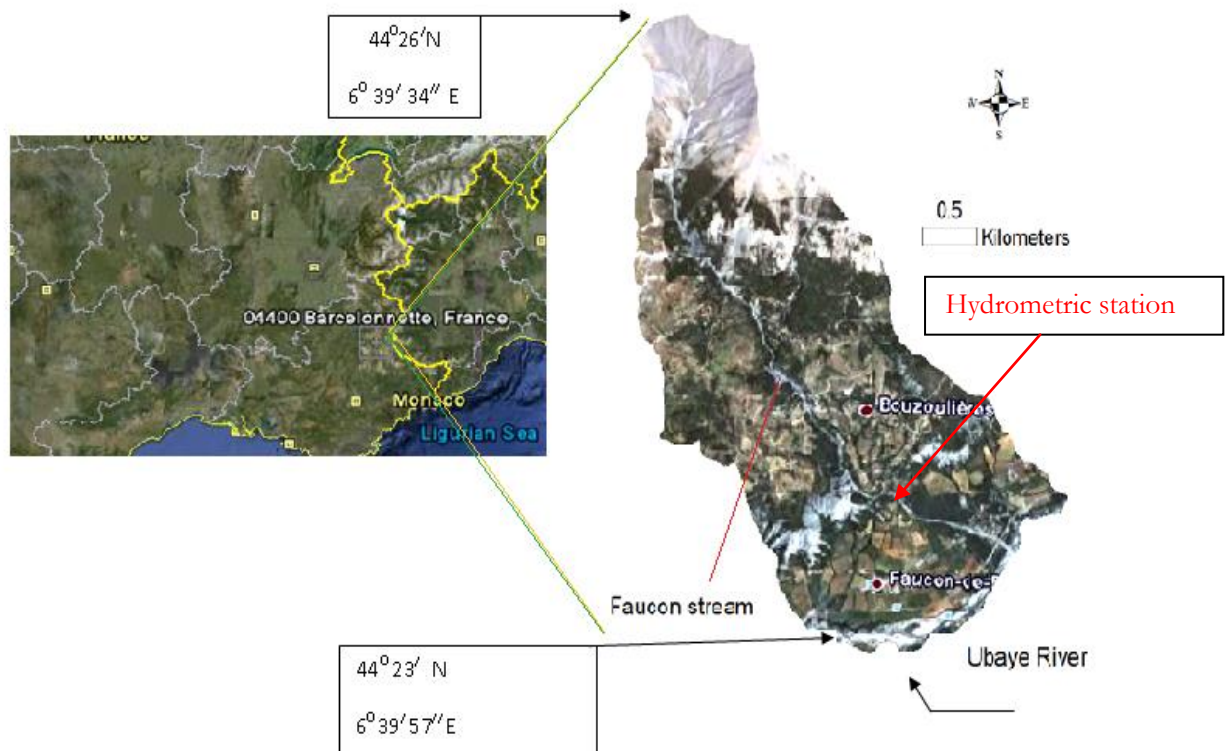


Figure 1. The Faucon Sub basin (OMIV-EOST 2010)

The area's geomorphology, debris flows run out and flood risk assessment were already studied as a part of Mountain Risks Project, but there are still many uncertainties about Soil properties and hydrology of the area which are to be scrutinized (Malet 2004; Remaitre 2005; Hosein 2010).

Geology of the catchment is composed of flyschs and limestones in the upper parts, and black marls in the lower parts (Figure 2). The entire area has various formations, like moraines and alluvial fan (OMIV-EOST 2010). In Figure 3, the geomorphic units of the basin are displayed (Remaitre 2005).

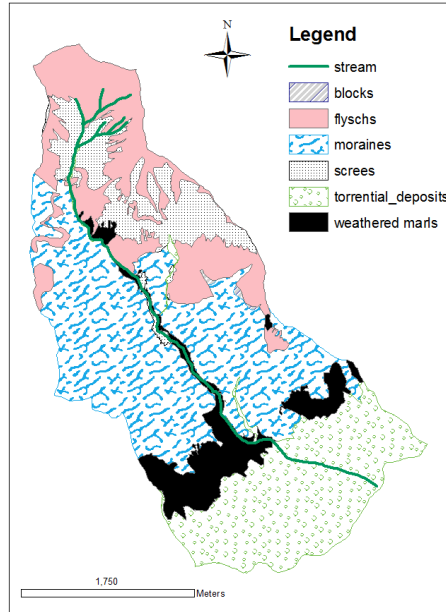


Figure 2. Geologic map of the Faucon sub basin (OMIV-EOST 2010)

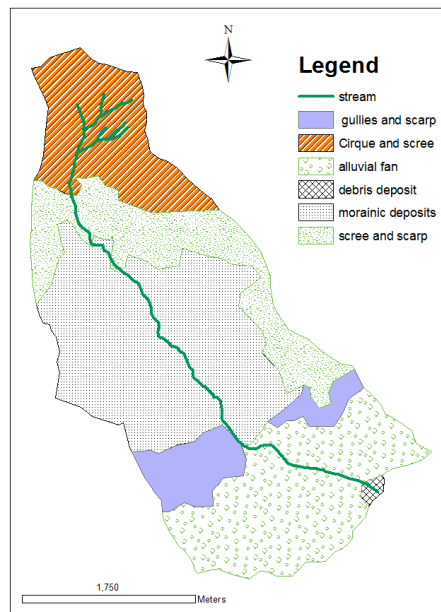


Figure 3. Geomorphic map of the Faucon sub basin (Remaitre 2005)

The Area's land use/land cover consists of farm lands, broad-leaved and coniferous forests, grass lands and urban units (Figure 4). Most of the arable and urban lands are seen together in the

alluvial fan. Lands on terraces and low gradient slopes are allocated to grazing and steeper slopes are mostly covered by trees (Hosein 2010).

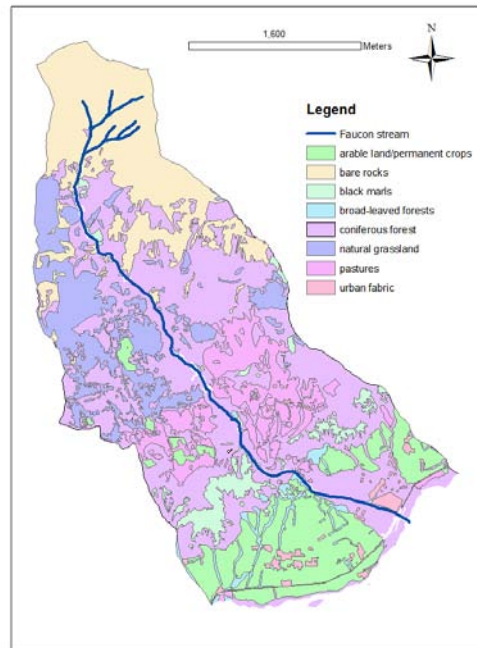


Figure 4. Land cover map of the Faucon sub basin (Mountain Risks 2010)

The watershed has a dry and Mediterranean climate. Summers are usually dry though some random storms may happen in the season. The lower parts of the watershed receive more rainfall than snow during winters while in the upper parts; precipitation is in form of snow. Most of rainfall occurs in autumn and spring (Flageollet, Maquaire et al. 1999). Based on the rainfall records from 1928 till 2009, measured at the Barcelonnette's station, located 2.5 Km southwest of Faucon alluvial fan, annual rainfall has been reported 733 mm. Due to lack of long period rainfall records at Faucon hydrometric station, the Barcelonnette's station data have been used for Faucon's studies (Hosein 2010; Mountain Risks 2010).

The discharge peak of the Faucon stream at apex of the alluvial fan, occurs during spring when both high rainfall and snowmelt take part in runoff generation (Remaitre 2005; Hosein 2010).

In Figure 5, the seasonal average of the precipitation (mm) based on records of 2003 until 2009 is shown. The data were taken from the Barcelonnette's station which is situated at elevation of 1132 meters, 200 meters lower than the Faucon hydrometric station¹. This means that the rainfall amount of the Faucon catchment should be more than that of the Barcelonnette's station. Table 1 also shows the return periods of rainfall in the Barcelonnette (Hosein 2010).

¹ The hydrometric station is located at the fan apex which coordinate in UTM (WGS 84) is (315276 E, 4919024 N)

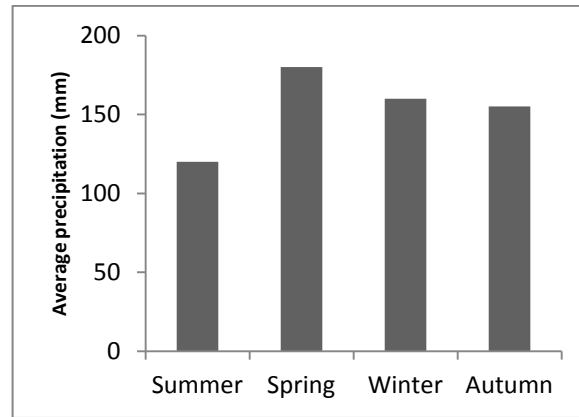


Figure 5. The Seasonal average rainfall of Barcelonnette (Mountain Risks 2010)

Return Period(yr)	Precipitation(mm)
5	46
10	64
15	71
20	79
50	89
100	97
500	114

Table 1. The rainfall return periods of the study area

No detailed soil survey has been done in the area, so there is no available soil map, but some general information says that the surface soil texture ranges from sandy silts in the moraine deposits to sandy clay in black marls areas (Malet 2004) mixed with 10-50 % gravel (Hosein 2010).

3. LITERATURE REVIEW

3.1. Statistics techniques for soil properties spatial prediction

3.1.1. Introduction to Geostatistical interpolations

Any kind of hydrologic models are sensitive to the soil hydraulic properties and the soil thickness (Herbst, Diekkrüger et al. 2006), therefore, the most accurate prediction of the soil properties spatial variations should be implemented. The techniques to predict the soil thickness and hydraulic properties of an area can be distinguished as: Non geostatistical and Geo-statistical interpolation methods (Dietrich 1995; Odeh 1995; Merz 1998; Kuriakose 2009). Using each of the mentioned techniques, leads to different realizations which by far affects the hydrologic modelling results significantly (Merz 1998; Kuriakose 2009). The Non geostatistical methods predictions were not always correct because sometimes they were based on invalid assumptions and the soil spatial variations are highly generalized with discrete spatial units (Zhu and Mackay 2001).

The Geostatistical interpolations, such as Ordinary Kriging, Regression Kriging and stochastic simulation, beget a continuous map of a spatial variable (Webster 2007) where the uncertainty can be calculated, based on the assumed model of spatial covariance.

The general assumption in the Regression Kriging which is going to be used in the research is that the mean of the predictand, varies as the location changes (Webster 2007). The trend of the mean variation is expressed as a regression model like this:

$$Z(S_0) = \sum_{k=0}^p (\beta_k) \cdot Q_k(S_0) + \sum_{i=1}^n \lambda_i \cdot E(S_i) \quad (1)$$

where, $Z(S_0)$ is the predicted value (predictand) at un-sampled point, β_k is the estimated slope coefficient of the model, Q_k is the predictor, S_i denotes the location, λ_i is the kriging weight determined by spatial dependence structure of the residuals and $E(S_i)$ is the residual from the linear model at location S_i . The β_k is estimated by either the OLS (Ordinary Least Squares) or the GLS (Generalized Least Squares) fitting method:

$$\beta_{GLS} = (Q^T \cdot C^{-1} \cdot Q)^{-1} \cdot Q^T \cdot C^{-1} \cdot Z \quad (2)$$

$$\beta_{OLS} = (Q^T \cdot Q)^{-1} \cdot Q^T \cdot Z \quad (3)$$

Where β is the vector of the regression coefficients, Q is the matrix of predictors at sampling locations (eqn 4), C is covariance matrix of residuals (eqn 5) and Z is vector of measured target variable.

$$Q = \begin{pmatrix} 1 & q1 \\ \vdots & \vdots \\ 1 & qn \end{pmatrix} \quad (4)$$

$$C = \begin{pmatrix} \text{cov}(q_1, q_1) & \cdots & \text{cov}(q_n, q_1) \\ \vdots & \ddots & \vdots \\ \text{cov}(q_1, q_n) & \cdots & \text{cov}(q_n, q_n) \end{pmatrix} \quad (5)$$

The difference between the GLS and OLS is that in the Ordinary Least Squares method the observations are considered independent (Bivand 2008), that is, no spatial auto correlation between residuals is assumed.

A function describing the spatial dependency of a stochastic process (Z) is called variogram. The very common method to compute the variogram is the method of moments (Matheron 1963; Webster 2007), described in the equation (6).

$$\gamma(h) = \frac{1}{2N(h)} \sum_{i=1}^{N(h)} \{Z(S_i) - Z(S_i+h)\}^2 \quad (6)$$

Where the $N(h)$ is the number of point pairs, S_i denotes the location of the stochastic process (Z) and h is the separation between the Z point pairs.

The first step to precede the kriging, is to select a model of spatial covariance for the experimental variogram and find the kriging variogram parameters by the least squares method (Webster 2007).

3.1.2. Conditional simulation

In the Kriging methods, a smoothed representation of reality is made, hence, the values which are greater than the average are underestimated and the values lower than the average are overestimated (Webster 2007). Here the need of simulation is felt, because the simulation results in more detailed realization of a random function.

There are two methods of conditional and unconditional simulation. In the unconditional simulation, the realization of a random function (i.e. the $Z(S_i)$ in the example) is randomly selected in the set of all possible realizations without considering the sample kriged map. But in the conditional simulation, the realizations are more realistic pictures of the spatial distribution. The simulation is done with regard to the sampling locations (Webster 2007).

But here a question arises: “How many simulations should be done?” the answer depends on the objective of study and the structure of the phenomenon. If the simulation is done considering a stationary field and an area more than the range of variogram, a single simulation is enough, while in non stationary fields such as petroleum reservoir, each simulation is one answer to the flow of petroleum, hence, several simulations are to be carried out if possible results are examined (Chiles 1999).

As discussed, in the conditional simulation, the prediction values are created based on the kriging results. The kriged estimates are assumed to have Gaussian distribution with normal variance and the mean from which the simulated data are randomly derived (Webster 2007).

The use of stochastic simulation is very much highlighted in studies where spatial variation of measured field is of importance (Goovaerts 2000). The choice of stochastic simulation is more preferred than the kriging based models for attributes like soil hydraulic conductivity (Goovaerts 2001). As one more example, the stochastic simulation method was compared with the regression Kriging in soil heterotrophic respiration modelling, the results showed that the stochastic simulation will produce significantly improved probability density function and the semivariogram of the original data (Herbst 2009).

3.1.3. Using environmental variables in soil properties prediction

In soil genesis, five major environmental factors of climate, fauna and flora effect, parent material (known as lithologic factor), relief (known as topographic factors) and time are involved (Jenny 1941). The SCORPAN model has incorporated those factors in spatially referenced format, as well as the coordinates and soil properties themselves into the digital soil mapping technique (McBratney, Mendonça Santos et al. 2003). Therefore, the consequent soil type and properties are influenced by each factor.

The correlation of environmental variables with the individual soil properties is a well known method for soil mapping (McKenzie and Ryan 1999). Substantiated by literature, using the environmental variables such as slope, land use and land cover as the predictors of the soil hydraulic properties will result in accurate outputs (Odeh 1995; Merz 1998; Kuriakose 2009). Also, Kuriakose et al., (2009) expressed that Land use/land cover can be used as a good predictor for the soil depth (thickness) prediction.

Based on the SCORPAN model, the relief factor highly influences the formed soil characteristics. According to a research, the topsoil moisture content spatial distribution has significant relationship with the topographic indices including, slope gradient, aspect, plan curvature, specific catchment area and stream power index (Florinsky, Eilers et al. 2002). Odeh et al., (1995) and Herbst et al. (2006) concluded that the regression Kriging by using the slope attributes as co-variables is the most appropriate method with the least prediction errors for the soil depth and hydraulic properties. Those variable which are derived from Digital Terrain Models, including the slope steepness, wetness index and slope shape are very much promising to be used as the predictors for soil depth (Ziadat 2010).

Herbst et al., (2006) concluded that the morphometric units have the highest correlations with the soil physical properties including saturated hydraulic conductivity. They also stated that the secondary terrain attributes like relative altitude and slope, have good potential to predict the soil properties.

Another study found that there is a strong relationship between soil properties and the land forms in young alluvial units (McKenzie and Austin 1993). It was also found that presence of impeding layers in shallow soils (< 1.5 m) determines the soil properties (McKenzie and Ryan 1999). Also, the lithologic units were good predictors of saturated hydraulic conductivity (McKenzie and Ryan 1999; Ferrer Julià 2004).

3.2. Hydrologic modelling

3.2.1. Introduction to the Limburg Soil Erosion Model (LISEM)

The LISEM is a physically based model which can simulate, erosion, runoff and sediment transport after each rainfall event (Jetten 2002). The model is raster based and uses PCRaster as the GIS environment (Jetten 2002; Hessel, Jetten et al. 2003).

3.2.2. Application of the LISEM model, in runoff simulation

Based on input data, the model can temporally and spatially simulate the overland flow of the watershed of study (De Roo 1996a). The LISEM model is recommended to be applied in assessing climate and land use change effects on basins hydrology (De Roo 1999). LISEM is a good model for hydrologic simulations during single rainfall events at scale of catchment which can be used for the runoff and erosion efficient mitigation actions (De Roo 1996). The user can also change the land use and soil properties scenarios in order to study their effects on the model.

De Roo et al. (1996 and 1999) carried out analysis on the model simulation and reported that the saturated hydraulic conductivity is the most sensitive variable in modelling. It was also concluded that the model outputs are far from perfect. The reasons are related to the spatial variability of soil saturated hydraulic conductivity and soil moisture storage at the catchment scale. Therefore, in order to obtain quantitative reliable results from the model, there should be very detailed and high resolution input data.

3.2.3. Theoretical basis of the LISEM

The rainfall intensities data are introduced to the LISEM as ASCII file. The precipitation depth (P in mm) is assumed to compose the water height (h) on the surface, and considering the surface slope angle of (α), the LISEM calculates the corrected surface water height (h') in mm:

$$h' = h + [P \times \cos(\alpha)] \quad (7)$$

The part of rainfall which is intercepted by the plants canopy is taken into account. Depending on the type of land cover and the user's objectives, several models can be introduced for interception calculations. The original equation that the LISEM uses is the Aston's model (Jetten 2002).

There are some sub-models which can be used to calculate water infiltration rate, according to data availability, user can decide which model to use (Jetten 2002). The possible models are as follows:

- (1) Green- Ampt model which is based on the Darcy's law,
- (2) Swatre model which uses the Richard's and continuity equations, and
- (3) Holtan model.

The Green-Ampt model which was used in the research requires the saturated hydraulic conductivity, soil thickness, initial soil moisture content and porosity. The model is based on the Darcy's law as explained in equation 8:

$$Q = K_s \left(\frac{M \partial h}{F} + 1 \right) \quad (8)$$

$$M = \theta_s - \theta_i$$

Where Q is the vertical flux (mm/h), K_s is the saturated hydraulic conductivity (mm/h), M represents available pore space, θ_s and θ_i are soil porosity and initial soil moisture content respectively, F is cumulative water infiltration (mm) and ∂h is matric suction (mm).

The surface storage of water is calculated by the Maximum Depression Storage (MDS). This value determines a threshold to which when water height reaches, water overflows micro depressions of ground surface. To compute the MDS, the following equation (Jetten 2002) is used:

$$MDS = (0.243 \times RR) + (0.010 \times RR)^2 + (0.012 \times RR \times S) \quad (9)$$

Where, The RR is the standard deviation of surface heights (cm) and S is the terrain slope (%).

The surface roughness is also taken into account for the flow path width application in the hydraulic equations. The flow width and hydraulic radius is assumed to have linear relation with the fraction of ponded surface (f_{pa}) in each grid cell (Jetten 2002). For the ponded surface fraction estimation, the Jetten and De Roo equation is used (Jetten 2002):

$$f_{pa} = 1 - e^{(-a \times h)} \quad (10)$$

The h is the water depth at the surface in mm, “ a ” is an empirical value calculated by the following formula:

$$a = 1.406 \times (RR)^{-0.942} \quad (11)$$

in which, the RR is in mm.

It is assumed that when the 10 percent of grid cell surface is ponded, the runoff starts. Then the equation (10) is solved and a threshold for water height is resulted which is called h_0 . If the threshold is larger than the **MDS**, then 90 percent of the **MDS** is filled and the runoff gradually increases non-linearly between the h_0 and the **MDS**. After the water height is more than the **MDS**, the runoff height increases linearly with the water height.

A grid cell may be covered by several land covers with different hydraulic characteristics. Each of the land cover types are taken into account in measuring the infiltration rate and runoff velocity. The runoff velocity is calculated by the Manning’s formula:

$$v = \frac{R^{\frac{2}{3}} \times \sqrt{S}}{n} \quad (12)$$

where, the v (m/s) is the velocity; R (m) is the hydraulic radius for which the average water height and flow width of grid cell is considered, S is the sine of slope and n is the Manning’s coefficient (Jetten 2002).

Then the discharge in each grid cell is calculated with Chow’s equations (Jetten 2002; Hessel 2005):

$$A = \alpha Q^\beta \quad (13)$$

$$\frac{\partial Q}{\partial x} + \alpha \beta Q^{\beta-1} \frac{\partial Q}{\partial t} = q \quad (14)$$

In which, Q ($\text{m}^3 \cdot \text{s}^{-1}$) is the discharge, q is the lateral inflow ($\text{m}^3 \cdot \text{s}^{-1} \cdot \text{m}^{-1}$) (this could be assumed as infiltration), A (m^2) is the wet cross sectional area of the channel, β is constant value of 0.6 (Govers 1990) and the α is calculated by the equation (15), x and t are the distance in flow direction (m) and time (s), respectively.

$$\alpha = \left(\frac{n}{\sqrt{S}} \times P^{2/3} \right) \quad (15)$$

in Equation 15, P (m) is the wetted perimeter of the stream channel.

A four point finite difference solution of the kinematic wave is also used together with the Manning's equation when the turbulent and distributed overland and channel flow routing is done over the Local Drainage Directions (LDD) map (Jetten 2002). Given that there are channels in some cells, a separate kinematic wave is processed for each channel. The channel is assumed to be located in the centre of the cell, and the velocity and height of water is the average of the height and velocity of water in different land covers of the cell.

4. METHODS AND MATERIALS

4.1. Data acquisition

Most of basic data required for the hydrologic modelling, had been acquired by the mountain Risks project. Other data including soil properties and some site descriptions were obtained during field observation and laboratory work (Table 2).

Data	Source
K_s (in $mm.hr^{-1}$)	Field work, some measurements are available from previous research (Hosein 2010)
Soil thickness (in mm)	Field work
Porosity (%)	Laboratory measurement
Soil field capacity moisture (in %) as the initial soil moisture	Laboratory measurement
Soil Bulk Density (in $g.cm^{-3}$)	Laboratory measurement
Soil texture	Field work
Fraction of soil covered by vegetation (%)	Field work
Plant height (m)	Field work
Hourly Rainfall data of Faucon	Available in mountain Risks project dataset
Faucon Stream temporal height (in mm)	Available in mountain Risks project dataset
InSAR DTM (5m resolution)	Available in mountain Risks project dataset
Land cover map	Available in mountain Risks project dataset
Roads map	Available in mountain Risks project dataset
Lithologic map	Available in mountain Risks project dataset
Geomorphologic map	Available in mountain Risks project dataset

Table 2. The list of data used for the LISEM model

4.2. Sampling Design

Prior to the fieldwork, the samples locations were determined based on the stratified purposive sampling strategy in which the geomorphologic and land cover maps were overlaid by the weighted sum operation in the ArcGIS, and on each 14 resultant units (Figure 6), a sampling point was selected, considering accessibility of the points and closeness to roads by using the Google earth image. More than 1 sampling point was selected on units which were large and covering more area. From previous research (Hosein 2010), there were some available soil data sampled from the middle of the catchment. Those points were also taken into consideration for the study.

In Figure 6, based on the overlaid units, the sampling points of the study area as well as the locations of available soil data from the previous study (Hosein 2010) are shown. Note that the area lower than the hydrometric station was later cut off, because there were no sampling points on that area.

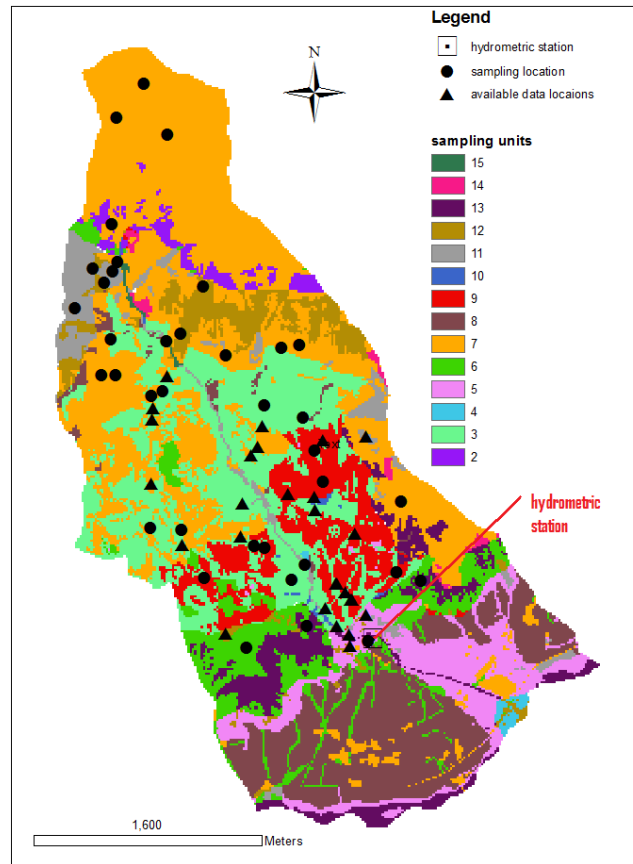


Figure 6. The sampling points; Note: available data locations represent the data acquired by previous study

4.3. Field observations

In the following sections, parameters which were measured in field and the methods of the measurements are explained. The results of the field observation are given in the Appendix I. Each of the following parameters were later used to make the LISEM input maps.

4.3.1. Soil texture classification

The surface soil texture classes were determined by the feel method (USDA 2010).

4.3.2. Saturated hydraulic conductivity (Ks) measurement

The single ring infiltrometer method was used to measure the Ks. In this method, a single ring was inserted vertically on ground and in the outer space of the ring, the near-saturation condition was provided by pouring water and keeping it wet. Then the inner space of the ring was filled with water to a certain height (15 cm). The water depth changes over determined time intervals were recorded until the

whole water infiltrates. The cumulative infiltration was plotted against the time and a line between the steady state portions of the infiltration plot, was fitted (Figure 7 shows the plot for one of the samples).

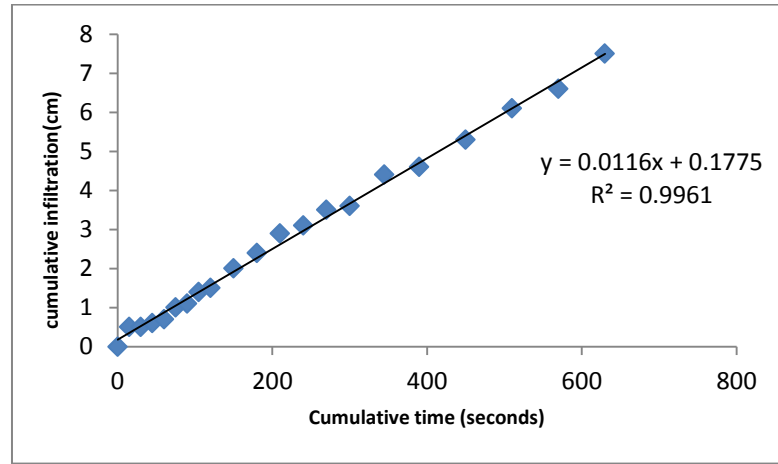


Figure 7. The Cumulative infiltration against Cumulative time (plot for one of the samples)

The slope of the line represents the flux velocity (cm.s⁻¹). According to Figure 7, the flux is 0.0116 (cm.s⁻¹) which was converted to (cm.min⁻¹):

$$q = 0.0116 \text{ (cm/s)} * 60 \text{ (s/min)} = 0.69 \text{ (cm/min)}$$

The following equation was used to calculate the Ks (Bagarello, Sferlazza et al. 2009; Farrell 2010):

$$q = ks \left\{ \left(\frac{C}{G \cdot \pi \cdot r} \right) + 1 \right\} \quad (16)$$

Where, q is the water flux in soil (cm.min⁻¹), Ks is the saturated hydraulic conductivity (cm.min⁻¹), C is the wetting front potential (cm of water) which was calculated by the Saxton pedotransfer function of Soil Water characteristics software (Saxton 1986). The Saxton function needs texture class and organic matter content of soil. Due to lack of organic matter measurements, the organic matter of soil was assumed 1%. The reason to choose this value is that the Saxton model was run using Organic matter ranges from 0 to 4, and it did not change the Ks value largely. The C factors of samples were also estimated by the Saxton function which ranges from 190 to 1530 cm for different samples. G is the shape factor for infiltration. This dimensionless parameter depends significantly on the ring radius, depth of ring insertion and water depth in the ring. The single ring infiltration calculation is very low sensitive to the errors in G estimation. Using the Reynolds and Elrick's graph (Figure 8) (Reynolds 1990), the G parameter was estimated for each soil sample by using the ring radius, insertion depth and average height of water in the ring (ponding depth). The average ponding depth was 15 cm, and the insertion depth was 4 cm. Based on the assumptions, the G factor was found 0.45. r is the ring radius which was 5 cm. Finally, the Ks was converted to (mm.hr⁻¹).

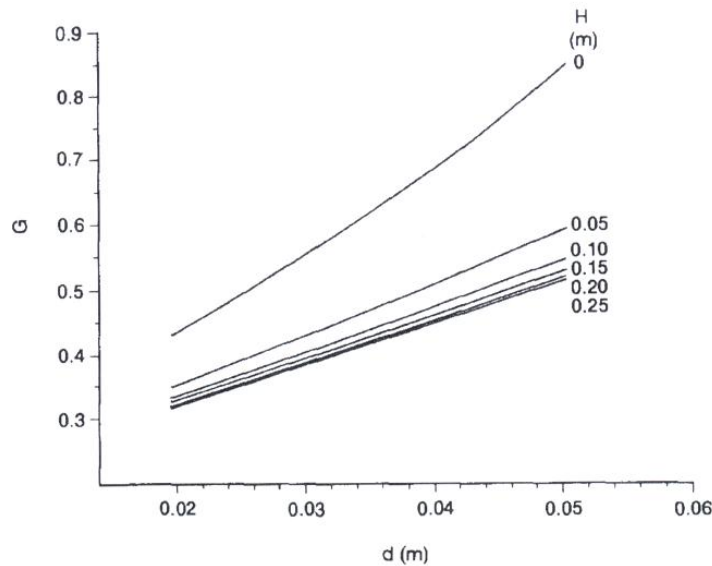


Figure 8. The Reynolds and Elrick's graph for G factor (Reynolds 1990);

$d(m)$ = the ring insertion depth, $H(m)$ = water height in the ring

In addition, the available K_s data measured in the moraine deposits area (Hosein 2010), were compared to the results of this study and due to having the same unit and being measured by the same method, they were taken into consideration for the interpolation. For some of the sampling points which were located on bare rocks, because of very steep slope, and impossibility of the measurements, value of zero was given as the K_s .

4.3.3. The soil thickness measurement

The soil thickness was determined by auger. In this method, an auger was pushed down into soil and continued until reaching bed rock. The vertical length of the auger hole was the soil thickness. For each sample point, 3 soil thickness measurements, each 10 meters apart, were done and the average was the final representation for the point soil thickness. Note that in some sampling areas, due to limitations, 1 measurement could only be done and in other areas where slope variations within a short distance was very large, more than 3 points were measured within distance of more than 10 meters (Table 4, Appendix I).

4.3.4. Soil surface stoniness

The soil surface stoniness means the area unit fraction of surface soil which is covered by stones. For determining the soil surface stoniness, the FAO fieldwork charts were used (FAO 2006).

4.3.5. Measurement of plants height and ground fraction covered by plant

At each sampling site, a 1×1 (m²) plot was made in which the fraction of the area covered by plants was estimated by eyeball (Jetten 2010). The trees height average was also eyeballed.

4.3.6. Roads width measurement

The width of impermeable roads was measured, which average² was given to the roads map so as to convert it to roads width map.

4.4. Laboratory work

4.4.1. Field capacity and porosity measurement

Undisturbed soil samples were taken by PF rings during the field work, then carried to laboratory and saturated. The weight of the samples at saturation point was measured (W1). The samples were left in the laboratory open air for 24 hours. Then the air dried soil weight was measured again (W2). After that, the samples were placed into Oven and dried completely for 24 hours at 105° C. The oven dried samples weight (W3) was measured as well. The difference of W1 and W3 was used to measure the soil porosity. The difference of W2 and W3 was also used to measure the soil Field Capacity. The field capacity moisture content was used as the LISEM input for the initial soil moisture content. The Field Capacity is a level at which soil moisture is between dry and saturation points. Because the area is neither wet nor dry and covered with plants which may adjust the soil moisture level, the Field Capacity was assumed as the initial soil moisture.

4.4.2. Soil Bulk Density

The Soil bulk density equates the division of dried Soil weight by the total volume of the soil. For most of the rings which were filled fully with soil, the volume of the ring (100 cm³) was used as the soil volume, but for those which were not fully filled, because of falling small part of soil from the rings during sampling, the height of soil was measured by a small graduated stick at laboratory before the saturation and drying process.

4.5. Analysis of the catchment hydrology

Based on the available measured data of the stream height between the dates of 1/1/2010 and 31/8/2010, and the field observation of the watershed outlet, the temporal discharge of the torrent was calculated using the Manning's formula (Eqn. 12). For this, average slope of the outlet was measured by Clinometer. The geometric shape of the stream Canal was more or less trapezium. The side lengths, outer and inner widths were measured by a measuring tape and the Nikkon Forestry 550 instrument. The shape and sides sizes of the Canal at the outlet are shown in Figure 9.

²The average of the roads width was 2 meters.

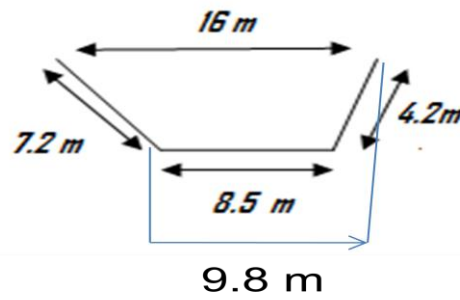


Figure 9. The Canal shape at the outlet; Note: the canal depth is 4 m.

The stream bed was covered with big boulders therefore by using the Canals Manning's coefficient table (Arcement 2010), the value of 0.06 was given as the roughness coefficient of the stream bed. Upon having the basic parameters of the Canal, the stream velocity was computed by the Manning's equation (Eqn.12). Then the discharge was calculated simply by multiplying the water velocity by the cross sectional area (Eqn.17). Note that the cross sectional area was calculated based on the water height variations.

$$Q \text{ (m}^3\text{s}^{-1}\text{)} = [\text{Velocity (ms}^{-1}\text{)}] \times [\text{cross sectional area (m}^2\text{)}] \quad (17)$$

After measuring the stream discharge values, temporal variations of discharge were plotted (Figure 10). According to Figure 10, there are 2 large peaks in the graph. The first peak which occurred on 4th of June, was selected for the model calibration.

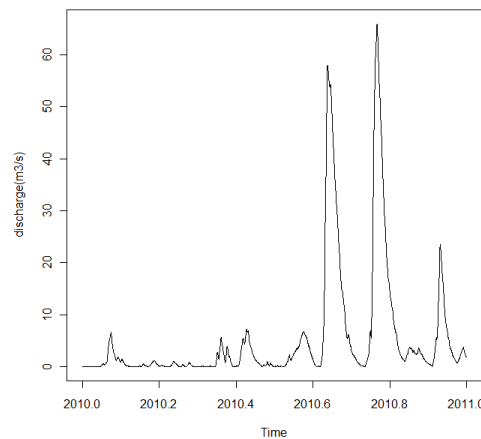


Figure 10. The temporal variations of the torrent discharge

At first, the runoff ratio of the peak was calculated by the following equation:

$$C = \sum_{i=1}^n \left(\frac{D_i \times [T_i \times 60]}{[A] \times [R_a]} \right) \quad (18)$$

Where “C” is the Runoff ratio, “D_i” is torrent discharge (m³/s) at duration time interval of T_i (minutes), and “n” is the number of the time intervals, “R_a” is the total amount of rainfall(m) and “A” is the area of the watershed to the gauging (hydrometric) station which was 9×10⁶ m².

Also, the rainfall intensity variation which caused the first large peak was plotted against time (Figure 11). The rainfall data were measured at the hydrometric station by the tipping bucket.

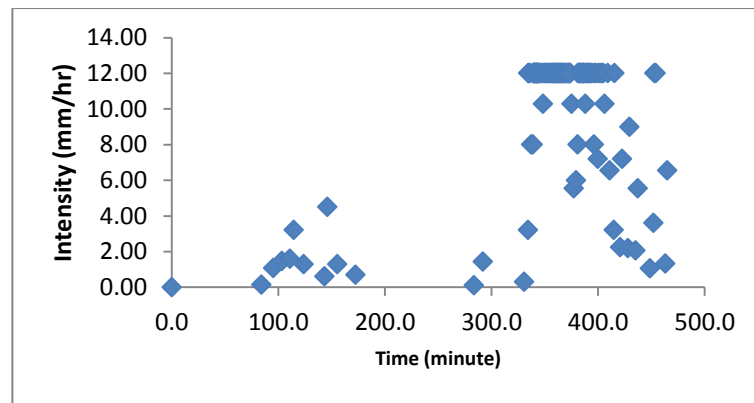


Figure 11. The rainfall intensity variation of the first peak

The runoff ratio was 1.1, which indicates that the stream discharge variations were not caused only by received rainfall. This could be related to the errors in the precipitation measurements, i.e., at higher elevations, the catchment receives more rain than the hydrometric station; this issue was not taken into account. In addition, the base flow of the torrent comes from underground (Remaitre 2005) which sources could be out of the catchment and at rainfall events the other catchments wherein the stream base flow originate, may receive much more rain than the Faucon and produce outflows which contribute to the discharge variations of the Faucon.

The same process was done for the other peaks of the discharge and same results were obtained. Therefore, the discharge values were not proper to be used in the model calibration.

4.6. Computing the environmental variables

4.6.1. Land cover and lithologic data

The land cover and lithologic maps were available as shape files, projected in Lambert zone III. The maps projection system was transformed to UTM (WGS84 zone 32N) and then the maps were converted to Raster and ASCII in ArcGIS³.

³ The 15 m resolution was given to the raster map. The reason to select this resolution will be explained at 4.8.1.

In order to use the maps in statistical modelling, the land cover and lithologic values were extracted at the sampling points and the resulted values along with the coordinates were written in excel table.

4.6.2. The terrain parameters

The Raster InSAR DTM with 5 m resolution, projected in Lambert zone III, was transformed to UTM (WGS84 zone 32N) in ArcGIS. The DTM was then imported to SAGA GIS software (Cimmery 2010). First the “Fillsink” operation was done on the DTM by Planchon/Darboux method. Then the morphometric parameters of LS factor, Slope, Aspect, Wetness index, Overland flow distance to channel network, Plan- Profile curvature and Convergence were derived by the morphometric operator of the SAGA GIS. Upon having the morphometric parameters, the resulted maps were exported from SAGA grid format to ESRI/ArcMap raster format.

In ArcGIS environment, the DTM and each of the DTM derived parameters were re-sampled by the nearest neighbour method which increased the resolution to 15m. The resultant terrain parameters values were later extracted at the sampling points and each value along with coordinates were recorded in Excel table.

4.7. Statistical modelling approach

An Excel file of the Ks and soil thickness measurements was made in which attributes namely coordinates, land cover classes, lithologic units and the terrain parameters for each point were added (appendix I). The file was later converted to CSV in order to become readable into the R. In appendix III, the script used for the R programming is available.

4.7.1. Study on the environmental variables as predictors of the soil properties

Each environmental variable including land cover, lithologic and the morphometric units were examined individually in a linear model to predict the soil thickness and Ks. The scatter plots, adjusted R² and diagnostic plots were used to justify the applicability of the variable in question as a predictor. After finding the variables which model with the soil properties had the highest adjusted R², good diagnostic plots and significant linear model parameters, the additive and interaction models between those variables and the soil properties, were investigated by using the forward stepwise method. In this procedure, variables were added one by one to the previous one so as to see the changes in the adjusted R² and diagnostic plots. In case of correlation coefficient increase, the variable was added to the model; otherwise, it would be removed. The process continued until reaching the highest adjusted R².

4.7.2. Kriging of the soil thickness and Ks

In order to see if there is any spatial structure among the soil data, the empirical variogram of the soil thickness and Ks were plotted as well as the residuals variogram of the soil properties modelled by the environmental predictors. Upon the spatial dependency existence, the Ordinary and Regression Kriging were later done. In case of having poor variogram, Thiessen polygons of the soil property were produced. For doing the Kriging, land cover map, re-sampled to 15 m resolution, was used as grid.

By doing the cross validation of the kriged maps, the Mean Error (ME) and Root Mean Squared Error (RMSE) were calculated so as to discuss the accuracy of the predictions. Finally, the created maps were exported to the ILWIS and then PCRaster.

4.7.3. The conditional simulation of the soil thickness and Ks

Upon making the kriged maps, the conditional simulation of the soil properties was carried out. The maximum number of nearest observations which would have been used for the simulation (nmax) and number of simulations (nsim) were set at 64 and 30, respectively.

4.7.4. Mapping other soil surface properties

The results of soil characteristics including the Field Capacity moisture (F.C.), soil porosity, Bulk Density and the soil matric potential, calculated by the Saxton pedotransfer function (section 4.3.2.), as well as soil surface stoniness, were recorded in a CSV file and read in the R. First the ordinary variograms of the soil properties were computed and those having spatial structure were used in the Ordinary Kriging, in case of having no structure, the average of the soil properties was just used for mapping.

The Manning's roughness coefficient and the Random Roughness maps were also provided. For this, the Manning's coefficients were obtained from the Chow's table (Prachansri 2007). The Random Roughness value was assumed 0.5 (cm) for all the land cover types (Renard 2000; Prachansri 2007), except for areas which were introduced as bare rock in the land cover map. According to the field observations, the surface roughness in such those areas is high, therefore the Random Roughness was estimated 1.9 (cm), using the following equation (Mwendera and Feyen 1992):

$$n = 0.014 \times RR^{2.692} \quad (19)$$

Where, RR is the Random Roughness (cm) and n is the Manning's coefficient. The equation 19 was also used for the torrent RR. In table 3, the Manning and RR values for each land cover unit are shown.

Land cover	Manning's value	RR (cm)
Forest	0.2	0.5
Grassland	0.24	0.5
Torrent	0.05	1.7
Arable land	0.06	1.80
Bare rock	0.06	1.9

Table 3. The Manning and Random Roughness values of land cover units

(Mwendera and Feyen 1992; Renard 2000; Prachansri 2007)

4.7.5. Mapping of plants height, ground fraction covered by plants and the Leaf Area Index (LAI)

The plants height and fraction of ground covered by plants canopy were obtained during the field work (Table 1, appendix I). For the pastures and grasslands, the plants height was assumed 0.05 m; then for each land cover unit, average canopy cover (in percentage) and plant height (in meters) were assigned. Note that there was high variability within each land cover unit but it was ignored in the study and just one averaged value was given to each unit. After making the maps by assigning the corresponding values to each land cover unit, they were exported to the ILWIS where the Raster operation was used to produce the LAI map. The LAI was calculated using the WOFOST- Diepen equation (Jetten 2010) as follows:

$$\text{Cover} = 1 - \exp(-0.4\text{LAI}) \quad (20)$$

In which, the Cover represents the canopy cover (in percentage) and the LAI is the Leaf Area Index.

4.8. Hydrologic modeling

4.8.1. Preparing the LISEM input maps

All the produced maps were exported to the ILWIS where re-sampled by the Nearest Neighbour method so that they all have the same size and number of cells.⁴ Note that minimum value of 10 mm was assigned to all zero and negative values of the soil depth (thickness) maps. Since the LISEM assumes that the stream width is less than cell size (Hessel 2005) and maximum width of the Faucon stream was 9 meters, the cell size was set at 15 meters. Also, based on Literature (Hessel 2005), using grid size of less than 15 meters in the LISEM, results in realistic outputs. Final maps were imported to the PCRaster via the ILWIS. For some maps such as hard surfaces and compact surfaces which were not necessary for the study, masks of zero values were produced and assigned to them.

Using the PCRaster commands (Appendix IV), the Local Drain Direction (LDD) was created from the DTM. The LDD was later used to make the outlet, channel mask, channel LDD and sub basins maps. From the sub basins map, the stream basin map was pulled out and used as mask map (Figure 12). The area of the mask map was 526 ha.

Roads width map was produced from the roads map. According to the field observation, the width of the roads was assumed two meters. Channel width, channel side and channel slope maps were created using the DTM, LDD and channel mask maps. The channel geometric shape was assumed rectangular and the Manning's coefficient, Cohesion and Ks values of the channel were assumed 0.06, 10 (kPa) and 0 (mm/hr), respectively. Other maps including sine of slope angle, catchment boundary and area covered by rain gauge, were also produced from the DTM. Finally all the input maps were extracted by the mask map.

⁴ Land cover map was used as reference for the re-sampling.

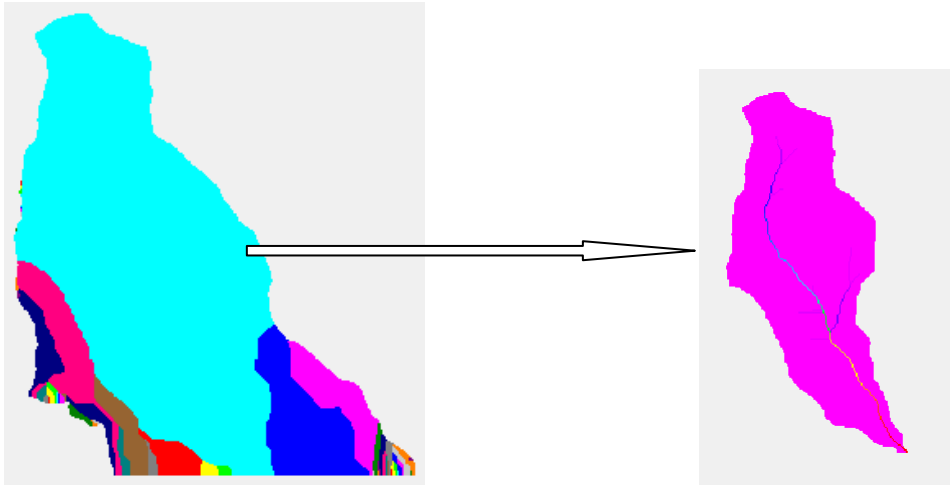


Figure 12. The main basin mask map (right) derived from the sub basins map (left)

4.8.2. Preparing rainfall intensity input for the LISEM

Three rainfall scenarios were designed based on past events. The area has experienced storm of 30 (mm/hr) intensity (Remaitre 2005). Also, according to the available rainfall records of 2010, the maximum rainfall intensity of 12 (mm/hr) was used for 2 durations of 60 minutes and 4 hours. The reason to use different rainfall intensities and durations was to see whether the soil properties spatial variations effects on simulated runoff change at various rainfalls. In Table 4, the synthetic rainfall scenarios are shown.

Rain intensity (mm.hr⁻¹)	12	12	30
Duration (hour)	1	4	1

Table 4. The synthetic rain scenarios used in the LISEM modelling

4.8.3. Run of the LISEM

In the model run file, all the input data directory were defined as well as the infiltration model of Green-Ampt layer 1. Then the impermeable layer option was checked. Also, the LISEM original storage equation for the interception was selected. The time step of the simulation was selected as 10 seconds because the cell size of all the maps was 15m. According to the Courant condition, for accuracy and stability, the time step must be smaller than the cell size when using the Kinematic wave equation (Hessel 2005).

5. RESULTS AND DISCUSSION

5.1. Statistical analysis on data

5.1.1. The Ks and soil depth (thickness) frequency distribution

Figure 13 compares the soil properties data box plots of the previous and the present studies. The Ks values were measured by same methods in the two studies but the box plots are largely different. The Ks box plot of the present study shows no symmetry which median is around 20 ($\text{mm}\cdot\text{hr}^{-1}$) and maximum reaches 400 ($\text{mm}\cdot\text{hr}^{-1}$) while the previous study results have median of 200 ($\text{mm}\cdot\text{hr}^{-1}$) and maximum is above 1500 ($\text{mm}\cdot\text{hr}^{-1}$). The distinction of the results could be relevant to the sampling locations differences. The highest values of the Ks were at points which were not sampled in the present study. The soil thickness box plot of the present study looks symmetric while that of the previous study has skewness. In both cases, the soil thickness medians are just above 100 (mm) and minimums are close to zero (mm). The maximum soil thickness of 300 (mm) was observed in the present study.

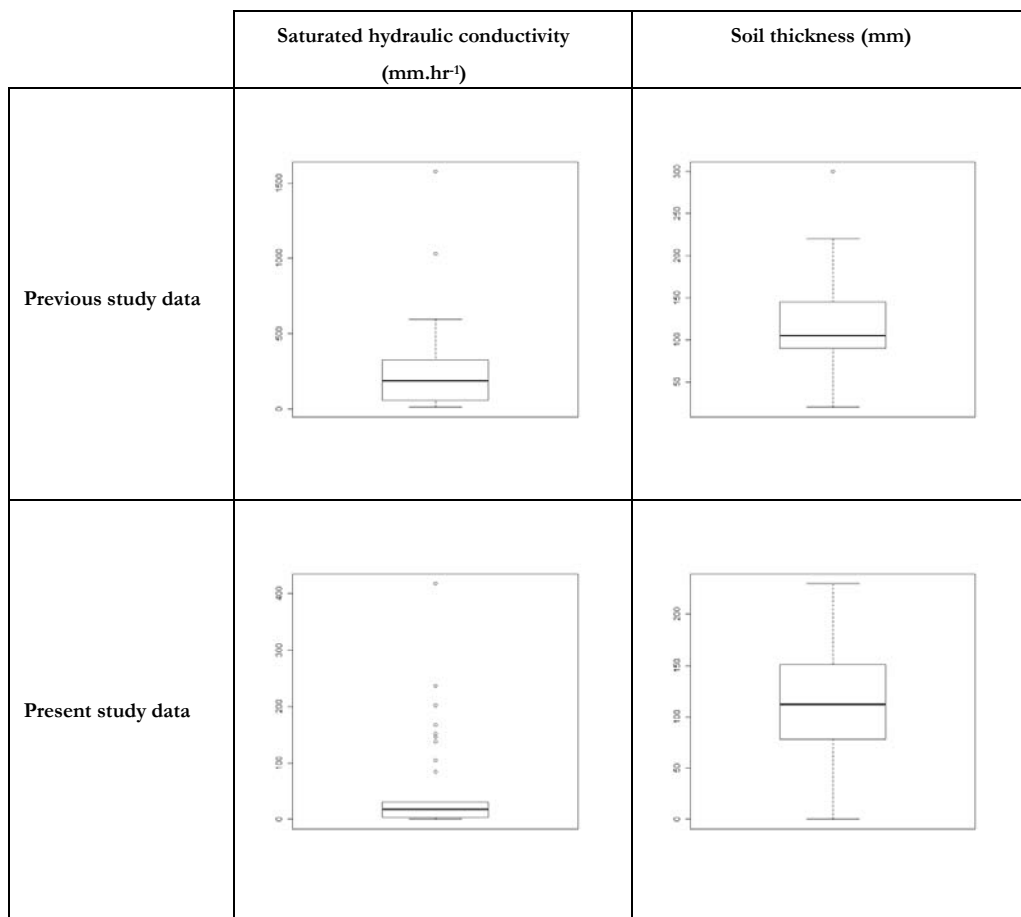


Figure 13. Comparison of previous and present studies data by box plots

The K_s and soil thickness of the two studies were analyzed together which statistical summary says that these soil properties distributions are not symmetric (Figure 14). The reason could be related to small number of samples and the applied sampling method. The soil data are not from a random sample but a purposive. Also, the differences of the present and previous researches data could highly influence the frequency distributions of the soil properties.

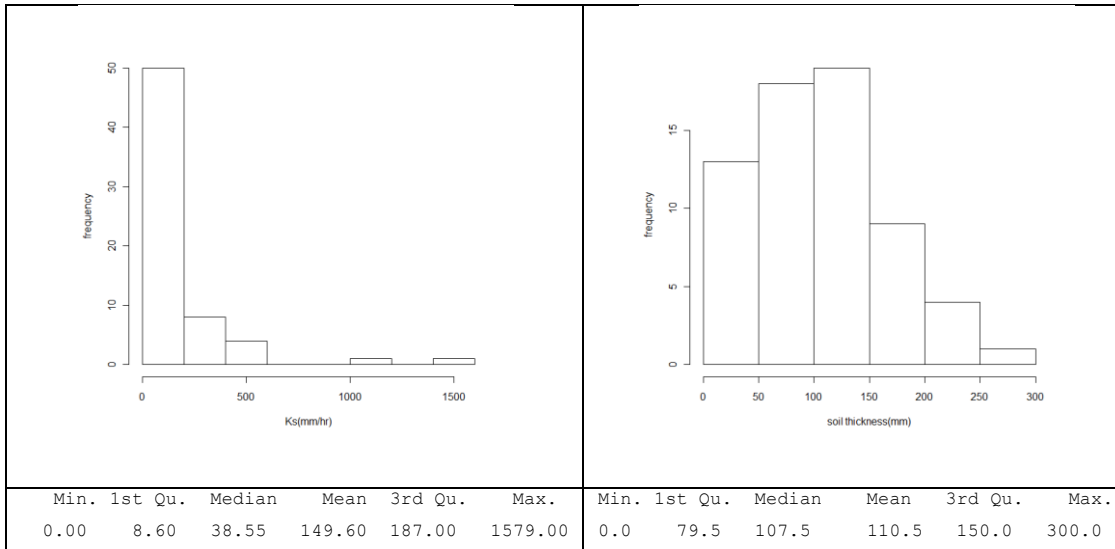


Figure 14. The frequency distribution of K_s (left) and soil thickness (right)

According to Figure 14, the K_s modal value is in the range of 0 to 200 ($\text{mm}\cdot\text{hr}^{-1}$) which includes both of high and low K_s values. Apart from this, other bins of the K_s histogram show high K_s value. The soil thickness ranges from 0 to 300 (mm) which indicates soil shallowness in the catchment. Based on these, the study area soil could be allocated to dual soil hydrologic group of A/D (USDA 2007) which means the soil saturated hydraulic conductivity may be favourable for water infiltration (in case of $K_s > 140 \text{ mm}\cdot\text{hr}^{-1}$), but due to shallowness of soil, there is high potential of runoff generation.

Figure 15 shows post plot of the measured K_s data at sampling points. According to the figure, there are some points which are largely different from the other close by points, i.e. K_s values of 1579 ($\text{mm}\cdot\text{hr}^{-1}$). The large K_s points were mostly located in the forest zones. The reason for the high K_s could be related to the local variability in such areas which is caused by trees roots made fissures, as well as the biological activities of animals.

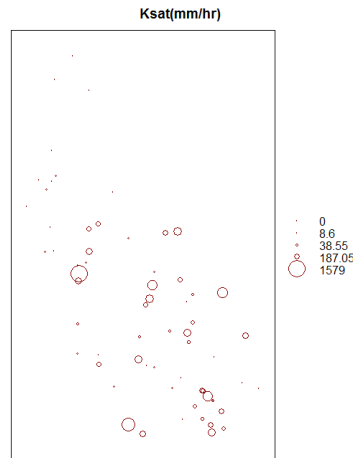


Figure 15. The post plot of the Ks field measurements

Post plot of soil thickness (Figure 16) shows that it does not differ much at close range. Outstanding large soil depths are located in forest and meadow zones. The reason could be related to the soil protection by the plants and the yearly addition of the organic matter to soil.

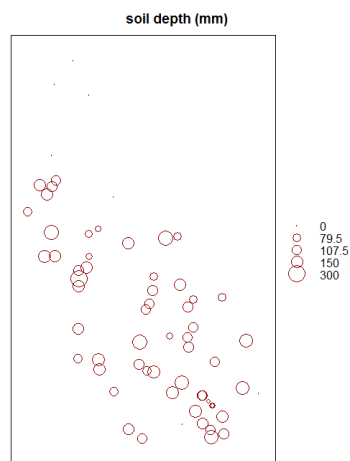


Figure 16. The post plot of soil depth

The Ks Coefficient of Variation (CV) was 173 percent which proves the high variability of Ks. The soil thickness CV was 58 percent which indicates low variability of this parameter.

5.1.2. Exploratory graphics: target vs. environmental variables

The first step to examine the correlation possibility between each variable and the soil properties was to look at scatter plots (appendix II). Figure 17 shows box plots explaining the Lithologic and land cover unit's relation with the Ks and soil depth (thickness).

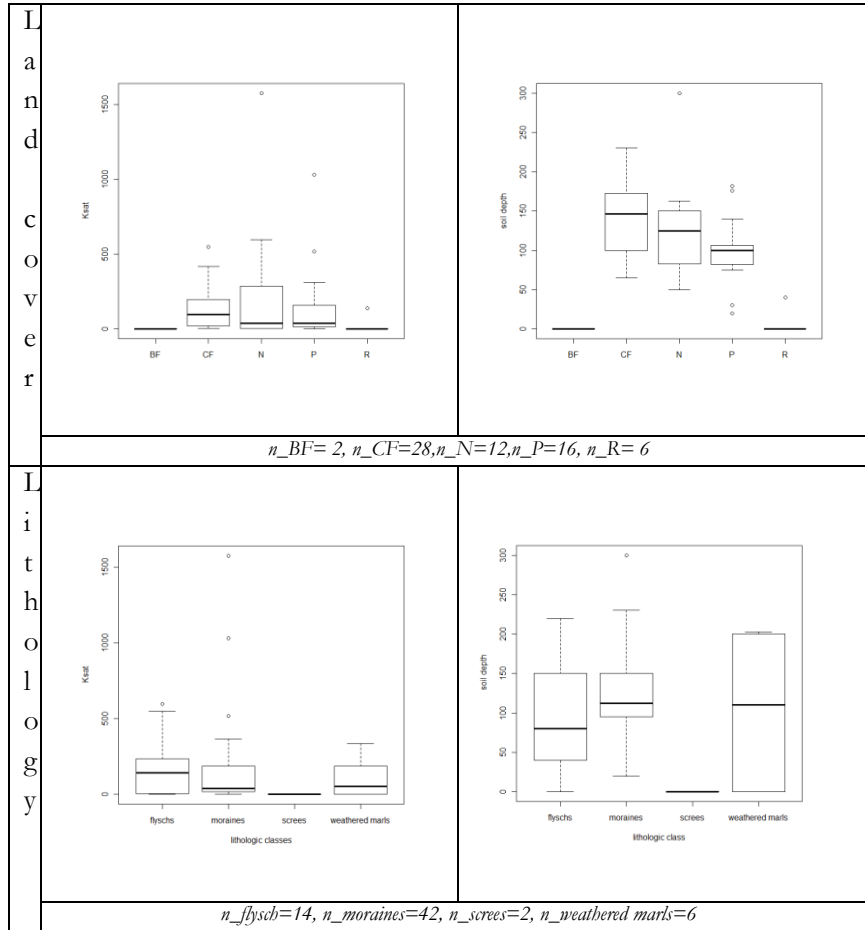


Figure 17. Box plots of the soil thickness (right) and Ks (left) against the Lithologic and land cover units; Note 1: the Ks is in (mm/hr) and soil depth in (mm); Note 2: BF = broad-leaved forest; CF = Coniferous forest; N = Natural grassland; P = pastures; R = bare rock; Note 3: “n” indicates number of sampled points in each unit, e.g., n_{flysch} denotes number of points in flysch unit and n_{BF} means number of points in broad leaved forest unit.

According to Figure 17, the medians of Ks in different land cover and Lithologic units have no large variations though in coniferous forest and flyschs units, the Ks median is the highest. Also the Ks box plots in any of the lithologic and land cover units are not symmetric.

The soil depth (thickness) has the highest median in the coniferous forest unit. The box plot of soil depth in the coniferous forest unit looks closer to symmetric than in other land cover units. Also the highest median of soil depth (thickness) is related to the lithologic unit of Moraines and the box plot of the flyschs looks close to symmetric. Altogether, soil depth seems to be related to the land cover and Lithologic units.

Figure 18 illustrates an example of the soil depth (thickness) and Ks relation with two morphometric variables of slope and convergence. As the figure shows, slope seems to have relation with only soil depth though the relation is not strong. The graph indicates that soil depth values close to zero are mostly concentrated at high slopes. This could be relevant to effect of terrain slope on soil erosion and deposition (Milevski 2007). Also, very weak relation between convergence and Ks is seen.

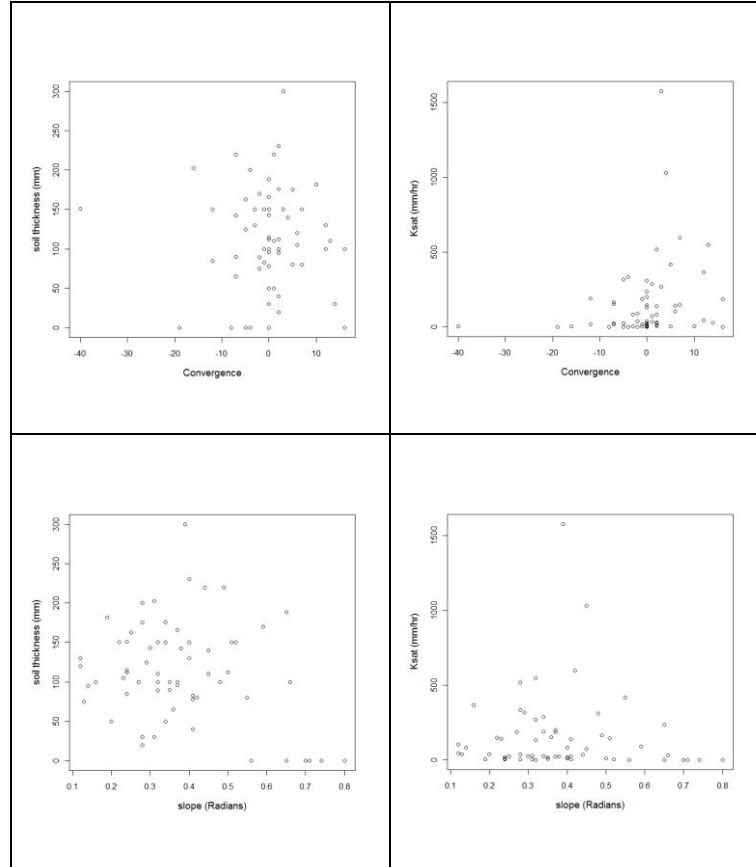


Figure 18. Scatter plots of soil depth (thickness) and K_s against slope and convergence variables

5.1.3. The linear model analysis between the soil parameters and the environmental factors

In table (5), linear models goodness-of-fit are shown by adjusted R^2 . The linear models validity is based on the models diagnostic plots. Those models which had no good diagnostic plots were invalid.

<i>variables</i>	Soil depth (thickness)		Saturated hydraulic conductivity(K_s)	
	<i>Adjusted R²</i>	<i>Model validity</i>	<i>Adjusted R²</i>	<i>Model validity</i>
Land cover	0.44**	valid	0.007	invalid
Lithology	0.08*	invalid	-0.033	invalid
Slope	0.07*	invalid	-0.01	invalid
Coordinates	0.09*	invalid	-0.01	invalid
Aspect	0.005	invalid	0.02	invalid
Profile curvature	-0.01	invalid	0.003	invalid
Plan curvature	-0.01	invalid	0.01	invalid
Convergence	-0.01	invalid	0.03*	invalid
Wetness index	-0.003	invalid	0.004	invalid
Overland flow distance to channel network	0.05*	invalid	0.03	invalid
Elevation	0.03*	invalid	0	invalid
LS	-0.01	invalid	-0.01	invalid

Table 5. The soil properties linear models validity; Note: <*> explains the statistical significance of the variable coefficient in model at $p=0.05$ significance level; <***> explains the statistical significance of the variable coefficient in model at $p= 0.01$ significance level

According to the results of table (5) none of the variables were good predictors for Ks. Only Convergence had significant relation with the Ks but due to low R² and poor diagnostic plots (Figure 19), the relation is not meaningful. Diagnostic plots of the Ks and convergence model is not good. The residuals QQ plot does not show normal distribution. For high theoretical quantiles, the standardized residuals go beyond +1. Also, as fitted values increase, the residuals deviate from zero. Hence, the Ks could not be predicted by any of the variables. The reason could be relevant to the Ks essence. Though the landscape, bed rock and land cover/land use can influence the soil behaviour, but the Ks is more dependent on complex internal and micro processes in soil environment than the external area, so that the effect of the surrounding environment is lessened.

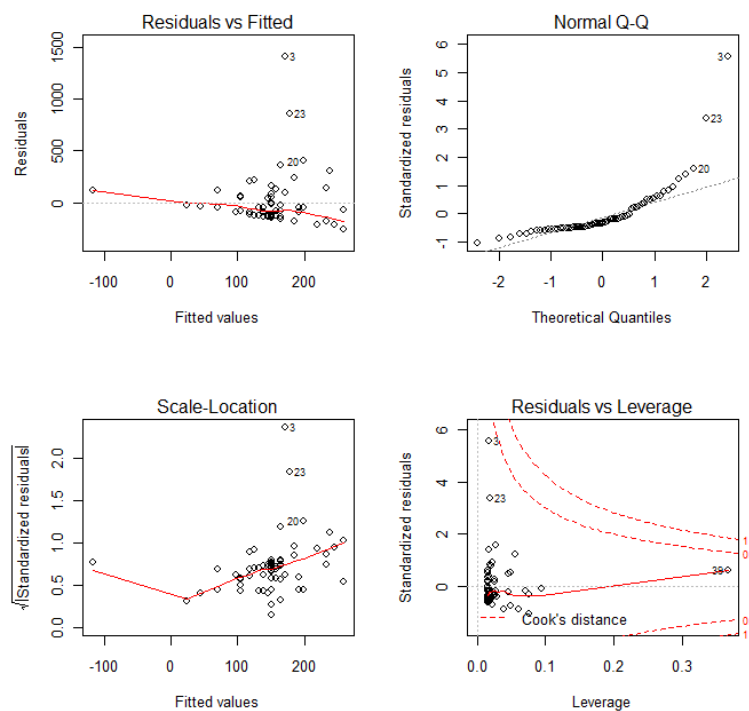


Figure 19. Diagnostic plots of the Ks model by convergence variable

Variables which had significant relation with soil depth (thickness) did not have good diagnostic plots to show the models validity. Only land cover class was the best explanatory variable. The land cover class correlation with the soil depth (thickness) was found to be the highest (Adjusted R² = 0.44) and resultant linear model parameters were very significant at p = 0.01 level of significance. The model diagnostic plots were also good. This could be relevant to the land cover/land use influence on soil protection and erosion.

Upon the stepwise forward modelling, adding terrain parameter of the overland flow distance to channel network, raises the soil thickness model fit slightly (Adjusted R² = 0.46). Therefore, additive model of land cover class and overland flow distance to channel network, had the highest correlation coefficient. That is, just under half of the soil thickness variance is explained by land cover class and overland flow distance to channel network. Diagnostic plots of the model were examined (Figure 20). Based on Figure 20, the diagnostic plots look good. According to the QQ plot, the model residuals are more or less normally distributed. There are some poorly fit points which are shown in the plots (i.e., point 3, 38 and 53).

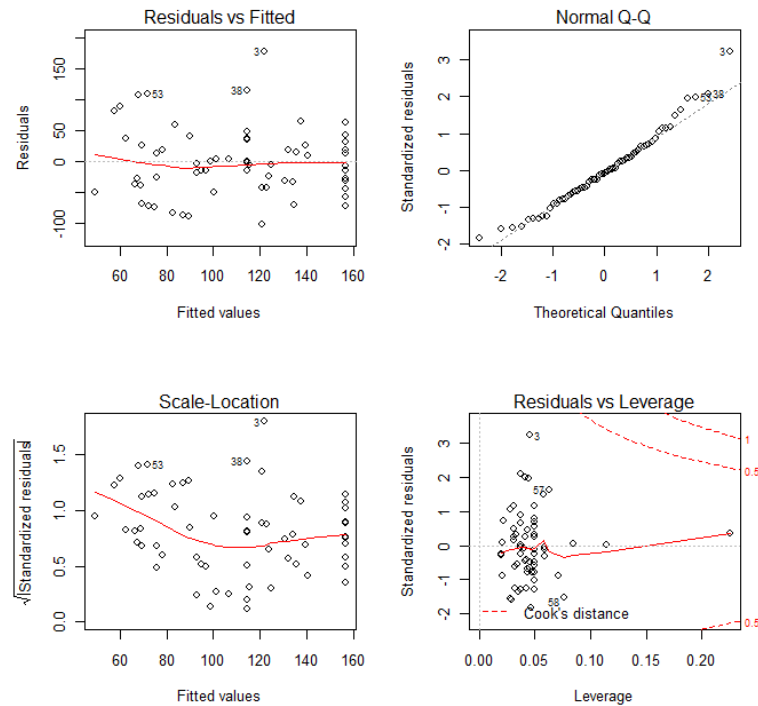


Figure 20. The diagnostic plots of soil depth modelled by land cover and overland flow distance to channel network

5.1.4. The Ordinary Kriging (OK) of the soil depth (thickness) and Ks

The empirical variograms of soil depth (thickness) and Ks were plotted in order to understand if there is any spatial structure or not (Figure 21). The best model to fit the soil thickness variogram was Circular.

The Ks variogram is far from perfect. As it is seen in the variogram, there are 36 point pairs at close range which have high variability and disturb the monotonic increase of the variogram. This could be related to the high variability of Ks at short range (Figure 15).

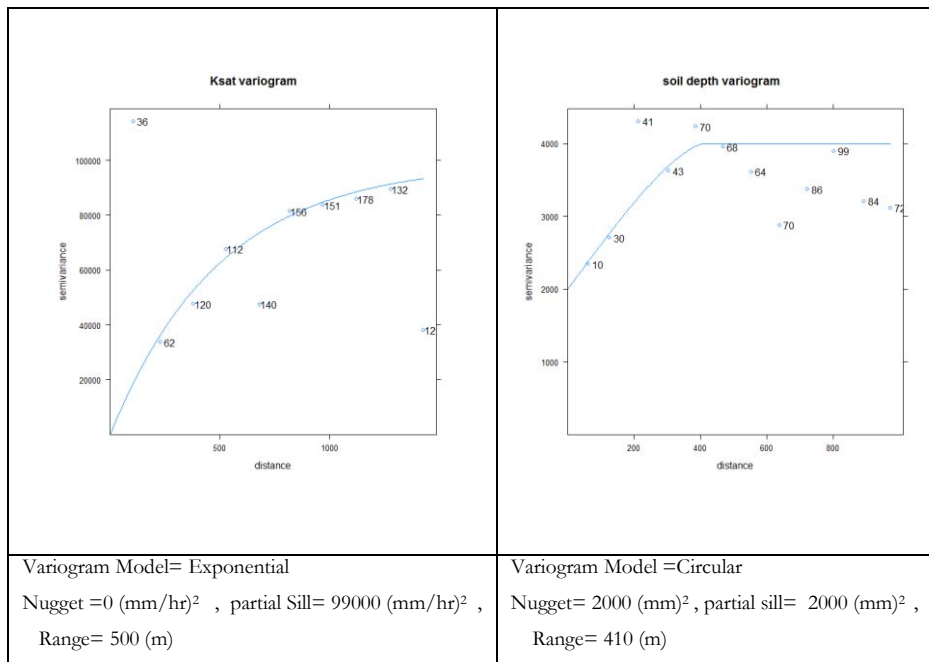


Figure 21. The empirical variograms for Ks (left) and soil depth (right)

The Ks variogram without the previous research data was also examined in order to see if there is any improvement, but very poor variogram was resulted (Figure 22).

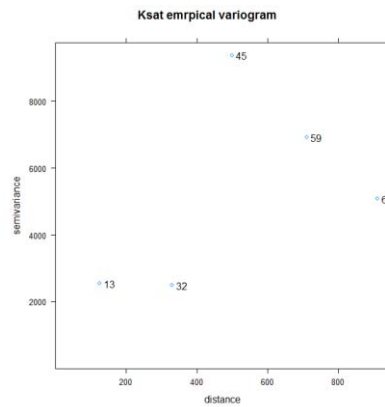


Figure 22. The sample variogram of the Ks data without the previous research points

Due to this result and high variability of the Ks, the data transformation might be helpful to obtain acceptable variogram (section 5.1.5.).

An Ordinary Kriging (OK) prediction was made for the variable with a variogram that could be modelled, i.e., soil thickness. In figure 23, the results of the OK for soil depth (thickness) is shown.

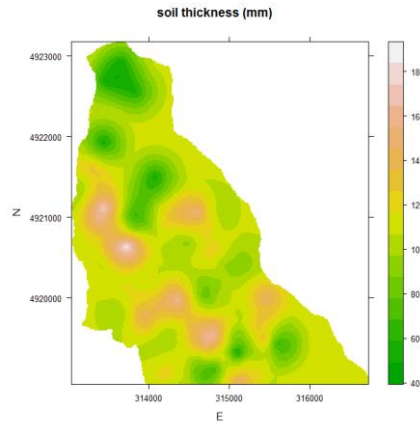


Figure 23. The map of soil depth (thickness) made by the Ordinary Kriging

Figure 24 shows the Kriging variance values ranging from 2400 to 4200 (mm^2). According to the figure, the least variances, which are close to the nugget variance, belong to areas near sampling points.

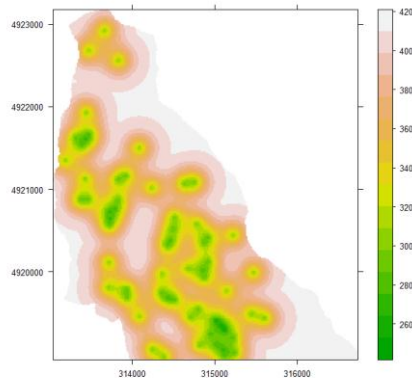


Figure 24. The soil thickness ordinary kriging variance (mm^2)

The Kriging residuals were obtained by the Kriging cross validation. The prediction residuals histogram is also shown in Figure 25. According to the figure, the soil depth kriging residuals look roughly normally distributed. The residuals were also used to calculate the Mean Error (ME) and Root Mean Squared Error (RMSE) which are -0.67 (mm) and 63.7 (mm), respectively. The prediction RMSE is lower than average soil thickness⁵. That is, the RMSE is 57 percent of the average soil thickness.

⁵ Average soil thickness is 110.5 (mm).

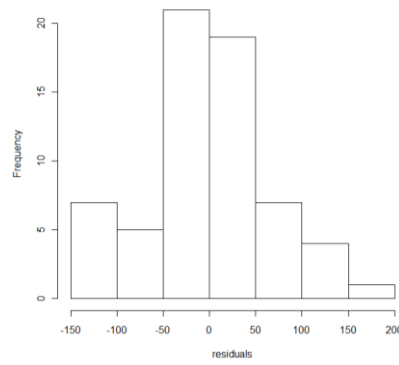


Figure 25. The Ordinary Kriging residuals histogram

5.1.5. The Ks data transformation and Ks mapping

Due to lack of good variogram for Ks, the normalization methods were applied to make the distribution close to normal. The common methods of “Logarithm” and “Square root” were not useful. Therefore another method, called Box-Cox (Sakia. 1992), was used in which the following formula was applied on the Ks values:

$$Y = G(K_s) \cdot \text{Log}(K_s) \quad (21)$$

Where, Y is the normalized value and G (Ks) is the Geometric mean of the Ks.

Figure 26 shows the new values distribution which looks close to normal and there is no high skewness. Then the linear model with the environmental variables was tried but no strong relationship was found.

The variogram of the normalized Ks was plotted which shows good spatial structure with monotonic increase at the short range (Figure 27).

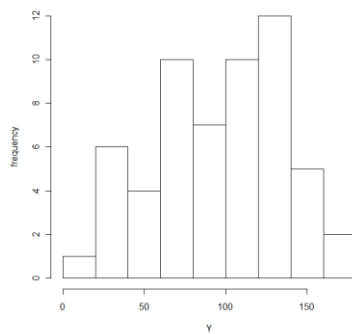


Figure 26. The normalized Ks distribution

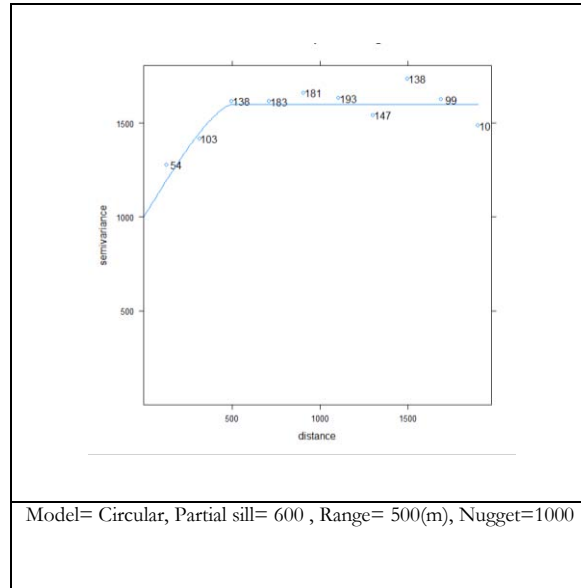


Figure 27. The normalized K_s variogram

The Ordinary Kriging was then done which resultant map and the kriging variance map are shown in Figure 28.

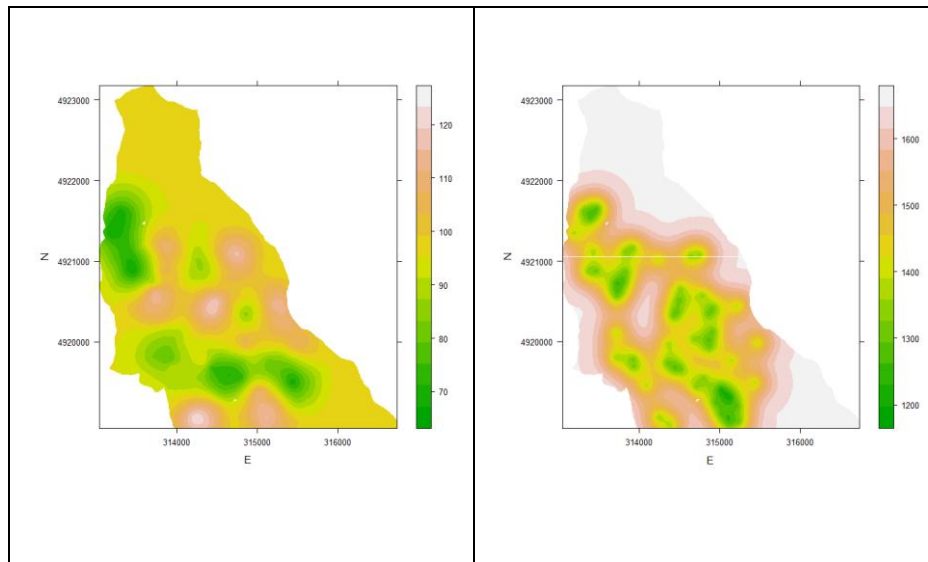


Figure 28. The ordinary kriging of normalized K_s (left) and the kriging variance (right)

Upon the kriging cross validation, the prediction residuals were obtained (Figure 29). As Figure 29 indicates, the residuals distribution looks like normal which mean is close to zero. The ME and RMSE were -0.2 [$\text{mm}\cdot\text{hr}^{-1}\log(\text{mm}\cdot\text{hr}^{-1})$] and 32 [$\text{mm}\cdot\text{hr}^{-1}\log(\text{mm}\cdot\text{hr}^{-1})$], respectively.

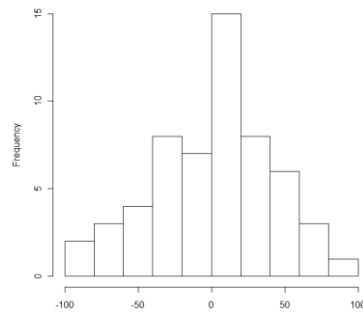


Figure 29. The normalized K_s kriging residuals histogram

Unfortunately no proper method was found in order to back transform the resultant kriged map into original K_s map. Because of this limitation, Thiessen polygons map of the K_s was produced and it was used for the modelling (Figure 30).

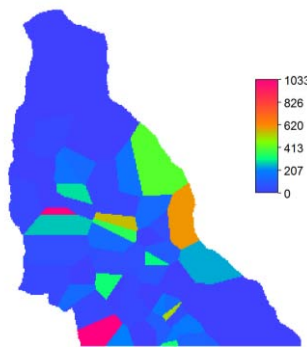


Figure 30. K_s map produced by Thiessen polygons method; Note: K_s ($mm.br^{-1}$)

5.1.6. The Regression Kriging (RK) of the soil depth (thickness)

Since, the soil K_s was not predicted by any of the environmental variables; it could not be used for the regression kriging. Thus, the RK was applied only for the soil depth prediction. At first, the autocorrelation of the soil depth model residuals was investigated by variogram (Figure 31). The Circular model was fitted on the variogram. Because of having spatial structure in the residuals, the next step which is the Regression Kriging was preceded (Figure 32).

As Figure 32 shows, the RK produced soil thickness map which represents the "Land cover class" and "overland flow distance to channel network" variables. The map made by the RK also shows more variability than the OK map. The RK variance ranges from 0 to 3000 (mm^2). The range of the RK variance is lower than that of the OK.

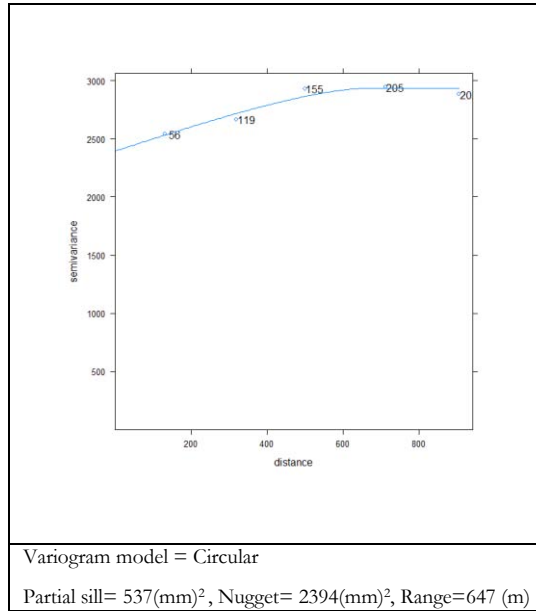


Figure 31. The variogram of soil depth model residuals

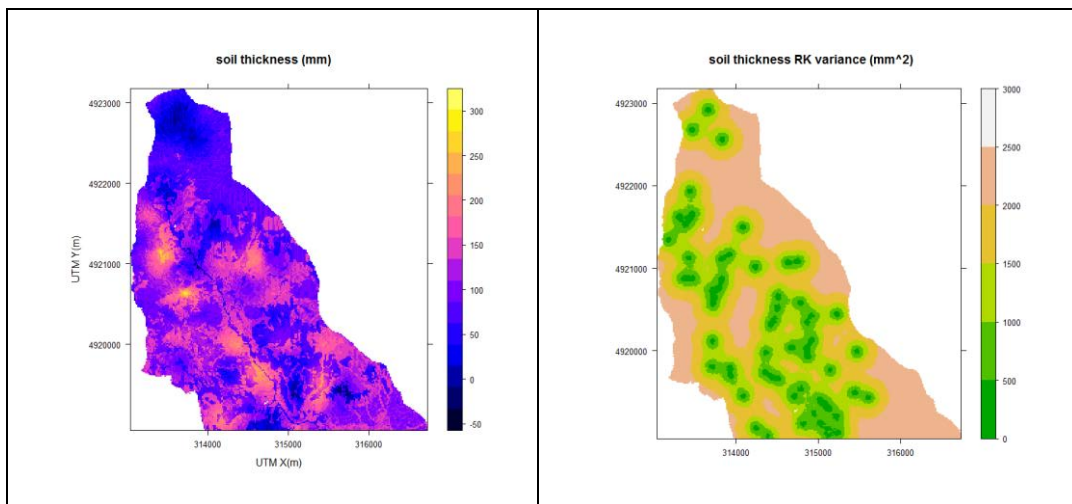


Figure 32. The Regression Kriging of the soil depth (left) and the Kriging variance (right)

The kriging residuals resulted from the cross validation, look more normally distributed than the Ordinary Kriging residuals (Figure 33).

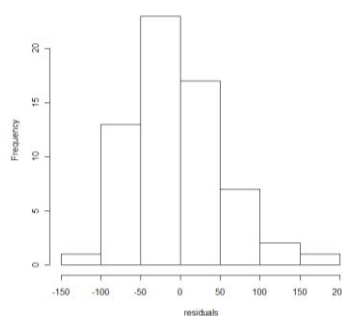


Figure 33. The RK residuals histogram

Upon the cross validation, the Kriging accuracy was assessed. The ME and RMSE are -2 (mm) and 60 (mm), respectively. The regression kriging RMSE is 54 percent of the average soil depth which is slightly lower than that of Ordinary Kriging. Therefore, the accuracy of the RK is better than the OK. The disadvantage of the RK is production of unreal negative values (Figure 32) which are the interpolation artefacts.

5.1.7. Conditional simulation

The Kriging has smoothing effect which causes the over and under estimation of real values, it also does not reproduce a normal frequency distribution histogram (Yamamoto 2005). The conditional simulation is a well known method to remove the smoothing effect. Therefore, the simulated maps and consequent histograms were produced. Four realizations of the ordinarily kriged soil thickness simulation are shown in Figure 34. Also, the soil thickness map resulted from the RK, was used in the simulation which example of four simulated fields are shown in Figure 35. According to the figures 34 and 35, the conditional simulation, generated negative values of soil thickness as artefacts.

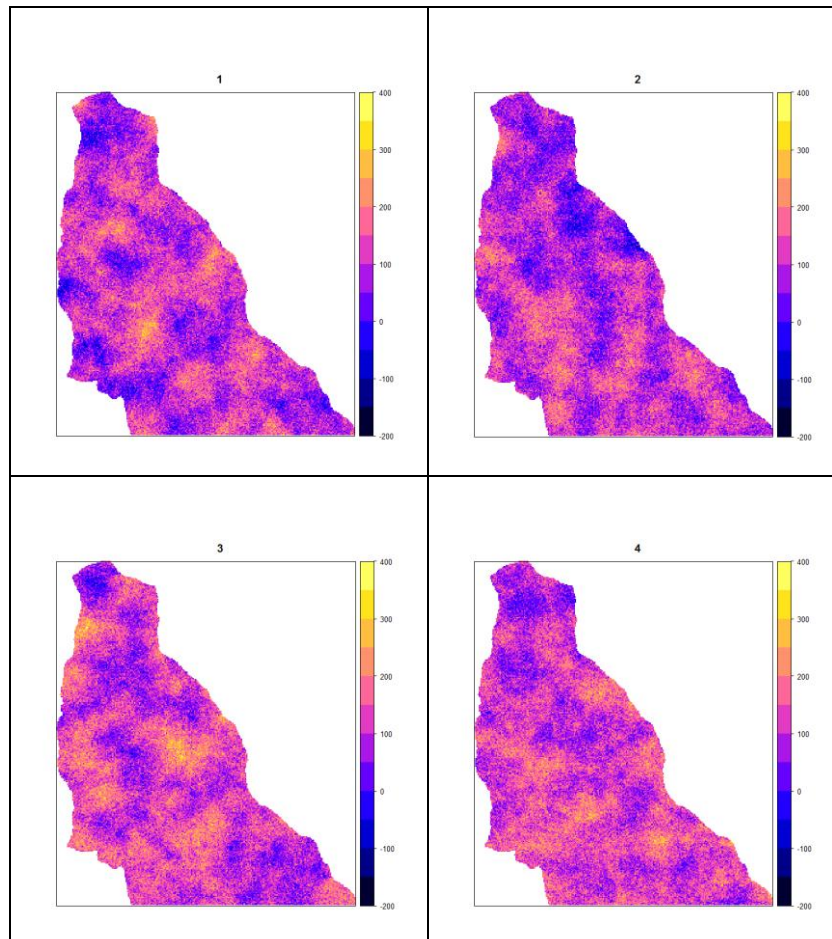


Figure 34. Four simulated fields of soil depth (thickness) map by OK

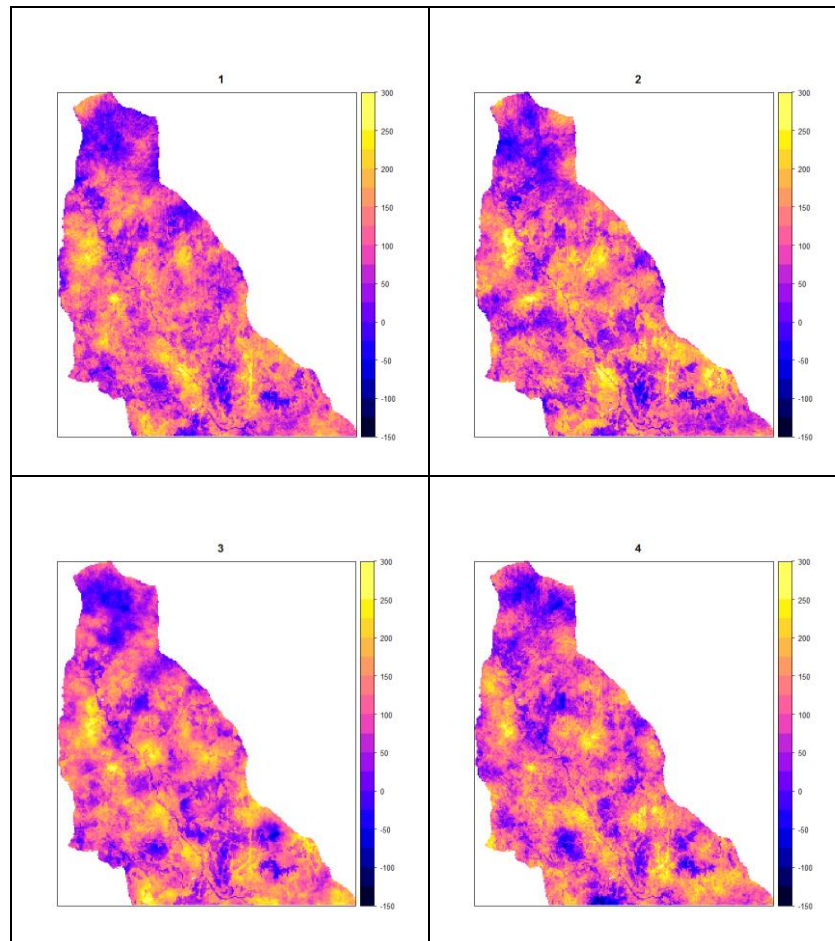


Figure 35. Four simulated fields of soil depth (thickness) created by the RK

Compared to the Kriged maps, the simulation results are much detailed with different realizations. According to Figure 36, conditional simulation has reproduced values with normal distribution as opposed to the Kriging. This emphasizes that simulation has removed the smoothing effect.

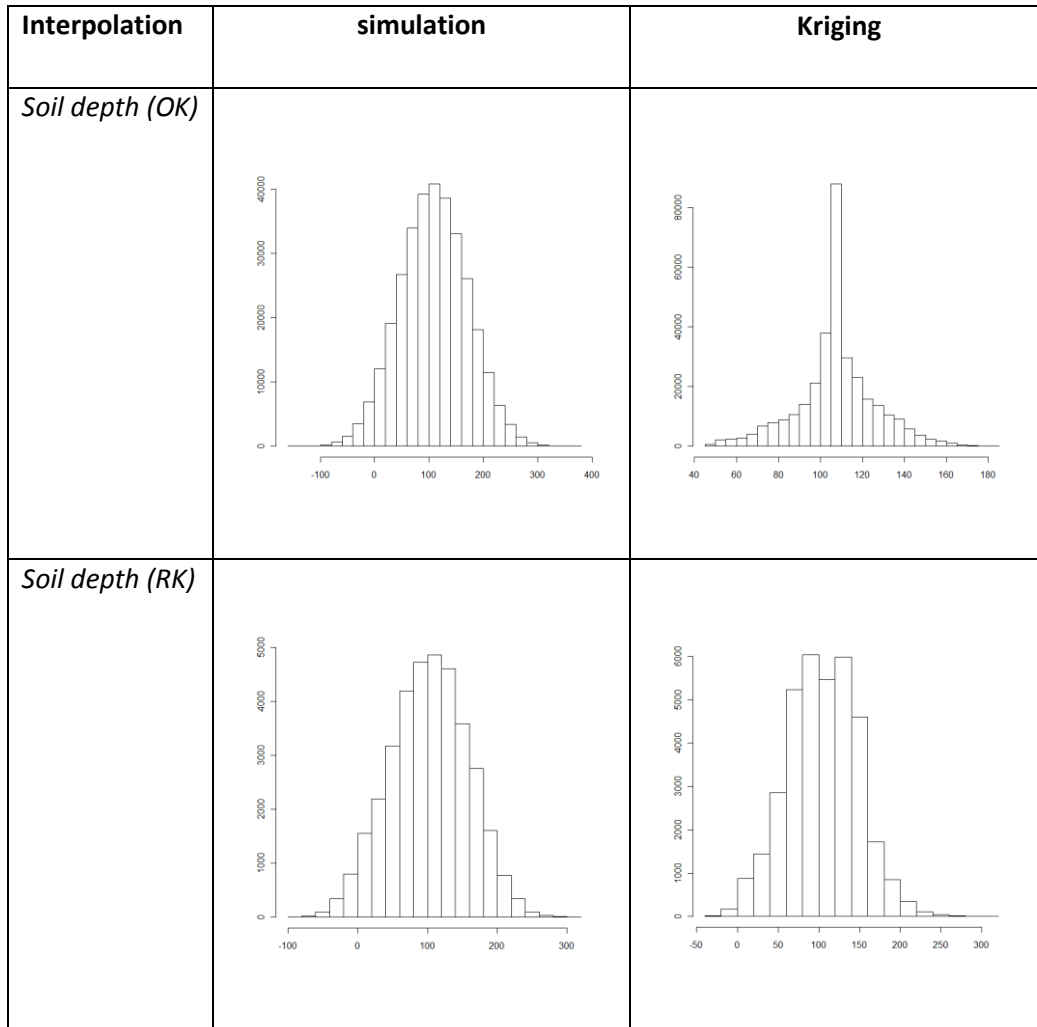


Figure 36 .The histograms of Kriged and simulated values; Note: x axis shows soil thickness (mm) and y axis frequency

5.2. Mapping of the surface stoniness and other soil properties

The soil porosity spatial analysis shows relatively good autocorrelation, for which interpolation, the OK was used (Figure 37). The map of soil porosity looks unrealistically much smooth and generalized. This could be related to the sampling scheme which caused to obtain low variability of this soil parameter.

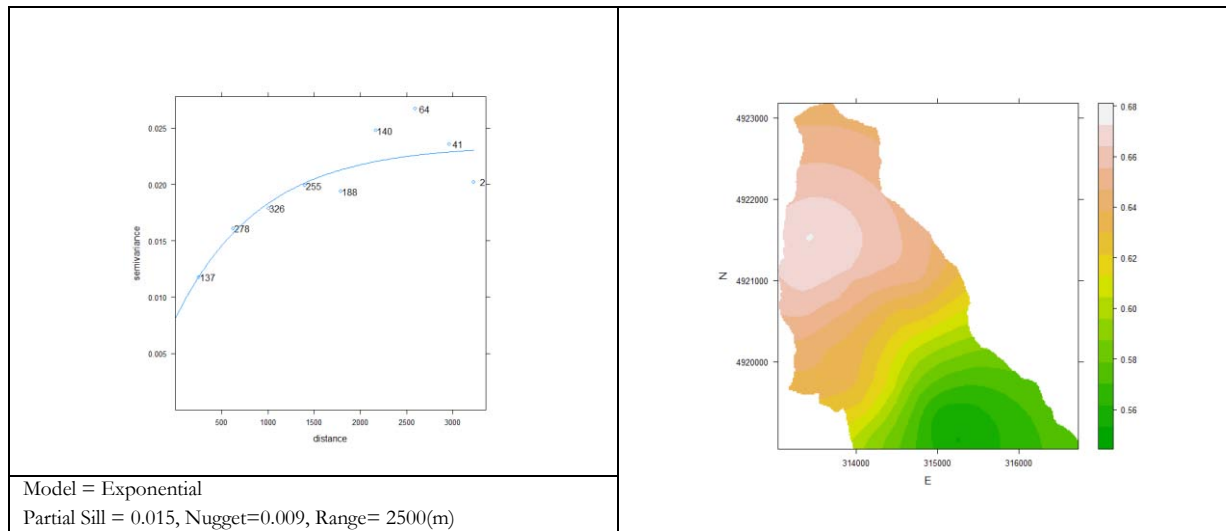


Figure 37. The soil porosity variogram (left) and map (right) produced by the OK

The surface stoniness variogram indicates existence of spatial structure (Figure 38); the Spherical model was best to fit. Based on this, the Ordinary Kriging was preceded.

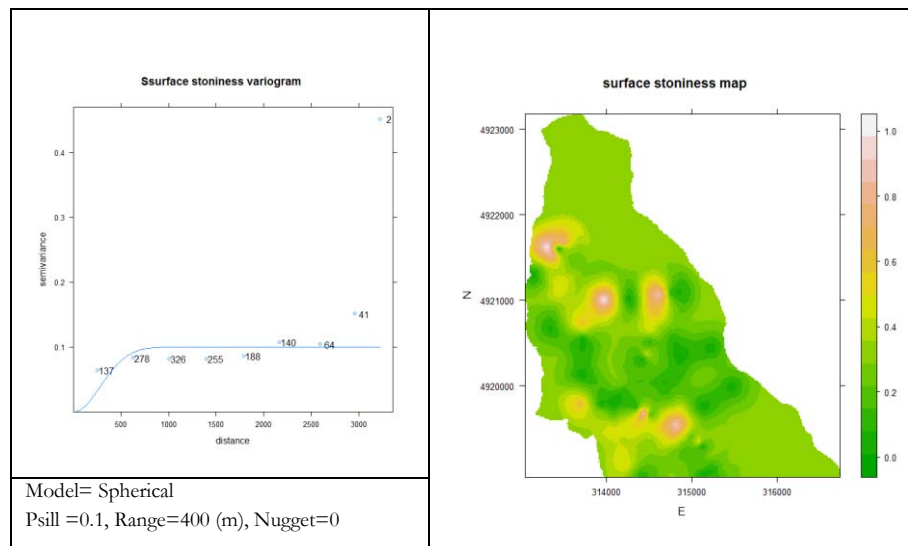


Figure 38. The surface stoniness variogram (left) and map produced by OK (right)

The variogram of soil Field Capacity moisture (F.C.) shows more or less spatial autocorrelation (Figure 39), for which the Circular model was the best to fit. According to the variogram model, the OK interpolation was applied to map this soil characteristic (Figure 39). The F.C. map looks unrealistic and much smoothed. The reason could be related to the sampling plan which resulted in having low variability of this parameter. Also, there were not enough F.C. data from the previous study which might highly influence the interpolation.

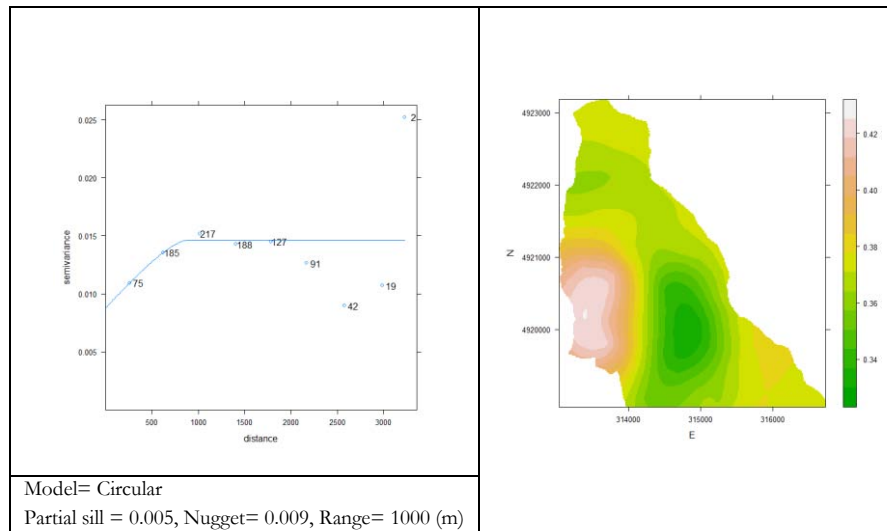


Figure 39. The Soil Field Capacity variogram (left) and map (right) produced by the OK

The soil bulk density (gcm^{-3}) spatial correlation was also examined (Figure 40). As the variogram shows, the points are spatially correlated. Therefore the Ordinary Kriging could be used and the resultant map is shown in Figure 40.

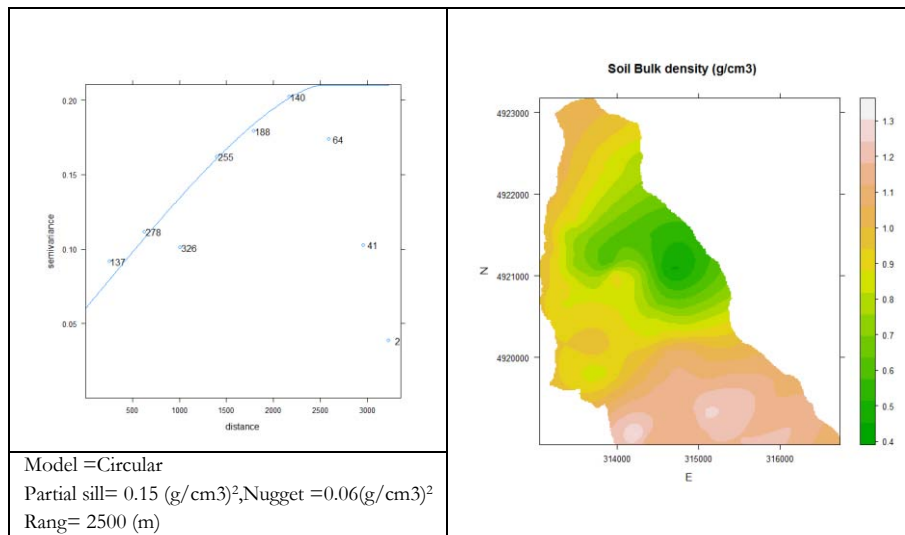


Figure 40. The soil Bulk Density variogram (left) and map (right) produced by the OK

According to the figure 40, there are Bulk Density values of less than $0.9 \text{ (gcm}^{-3}\text{)}$ which are only expected to occur in organic soils or those from very porous young volcanic ash, neither of which is the case here. As the map shows, points having such values are concentrated in the eastern part of the catchment where forest zones are located. During the field work many soil samples of such areas were very light, highly mixed with organic and turf-like matters in which matted roots, grass and leaves remnants were found.

The soil texture classes were used to derive the soil matric potential in water cm (section 4.3.2.). The variogram of the results is shown in Figure 41. As it is seen in the figure, Nugget model was fitted

on the variogram which indicates the lack of spatial structure. Therefore, the average matric potential was used for the mapping.

The mentioned mapped soil properties were used as input for the modelling though they were heavily influenced by the sampling scheme and small number of samples in some cases.

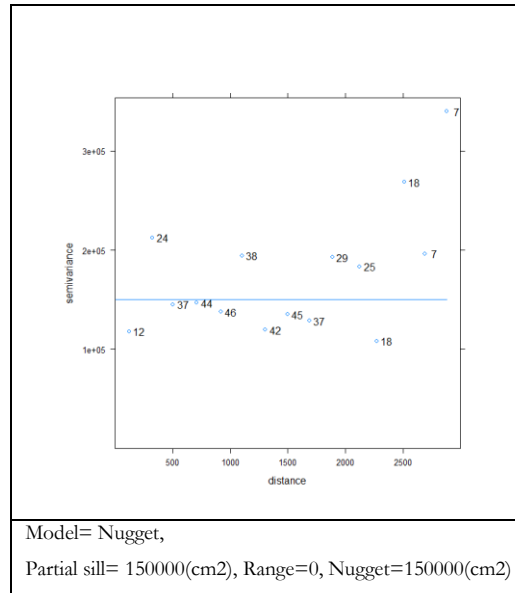


Figure 41. variogram of the soil matric potential

5.3. The LISEM output Analysis

5.3.1. The effect of different soil thickness interpolation methods on hydrograph

Since, no Kriging could be done on Ks, only Soil depth (thickness) maps spatial variations effect on hydrographs were compared.

Figure 42 shows modelled discharge hydrographs produced by applying two soil depth (thickness) maps and different rainfall scenarios. The applied maps were named “sdok” and “sdrk” which stand for ordinary kriging and regression kriging of soil depth, respectively.

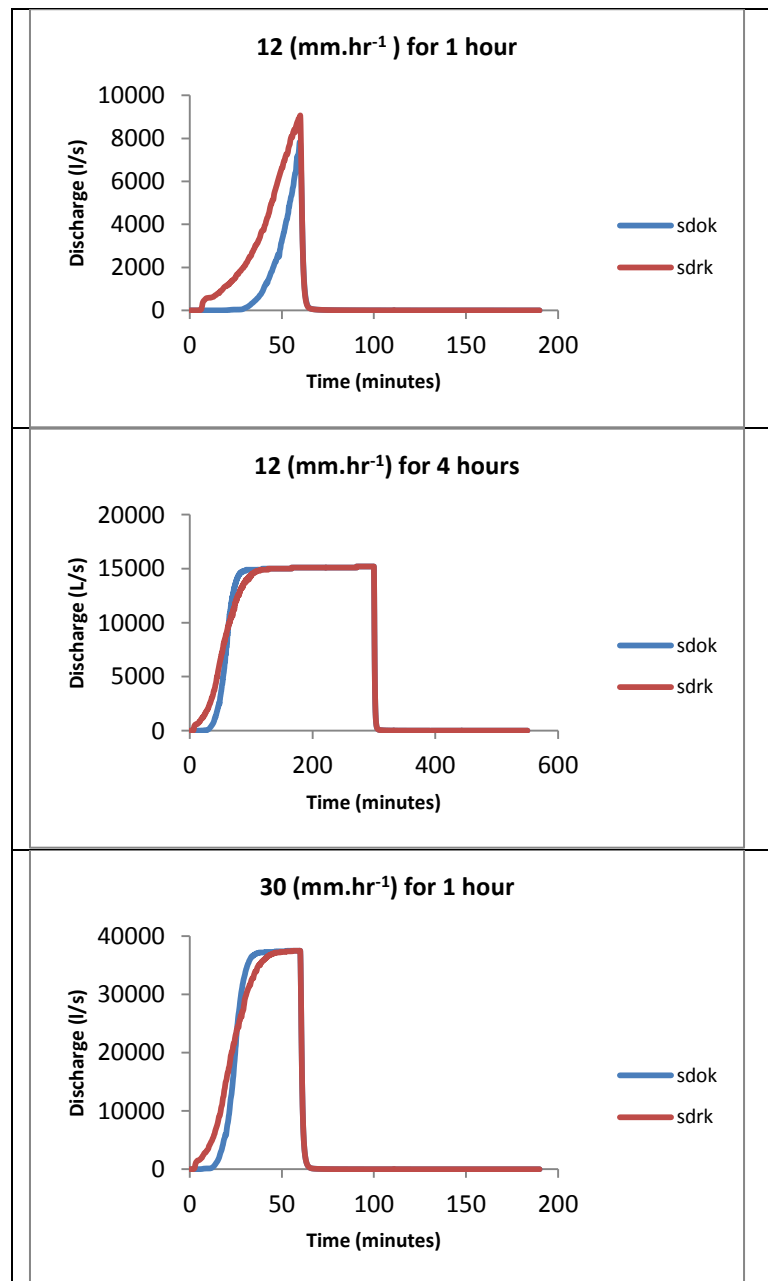


Figure 42. Hydrographs resulted from application of soil thickness OK and RK at 3 rainfall scenarios

According to Figure 42, in the beginning of rainfall, the “sdrk” hydrographs have more discharge than the “sdok”, while at peak the differences reduce. In table 6 the hydrographs characteristics are shown. Based on the table, at scenario (A) where rainfall intensity and duration is the least, the “sdrk” hydrograph has more discharge peak than that of “sdok”. As the rainfall duration increases at scenario (B), the peaks of discharge become equal and at scenario (C) where the rainfall intensity is the most, the discharge peak of the “sdok” is more than that of “sdrk”. Also, the table indicates that the peak times don’t differ much at the three rainfall scenarios but the total discharges are different. At the three rainfall scenarios, the “sdrk” produced more total discharge than “sdok”. As rainfall intensity or duration increases, the total discharge differences decrease.

(A) :rainfall scenario=12 (mm.hr⁻¹) for 1 hour		
<i>soil depth interpolation method</i>	<i>sdok</i>	<i>sdrk</i>
peak time (min)	59.6	60
total discharge (m3)	5359	11793
Discharge peak (l/s)	7827	9073
(B) :rainfall scenario=12 (mm.hr⁻¹) for 4 hours		
<i>soil depth interpolation method</i>	<i>sdok</i>	<i>sdrk</i>
peak time (min)	299.8	299.8
total discharge (m3)	219123	222643
Discharge peak (l/s)	15162	15162
(C) :rainfall scenario=30 (mm.hr⁻¹) for 1 hour		
<i>soil depth interpolation method</i>	<i>sdok</i>	<i>sdrk</i>
peak time (min)	59.8	60
total discharge (m3)	83018	86538
Discharge peak (l/s)	37549	37533

Table 6. Hydrographs characteristics resulted from different interpolation methods at different rainfall scenarios; Note: ordinary kriging of soil depth is shown as “sdok” and regression kriging of soil depth shown as “sdrk”.

The hydrographs means at each rainfall scenario were compared by the Mann Whitney U test (Wilcox test). The reason to use the Wilcox test instead of t-test, was lack of normal distribution in hydrographs (Bhattacharjya. 2004). The test results revealed that at scenario (A), the means of the hydrographs are significantly different at 95 % confidence interval. The hydrographs means have no significant difference at scenarios (B) and (C).

The hydrologic differences that the soil thickness maps caused could be related to dissimilarity of soil thickness spatial variations which brings about various total soil volumes as such. Figure 43, illustrates total soil volume of the two soil thickness maps. According to the figure, the “sdrk” has less soil volume than “sdok”. This means that the “sdrk” has less infiltration capacity for water which increases the saturation overland flow. The peak discharge behaviour at scenario (A) confirms the saturation overland flow differences. At scenarios (B) and (C), both “sdrk” and “sdok” have probably

reached near the saturation level at the peak time; hence, the soil thickness differences have no effect on water infiltration and the peak discharges are equal or marginally different.

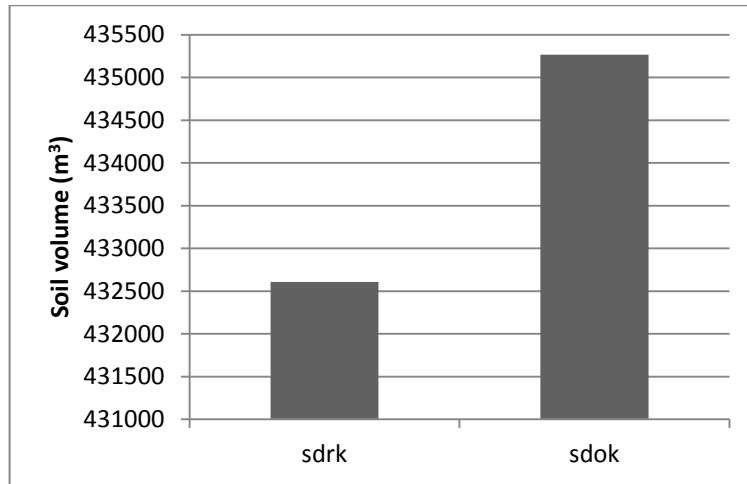


Figure 43. Comparison of the two soil depth maps total soil volume; Note: *sdok*= soil depth map produced by the OK; *sdrk*= soil depth map produced by the RK

5.3.2. The effect of different simulated fields on the resultant hydrographs

Since, RK produced more accurate map than OK, the RK simulation was used in this part. Three simulated fields of the soil depth (thickness) were selected and applied to the LISEM modelling at the three rainfall scenarios. The modelled hydrographs are illustrated in Figure 44. The 4th, 10th and 30th simulated fields are shown as “sdrk4”, “sdrk10” and “sdrk30”, respectively.

Table 7 shows the hydrographs characteristics resulted from soil depth simulated fields at the three rainfall scenarios.

(A): Scenario of 12 (mm.hr⁻¹) rain for 1 hour	<i>sdrk4</i>	<i>sdrk10</i>	<i>sdrk30</i>
Discharge peak (L/s)	8417	8179	9405
peak time (min)	60	60	60
total discharge (m3)	13431	13438	16402
(B): Scenario of 12 (mm.hr⁻¹) rain for 4 hours	<i>sdrk4</i>	<i>sdrk10</i>	<i>sdrk30</i>
Discharge peak (L/s)	15162	15162	15162
peak time (min)	299.8	299.8	299.8
total discharge (m3)	222559	221474	226143
(C): Scenario of 30 (mm.hr⁻¹) rain for 1 hour	<i>sdrk4</i>	<i>sdrk10</i>	<i>sdrk30</i>
Discharge peak (L/s)	37516	37495	37510
peak time (min)	60	60	60
total discharge (m3)	86457	85374	90046

Table 7. Hydrographs characteristics resulted from simulated fields of soil thickness at three rainfall scenarios

The hydrographs means at the three rainfall scenarios were compared by the Wilcox test. According to test results, the hydrographs means of the scenario (A) are significantly different at 95 %

confidence interval while the means of hydrographs at scenarios (B) and (C), have no significant difference.

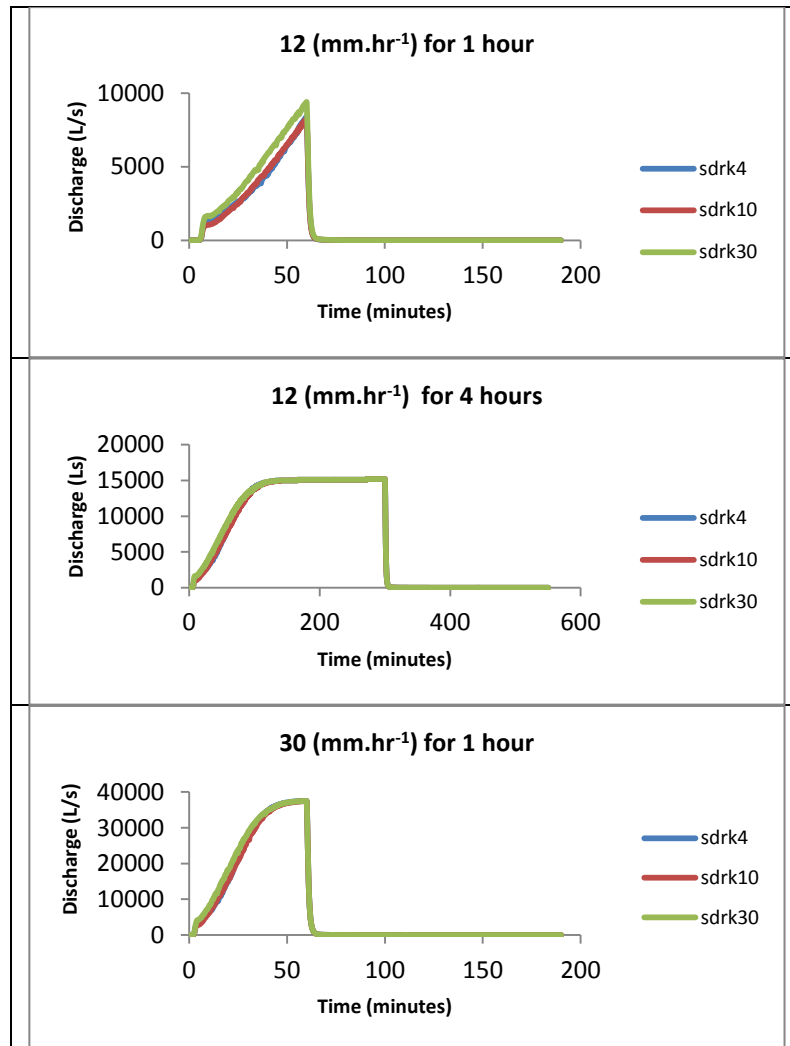


Figure 44. Hydrographs resulted from application of soil depth RK simulations

Based on Table 7 and Figure 44, the “sdrk30” produced the most discharge at the three rainfall scenarios. At scenario (A) where the rainfall intensity is the lowest, the “sdrk30” caused the highest peak of discharge. At scenarios (B) and (C) where rainfall duration and intensity increased respectively, the discharge peaks differences reduced.

The variations of the hydrographs characteristics could be related to the soil volume differences caused by the simulated fields. Figure 45 shows the total soil volumes of the three simulated fields. The “sdrk30” has the lowest and “sdrk4” the highest soil volume. Consequently, the “sdrk30” produced the most and “sdrk4” the least saturation overland flow at scenario (A). At scenarios (B) and (C), the near saturation point might be reached which resulted in reduction of soil thickness effect on saturation overland flow generation.

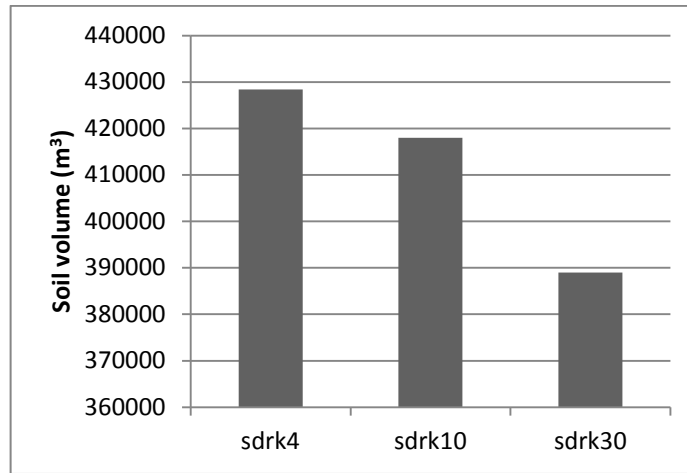


Figure 45. Total soil volumes of the simulated fields

5.3.3. Comparison of RK, OK and simulated fields in hydrograph modelling

In table below, the hydrographs characteristics resulted from RK, OK and RK simulated fields, are brought up. The peak time at the three rainfall scenarios are nearly equal. At scenario (A), the discharge peaks and total discharges resulted from OK, RK and simulated fields, are mainly different while at scenarios (B) and (C), the differences largely reduce.

(A) :12(mm.hr⁻¹) for 1 hour	sdok	sdrk	sdrk4	sdrk10	sdrk30
peak time (min)	59.6	60	60	60	60
discharge peak (l/s)	7827	9073	8417	8179	9405
total discharge (m ³)	5359	11793	13431	13438	16402
(B):12(mm.hr⁻¹) for 4 hours	sdok	sdrk	sdrk4	sdrk10	sdrk30
peak time (min)	299.8	299.8	299.8	299.8	299.8
discharge peak (l/s)	15162	15162	15162	15162	15162
total discharge (m ³)	219123	222643	222559	221474	226143
(C):30(mm.hr⁻¹) for 1 hour	sdok	sdrk	sdrk4	sdrk10	sdrk30
peak time (min)	59.8	60	60	60	60
discharge peak (l/s)	37549	37533	37516	37495	37510
total discharge (m ³)	83018	86538	86457	85374	90046

Table 8. Comparison of hydrographs resulted from RK, OK and simulated fields

The Wilcox test results also say that the means of hydrographs produced by OK, RK and simulated fields are significantly different at scenario (A) while at scenarios (B) and (C), there is no significant difference between the means of the hydrographs.

As a whole, various spatial patterns of soil thickness have no significant effect on hydrograph modelling at rainfalls of high intensity and/or long duration.

6. CONCLUSIONS

In this part, based on the results, the research questions with corresponding answers are brought as the conclusions:

- 1- How well can the land cover types, lithologic units and the terrain parameters of the area (including the elevation, LS factor, slope, aspect, wetness index, overland flow distance to channel network, plan- profile curvature and convergence), or their combinations predict the soil thickness and saturated hydraulic conductivity?

None of the environmental variables in question are good predictors for the Ks. This result contradicts the findings of Herbst et al., (2006) which say relative elevation and slope significantly predict the Ks. The contradictory result in this case may be caused by very short range variability of Ks which was not averaged out by repeated measurements.

The additive linear model of land cover and terrain parameter of overland flow distance to channel network, satisfactorily predicted the soil thickness; this confirms the results of Kuriakose et al., (2009) in which using variable of land cover and land use (i.e., anthropogenic land cover) along with elevation, slope and aspect could best predict the soil thickness. The land cover effect could be discussed by the plants role in soil genesis (Jenny 1941) and soil protection (Foth 1984). The plants roots excrete acidic materials and provide environment for micro organisms to accelerate weathering. Plant litter accumulation and decomposition has also effect on soil thickness. The topography has also one of the important roles in soil genesis as well as soil erosion and accumulation (Jenny 1941; Foth 1984; Milevski 2007), so that thicker soils would be expected in lower elevations and gentler slopes which have concave curvature. However in different studies different terrain parameters have been found as soil thickness explanatory variable, for example, Herbst et al.,(2006) reported that tertiary morphometric parameter of slope elements has the highest correlation with the soil thickness while Kuriakose et al., (2009) and the present study found other terrain parameters. In the present study the minor effect of overland flow distance to channel network may be a proxy for soil thickness prediction. This terrain parameter could be representative for the effect of slope and curvature on soil thickness.

- 2- Is a regression kriging with one or more of the above –mentioned environmental variables, able to satisfactorily predict spatial variation in soil thickness and hydraulic conductivity?

The Regression Kriging of soil thickness by the “Land cover” and “overland flow distance to channel network” variables have better and more accurate results than the Ordinary Kriging. This finding is compatible with that of Kuriakose et al., (2009). The RK prediction was however fairly uncertain (RMSE 60 mm, over half the median thickness 107 mm, see Fig. 14), and away from sample points the kriging prediction variance and standard deviation was of the same order of magnitude, about 500 (mm²) and 22 mm, respectively (Fig. 32). This uncertainty is expected to have a major effect on any model sensitive to soil thickness. The reason for the high uncertainty is few points and poor spatial structure with high nugget effect.

Neither the Regression Kriging nor the Ordinary Kriging could be used for the Ks prediction; because there was no identifiable local spatial dependence. This goes further than the previous answer (Ks not dependent on environmental predictors), showing that with this sample, nearby observations are no more similar than randomly-distributed ones. The physical cause of this may be internal processes such as biologic activities occur in soil which causes close by variations.

Kuriakose et al., (2010) also reported due to high variability of Ks, poor performance of the kriging could be done.

- 3- Does the modelled hydrologic response to a rainfall event at the catchment outlet, change with different interpolation methods of soil thickness?

Depending on rainfall intensity and duration, the hydrologic responses differ. At rainfall of low intensity and/or short duration, various spatial patterns of soil thickness result in significantly different hydrographs. As the intensity or duration of rainfall increases, the hydrographs differences lessen so that they can become insignificant; this is because at rainfalls of short duration or low intensity, the soil may not reach near saturation level, hence, shallower soils are saturated faster and produce more runoff than the deeper soils. But at higher intensity or duration of rainfall, all soils may have reached the saturation; therefore, the soil thickness variations make no more differences in the runoff generation.

- 4- How much do simulated fields vary in their runoff predictions?

Each simulated field gives a different realization of soil thickness and soil volume. Therefore, runoff hydrographs modelled by various simulated fields of soil thickness are different as long as the near saturation point is not reached. As the soil saturation occurs by rainfalls having either long duration or high intensity, the simulated fields' variation effects become less.

The infiltration capacity, determined by soil thickness, porosity and initial soil moisture, does influence the LISEM model results. As De Roo et al.,(1999) found the LISEM sensitive to initial soil moisture content, the present study, found out that the LISEM was sensitive to the soil thickness variations when soil is not saturated. When soil reaches saturated level, the LISEM is no more sensitive to the soil thickness variations and the simulated hydrographs are not largely different.

As a whole, using various interpolation methods of soil thickness does not make differences in runoff simulation when it is based on rainfalls of high intensity and/or long duration. Therefore, using simple methods of interpolation could be sufficient.

According to the conclusions and the study deficiencies, the following recommendations can be taken into consideration for further studies:

- 1- In the present study, the combination of land cover class and overland flow distance to channel network was found to predict the soil depth satisfactorily. This should be worked out in other catchments with different climatic situations in order to examine the climatic parameters applicability as covariables of the soil depth prediction. Since, rainfall is important parameter in soil erosion, it will be interesting to see the variations of rainfall at different elevations of a catchment and scrutinize the rainfall variation effect on the soil depth prediction. Unfortunately due to lack of such climatic data in the study area, the rainfall variation effect could not be examined.
- 2- The Ks could not be predicted by any of the environmental variables. This can be tested at other catchments as well.

There are pedotransfer functions which can predict the Ks (Saxton 1986; Wosten 2001; Saxton 2006) by using parameters such as Organic carbon, texture etc. The functions can be calibrated at the catchment of study, then the relationship of the environmental variables with the parameters be investigated. In case of having acceptable mathematical relationship, the best environmental variables may be used as predictors in the pedotransfer functions.

- 3- The high variability of Ks caused not to have good variogram for this soil property. Box-Cox transformation resulted in good variogram for the Ks but due to lack of time no proper method for the Kriging results back transformation could be found. As the Ks variations are very much important in the hydrologic modelling (refer to 3.2.2.), It is suggested to continue this work in order to use the available Ks data in making ordinarily kriged Ks map. Then, the effect of Ks simulation and different interpolation methods on the hydrograph characteristics will be interesting subject to look into.
- 4- Due to the data base problems, no calibration on the LISEM model results could be done, but it is highly advised to see how close the modelled hydrographs are to the measured hydrograph. For this, the rainfall at different elevations of the catchment as well as the discharge at the outlet should be measured. It is also recommended to study the hydrology of Faucon and the base flow sources. Having more information of the catchment hydrology will be helpful in the runoff ratio analysis and end up better modelling and the calibration.
- 5- As the runoff and soil properties are important factors in soil erosion, the same study can be used for erosion and gully option of the LISEM and see how the soil properties spatial variations may affect soil erosion prediction. Also, the sensitivity of gullies spatial variations to the soil properties interpolations could be an interesting subject.
- 6- The same study can be done by using other hydrologic models such as AvSWAT so as to find out how sensitive various hydrologic models results are to the soil properties spatial variations.

LIST OF REFERENCES

- Arcement, G. J., Jr., V.R., Schneider, USGS, (2010). "Guide for Selecting Manning's Roughness Coefficients for Natural Channels and Flood Plains, United States Geological Survey Water-supply Paper 2339, Metric version." Retrieved on October 14th 2010, from <http://www.fhwa.dot.gov/BRIDGE/wsp2339.pdf>.
- Bagarello, V., S. Sferlazza, et al. (2009). "Comparing two methods of analysis of single-ring infiltrometer data for a sandy-loam soil." *Geoderma* **149**(3-4): 415-420.
- Bhattacharjya, R. K. (2004). "Optimal design of unit hydrographs using probability distribution and genetic algorithms." *Sadhana* **29**, part 5: 499-508.
- Bivand, R. S., Edzer J., Pebesma, Birgilio Gomez-Rubio (2008). "Applied Spatial Data Analysis with R." Springer.
- Chiles, J.-P., Pierre, Delfiner, (1999). "Geostatistics: Modeling Spatial Uncertainty." *John Wiley and Sons, Inc.*
- Cimmery, V. (2010). "User Guide for SAGA (version 2.0.5)." Retrieved on January 16th 2011 from : <http://www.saga-gis.org/en/about/references.html> **volume 1 and 2.**
- De Roo, A. P. J. (1996a). "the LISEM project: An Introduction." *Hydrological Processes* **10**: 1021-1025.
- De Roo, A. P. J., R.J.E., Offermans, N.H.D.T., Cremers (1996). "LISEM: A single-event physically based hydrological and soil erosion model for drainage basins.II: Sensitivity analysis, validation and application." *Hydrological processes* **10**: 1119-1126.
- De Roo, A. P. J., V.G., Jetten, (1999). "Calibrating and validating the LISEM model for two data sets from the Netherlands and South Africa." *Catena* **37**: 477-493.
- Dietrich, W. E., Reiss, R., Hsu, M.-L, Montgomery, D.R., (1995). "A process-based model for colluvial soil depth and shallow landsliding using digital elevation data." *Hydrological processes* **9**: 383-400
- FAO (2006). "Guidelines for soil description." *Food and Agriculture Organization of the United Nations 4th Edition.*
- Farrell, Z. (2010). "Single Ring Falling Head Infiltrometer." Retrieved on October 2010: <http://www.usyd.edu.au/agric/web04/Single%20ring%20final.htm>.
- Ferrer Julià, M., Estrela Monreal, T., Sánchez del Corral Jiménez, A., García Meléndez, E. (2004). "Constructing a saturated hydraulic conductivity map of Spain using pedotransfer functions and spatial prediction." *Geoderma* **123**(3-4): 257-277.
- Flageollet, J.-C., O. Maquaire, et al. (1999). "Landslides and climatic conditions in the Barcelonnette and Vars basins (Southern French Alps, France)." *Geomorphology* **30**(1-2): 65-78.
- Florinsky, I. V., R. G. Eilers, et al. (2002). "Prediction of soil properties by digital terrain modelling." *Environmental Modelling & Software* **17**(3): 295-311.
- Foth, H. D. (1984). "Fundamentals of Soil Sciences." *John Wiley and Sons, Inc. Seventh Edition.*
- Goovaerts, P. (2000). "Estimation or simulation of soil properties? An optimization problem with conflicting criteria." *Geoderma* **97**(3-4): 165-186.
- Goovaerts, P. (2000). "Geostatistical approaches for incorporating elevation into the spatial interpolation of rainfall." *Journal of Hydrology* **228**(1-2): 113-129.
- Goovaerts, P. (2001). "Geostatistical modelling of uncertainty in soil science." *Geoderma* **103**(1-2): 3-26.
- Govers, G. (1990). "Empirical Relationships for the Transport Capacity of Overland Flow." *IAHS Publication* **189**: 45-63.
- Grayson, R., Bloschl, G. (Eds) (2001). "Spatial Patterns in Catchment Hydrology; Observations and Modeling." *University Press, Cambridge*: 404.
- Herbst, M., B. Diekkrüger, et al. (2006). "Numerical experiments on the sensitivity of runoff generation to the spatial variation of soil hydraulic properties." *Journal of Hydrology* **326**(1-4): 43-58.
- Herbst, M., B. Diekkrüger, et al. (2006). "Geostatistical co-regionalization of soil hydraulic properties in a micro-scale catchment using terrain attributes." *Geoderma* **132**(1-2): 206-221.
- Herbst, M., Prolingheuer, N., Graf, A., Huisman, J. A., Weihermüller, L., Vanderborght, J., Vereecken, H. (2009). "Multivariate conditional stochastic simulation of soil heterotrophic respiration at plot scale." *Geoderma In Press, Corrected Proof.*
- Hessel, R. (2005). "Effects of grid cell size and time step length on simulation results of the Limburg soil erosion model (LISEM)." *Hydrological processes* **19**: 3037-3049.
- Hessel, R., V. Jetten, et al. (2003). "Calibration of the LISEM model for a small Loess Plateau catchment." *CATENA* **54**(1-2): 235-254.
- Hosein, T. (2010). "Alluvial Fan Flood Hazard Assessment based on DTM Uncertainty." *MSc Thesis, ITC, Enschede.*

- Jenny, H. (1941). "Factors of Soil Formation, a system of Quantitative Pedology." McGraw-Hill, New York, NY.
- Jetten, V., Menno, Straatsma, Dinand, Alkema (2010). "Spatial Modelling of Natural Hazard processes, GH Module 8." ESA Department, ITC, Enschede.
- Jetten, V. G. (2002). "LISEM user manual." Utrecht center for Environment and Landscape Dynamics, Utrecht University, The Netherlands.
- Jetten, V. G. (2002). "LISEM user manual." Utrecht center for Environment and Landscape Dynamics, Utrecht University, The Netherlands.
- Kuriakose, S. L. (2010). "Physically-based dynamic modelling of the effect of land use changes on shallow land slide initiation in the western Ghats of Kerala, India." Ph.D. Thesis. University of Twente (ITC) and University of Utrecht (Faculty of Geosciences), Enschede.
- Kuriakose, S. L., Sanjaya Devotka, D.G. Rossiter, V.G. Jetten (2009). "Prediction of soil depth using environmental variables in an anthropogenic landscape, a case study in the Western Ghats of Kerala, India." CATENA 79(1): 27-38.
- Kutilek, M., Donald R., Nielsen, (1994). "Soil Hydrology." CATENA VERLAG GeoEcology publications.
- Malet, J.-P., Alexander, Remaitre, Olivier, Maquaire, (2004). "Runout modeling and extension of the threatened area associated with muddy debris flows." Geomorphologie: relief, processus, environment 10 N0 3: 195-209.
- Matheron, G. (1963). "Principles of geostatistics." Economic Geology 58: 1246-1266.
- McBratney, A. B., M. L. Mendonça Santos, et al. (2003). "On digital soil mapping." Geoderma 117(1-2): 3-52.
- McKenzie, N. J. and M. P. Austin (1993). "A quantitative Australian approach to medium and small scale surveys based on soil stratigraphy and environmental correlation." Geoderma 57(4): 329-355.
- McKenzie, N. J. and P. J. Ryan (1999). "Spatial prediction of soil properties using environmental correlation." Geoderma 89(1-2): 67-94.
- Merz, B., András Bárdossy, (1998). "Effects of spatial variability on the rainfall runoff process in a small loess catchment." Journal of Hydrology 212-213: 304-317.
- Milevski, I. (2007). "Morphometric elements of terrain morphology in the Republic of Macedonia and their influence on soil erosion." International Conference; Erosion and Torrent Control as a Factor in Sustainable River Basin Management.
- Minasny, B., McBratney, A.B., (1999). "A rudimentary mechanistic model for soil production and landscape development." Geoderma 90: 3-21.
- Mountain Risks (2010). "the Faucon watershed: the 2003 debris-flow even (part 1)." Retireved on 17 August 2010, from http://www.unicaen.fr/mountainrisks/spip/IMG/pdf/13_Faucon_pit_stop_1.pdf.
- Mwendera, E. J. and J. Feyen (1992). "Estimation of depression storage and Manning's resistance coefficient from random roughness measurements." Geoderma 52(3-4): 235-250.
- Neitsch, S. L., J.G. Arnold, J.R. Kiniry, J.R. Williams, K.W. King (2002). "Soil and Water Assessment Tool theoretical documentation." Texas Water Resources Institute, Colledge Station, Texas. TWRI Report, TR- 191.
- Odeh, I. O. A., A.B. McBratney , D.J.Chittleborough (1995). "Further results on prediction of soil properties from terrain attributes: heterotopic cokriging and regression-kriging." Geoderma 67(3-4): 215-226.
- OMIV-EOST (2010). "Barcelonnette area, Debris flows at Faucon. Services des Observatoires des instabilites de Versants. ." Retireved on 17 August 2010, from http://eost.u-strasbg.fr/omiv/barcelo_area_faucon.html.
- Prachansri, S. (2007). "Analysis of soil and land cover parameters for flood hazard assessment : a case study of the Nam Chun watershed, Phetchabun, Thailand. ." MSc Thesis, ITC, Enschede.
- Remaitre, A., J.P. Malet, et al., (2005). "Morphology and Sedimentology of a complex Debris Flow in a Clay-shale Basin." Earth surface processes and landforms: The Journal of the British Geomorphological Research Group 30(3): 339-348.
- Remaitre, A., J.P., Malet, et al., (2005). "Morphology and Sedimentology of a complex Debris Flow in a clay-shale basin. Earth surface processes and landforms." The Journal of British Geomorphological Research Group 30(3): 339-348.
- Renard, K. G., Foster, G.R., Weesies, G.A., McCool, D.K., Yoder, D.D., (2000). "Predicting Soil Erosion by Water: A Guide to Conservation Planning with the Revised Universal Soil Loss Equation (RUSLE)." The U.S. Department of Agriculture (USDA), Washington D.C.

- Reynolds, W. D., D.E., Elrick (1990). "Ponded Infiltration From a Single Ring: I. Analysis of Steady Flow." *Soil Science Society of America* **54**.
- Sakia, R. M. (1992). "The Box-Cox transformation technique: a review." *the Statistician* **41**: 169-178.
- Saxton, K., W.J., Rawls (2006). "Soil water characteristic estimates by texture and organic matter for hydrologic solutions." *Soil Science Society of America* **70**: 1569-1578.
- Saxton, K. E., W.J., Rawls, J.S., Romberger, R.I., Papendick (1986). "Estimating Generalized Soil-water Characteristics from texture." *Soil Science Society of America* **50**:1031-1036.
- Singh, V. P. (1997). "Effect of Spatial and temporal variability in rainfall and watershed characteristics on stream flow hydrology." *Hydrological processes* **11**: 1649-1669.
- USDA (2007). "Part 630 Hydrology, National Engineering Handbook." Retrieved on February 2011 from : <http://directives.sc.egov.usda.gov/OpenNonWebContent.aspx?content=17757.wba>.
- USDA (2010). "Determining Soil Texture by Feel Method Handout." Retrieved on 17 October, 2010, from http://www.mt.nrcs.usda.gov/about/lessons/Lessons_Soil/feelmethod.html.
- Warrick, A. W. and Nielsen D.R. (1980). "Spatial variability of soil physical properties in the field. In: Hillel, D. (Ed.) Application of Soil physics." *Academic Press, New York*: 319-344.
- Webster, R., and M., A.Oliver (2007). "Geostatistics for Environmental Scientists." *John Wiley and Sons, Ltd 2nd Edition*.
- Wosten, J. H. M., Ya.A., Pachepsky, W.J., Rawls (2001). "Pedotransfer functions: bridging the gap between available basic soil data and missing soil hydraulic characteristics." *Journal of Hydrology* **251**: 123-150.
- Yamamoto, J. (2005). "Correcting the Smoothing Effect of Ordinary Kriging Estimates." *Mathematical Geology* **37**(1): 69-94.
- Zhu, A. X. and D. S. Mackay (2001). "Effects of spatial detail of soil information on watershed modeling." *Journal of Hydrology* **248**(1-4): 54-77.
- Ziadat, F. M. (2010). "Prediction of Soil Depth from Digital Terrain Data by Integrating Statistical and Visual Approaches." *Pedosphere* **20**(3): 361-367.

APPENDIX I : TABLES OF APPLIED DATA

1. Table of the field observation records

Sample No.	X_UTM (m)	Y_UTM (m)	Soil thickness (cm)	Stoniness %	texture	landuse	ground cover fraction by plant	Remarks
1	314513	4919658	18	20%	sandy-loam	grass	1	
2	314924	4920124	9.5	15%	sandy-loam	grass	1	
3	314437	4919675	8.9	90%	silty loam	forest	0.6	
4	314513	4920658	7.8	50%	silty loam	forest	0.1	trees 6 m high
5	314759	4921082	8	10%	silty loam	forest	1	
6	313444	4921603	11	5%	Loam	grass	0.9	
7	313973	4921006	10.5	100%	clay loam	debrs flow	0	
8	313924	4921165	4	50%	loam	forest	1	tree 10 m high
9	314239	4921014	15	5%	silty loam	forest	1	tree 12 m high
10	314631	4921063	22.4	90%	silty loam	forest	1	
11	313827	4921111	6.5	50%	Loam	forest	0.5	on screes and debris flow
12	313432	4921124	23	50%	silty loam	forest	0.8	trees 10m high
13	313348	4920658	15.2	5%	clay loam	grass	1	
14	313184	4921343	8.4	10%	clay loam	forest	1	humus 2 cm
15	313930	4919788	17.5	5%	clay loam	grass	1	
16	313718	4920726	11.5	60%	clay loam	grass	0.8	
17	314704	4919439	16.7	60%	Loam	grass	0.9	
18	313710	4919802	8.5	60%	Loam	forest	0.5	trees 6 m high and sparse
19	314088	4919450	9	50%	silty loam	grass	0.8	
20	315471	4919987	18.8	2%	sandy-loam	forest	0.5	trees 15 m high
21	314784	4920576	15	10%	sandy-loam	forest	0.5	trees 10 m high
22	314862	4920342	11.2	0%	silty loam	grass	1	
23	313483	4921663	10	80%	silty loam	forest	0.6	trees 6 m high and sparse
24	313388	4921520	14.2	80%	sandy-loam	grass	0.6	high organic matter
25	313367	4920870	16.4	2%	silty loam	grass	0.9	
26	313801	4920757	14.4	50%	silty loam	forest	0.8	trees 10m high
27	315438	4919489	18.2	30%	silty clay loam	grass	0.6	
28	315241	4919008	12	5%	silty loam	forest	0.5	trees 15 m high
29	314389	4918959	9.6	10%	sandy-loam	forest	1	trees 5 m high sparse
30	314800	4919545	20.4	90%	silty clay loam	forest	0.3	trees 15 m high
31	313310	4921620	15	100%	silty loam	grass	0.4	

2. Example of one the Infiltration measurement sheets

time intervals(s)	infiltration(cm)	Cumulative time(s)	cumulative infiltration(cm)
15	0.5	0	0
15	0	15	0.5
15	0.1	30	0.5
15	0.1	45	0.6
15	0.3	60	0.7
15	0.1	75	1
15	0.3	90	1.1
15	0.1	105	1.4
30	0.5	120	1.5
30	0.4	150	2
30	0.5	180	2.4
30	0.2	210	2.9
30	0.4	240	3.1
30	0.1	270	3.5
45	0.8	300	3.6
45	0.2	345	4.4
45	0.7	390	4.6
60	0.8	450	5.3
60	0.5	510	6.1
60	0.9	570	6.6
		630	7.5

3. Table of measured Ks (the results of the present and previous study)

Note: X and Y are UTM coordinates of sampled points in meters.

X	Y	Ks (mm/hr)	X	Y	Ks (mm/hr)
315120	4919300	28.7	314923	4920124	84.1
313833	4920867	286.6	314513	4919658	25.6
313729	4920638	1579	313444	4921603	12.5
315014	4919407	188.1	313924	4921165	138
315115	4918970	335.8	314239	4921014	17.5
314861	4920020	310	314631	4921063	167.2
315146	4919761	9.4	313827	4921111	152
313717	4920109	47.4	313432	4921124	11
314675	4920035	37.2	313470	4920873	3.2
314465	4920370	367.8	313184	4921343	3.8
315130	4919300	39.9	313930	4919788	4.2
313722	4920558	268.7	313718	4920726	3.6
314945	4919239	90	314704	4919439	20.4
314350	4919739	319	313710	4919802	19.6
315024	4919407	133.6	314088	4919450	17.6
314497	4920512	548	315471	4919987	237
315107	4919049	186.7	314784	4920576	146
315080	4919349	519	314862	4920342	6.2
314423	4920312	141.6	313483	4921663	30.9
315227	4920440	597	313388	4921520	24.7
315224	4919193	191	313367	4920870	24
313935	4919684	149	313801	4920757	24.8
314243	4919058	1033	315438	4919489	2.8
314871	4919923	72	315241	4919008	104
314921	4920416	40	314389	4918959	202
314362	4919969	36.5	314800	4919545	3.5
315019	4919111	82.8	313310	4921620	5.7
314513	4920658	23.9	315609	4919430	0
314759	4921082	417.8	314813	4919109	0
314437	4919675	1.9	314085	4921495	0
314923	4920124	84.1	313442	4921929	0
314513	4919658	25.6	313833	4922559	0
313444	4921603	12.5	313472	4922676	0
313924	4921165	138	313666	4922920	0

4. Average soil thickness and variances; Note 1: these points are related to the present study; Note 2: the corresponding coordinates of each sample No. can be found at table 1 of the appendix.

sample No.	Average soil thickness(mm)	Variance (mm ²)
1	176.7	36.2
2	95.0	46.8
3	89.5	14.8
4	78.3	22.5
5	80.0	10.0
6	111.7	24.7
7	105.0	35.4
8	40.0	0.0
9	150.0	17.3
10	223.3	20.8
11	65.0	35.4
12	230.0	56.6
13	151.7	22.5
14	83.3	18.9
15	175.0	63.6
16	115.0	7.1
17	166.7	41.6
18	85.0	0.0
19	90.0	14.1
20	188.3	62.1
21	150.0	0.0
22	112.5	43.3
23	100.0	0.0
24	142.5	17.7
25	163.3	77.7
26	143.3	40.4
27	181.7	109.1
28	120.0	72.1
29	96.7	28.9
30	203.3	95.0
31	150.0	0.0

5. Soil data after laboratory analysis (x and y are UTM coordinates of sampled points in meters); Note: initial soil moisture equals the Field Capacity (F.C.) moisture

x	y	porosity	initial soil moisture	Bulk density (g/cm³)
314513	4919658	0.44	0.22	1.13
314924	4920124	0.58	0.29	1.17
314437	4919675	0.85	0.33	1.2
314513	4920658	0.47	0.23	0.45
314759	4921082	0.90	0.45	0.33
313444	4921603	0.71	0.34	0.69
313973	4921006	0.39	0.19	1.74
313924	4921165	0.85	0.39	0.12
314239	4921014	0.69	0.34	1.07
314631	4921063	0.76	0.38	0.15
313827	4921111	0.75	0.38	0.26
313432	4921124	0.70	0.35	0.56
313348	4920658	0.78	0.44	0.67
313184	4921343	0.69	0.34	1.29
313930	4919788	0.85	0.43	0.72
313718	4920726	0.65	0.33	0.8
314704	4919439	0.63	0.32	1.04
313710	4919802	0.74	0.64	0.44
314088	4919450	0.86	0.43	1.16
315471	4919987	0.53	0.44	1
314784	4920576	0.78	0.34	0.67
314862	4920342	0.59	0.29	0.72
313483	4921663	0.75	0.37	1.21
313388	4921520	0.78	0.39	0.45
313367	4920870	0.71	0.54	1.14
313801	4920757	0.85	0.65	0.59
315438	4919489	0.54	0.40	1.29
315241	4919008	0.36	0.17	1.34
314389	4918959	0.64	0.32	0.65
314800	4919545	0.44	0.30	1.16
313310	4921620	0.64	0.32	0.97
315120	4919300	0.51		1.5
313833	4920867	0.60	0.50	0.9
313729	4920638	0.52	0.50	1.1
315014	4919407	0.52		1.2
315115	4918970	0.59	0.60	1.1
314861	4920020	0.56	0.20	1.1
315146	4919761	0.59	0.30	1
313717	4920109	0.46	0.30	1.3

x	y	porosity	initial soil moisture	Bulk density (g/cm ³)
314675	4920035	0.49		1.4
314465	4920370	0.65		0.8
315130	4919300	0.48		1.3
313722	4920558	0.62	0.50	0.9
314945	4919239	0.49	0.40	1
314350	4919739	0.70	0.40	1
315024	4919407	0.52		1.2
314497	4920512	0.49	0.20	1.1
315107	4919049	0.54		1.1
315080	4919349	0.51		1.3
314423	4920312	0.64		0.6
315227	4920440	0.59	0.50	0.9
315224	4919193	0.51		1.1
313935	4919684	0.58	0.50	1
314243	4919058	0.38	0.20	1.9
314871	4919923	0.41	0.30	1.5

6. Table of the environmental variables used in linear modelling; Note1: the coordinates indicate the sample point's location where the environmental variables were extracted. Note2: the coordinates are in meter.

UTM X (m)	UTM Y (m)	Land cover	lithology	slope(R)	Aspect(R)
315120	4919300	pastures	moraines	0.31	3.5
313833	4920867	natural grassland	moraines	0.34	1.75
313729	4920638	natural grassland	moraines	0.39	2.39
315014	4919407	pastures	moraines	0.27	2.84
315115	4918970	coniferous forest	weathered marls	0.28	2.36
314861	4920020	pastures	moraines	0.48	3.37
315146	4919761	pastures	moraines	0.35	3.76

UTM X (m)	UTM Y (m)	Land cover	lithology	slope(R)	Aspect(R)
313717	4920109	natural grassland	moraines	0.12	2.73
314675	4920035	pastures	moraines	0.20	3.12
314465	4920370	coniferous forest	moraines	0.16	2.63
315130	4919300	pastures	moraines	0.28	2.95
313722	4920558	coniferous forest	moraines	0.32	2.24
314945	4919239	coniferous forest	moraines	0.59	4.07
314350	4919739	natural grassland	moraines	0.29	1.91
315024	4919407	pastures	moraines	0.32	2.71
314497	4920512	coniferous forest	flyschs	0.32	3
315107	4919049	coniferous forest	weathered marls	0.37	3.3
315080	4919349	pastures	moraines	0.28	3.04
314423	4920312	natural grassland	moraines	0.23	3.53
315227	4920440	natural grassland	flyschs	0.42	4
315224	4919193	coniferous forest	moraines	0.34	3.08
313935	4919684	coniferous forest	moraines	0.22	1.91
314243	4919058	pastures	moraines	0.45	4.02
314871	4919923	coniferous forest	moraines	0.45	2.83
314921	4920416	pastures	moraines	0.13	3.31
314362	4919969	coniferous forest	moraines	0.44	1.56
315019	4919111	coniferous forest	moraines	0.40	3.36
314513	4920658	coniferous forest	flyschs	0.41	3.42
314759	4921082	coniferous forest	flyschs	0.55	4.12
314437	4919675	pastures	moraines	0.32	1.4
314923	4920124	pastures	moraines	0.14	3.61
314513	4919658	pastures	moraines	0.34	1.58
313444	4921603	coniferous forest	moraines	0.50	2.12
313924	4921165	bare rocks	flyschs	0.41	3.77
314239	4921014	coniferous forest	flyschs	0.40	2.8
314631	4921063	coniferous forest	flyschs	0.49	3.56
313827	4921111	coniferous forest	flyschs	0.36	3.9
313432	4921124	coniferous forest	moraines	0.40	2.51
313470	4920873	natural grassland	moraines	0.24	2.39
313184	4921343	natural grassland	moraines	0.41	1.89
313930	4919788	coniferous forest	moraines	0.28	2.04
313718	4920726	natural grassland	moraines	0.24	2.06
314704	4919439	coniferous forest	moraines	0.37	1.45
313710	4919801	coniferous forest	moraines	0.24	3.44
314088	4919450	pastures	moraines	0.35	2.4
315471	4919987	coniferous forest	flyschs	0.65	3.51
314784	4920576	coniferous forest	flyschs	0.51	2.74
314862	4920342	pastures	moraines	0.24	3.53
313483	4921663	coniferous forest	moraines	0.66	1.63
313388	4921520	coniferous forest	moraines	0.38	1.21
313367	4920870	natural grassland	moraines	0.25	1.64

UTM X (m)	UTM Y (m)	Land cover	lithology	slope(R)	Aspect(R)
313801	4920757	natural grassland	moraines	0.30	2.31
315438	4919489	pastures	moraines	0.19	2.68
315241	4919008	coniferous forest	weathered marls	0.12	1.61
314389	4918959	coniferous forest	moraines	0.37	2.76
314800	4919545	coniferous forest	weathered marls	0.31	3.4
313310	4921620	natural grassland	flyschs	0.52	2.58
315609	4919430	broad-leaved forests	weathered marls	0.80	2.12
314813	4919109	broad-leaved forests	weathered marls	0.74	1.79
314085	4921495	bare rocks	scree	0.65	3.35
313442	4921929	bare rocks	scree	0.71	1.9
313833	4922559	bare rocks	flyschs	0.65	3.64
313472	4922676	bare rocks	flyschs	0.56	2.3
313666	4922920	bare rocks	flyschs	0.70	2.64

UTM X (m)	UTM Y (m)	Profile curvature (R/100m)	Plan curvature (R/100m)	Convergence
315120	4919300	-0.005	-0.059	14
313833	4920867	-0.03	0	1
313729	4920638	0.0001	0.028	3
315014	4919407	-0.007	-0.001	-1
315115	4918970	-0.018	-0.0018	-4
314861	4920020	0.0024	0.008	0
315146	4919761	0.018	0.04	0
313717	4920109	-0.0008	-0.001	12
314675	4920035	0.0005	-0.0015	0
314465	4920370	-0.0001	0.0025	12
315130	4919300	0.0003	-0.001	0
313722	4920558	-0.001	0.0001	3
314945	4919239	-0.005	-0.044	-2
314350	4919739	0.0006	-0.004	-5
315024	4919407	0.004	-0.0007	0
314497	4920512	-0.01	0.0001	13
315107	4919049	0.0004	0.007	16
315080	4919349	-0.0036	-0.002	2
314423	4920312	0.008	0.0008	6
315227	4920440	0.002	0.004	7
315224	4919193	-0.002	-0.002	-12
313935	4919684	0.0008	0.0007	7
314243	4919058	-0.003	0.017	4
314871	4919923	-0.03	0.0014	1
314921	4920416	0.0002	-0.028	-2
314362	4919969	0.001	0.001	1
315019	4919111	0.018	0.0038	-3

UTM X (m)	UTM Y (m)	Profile curvature (R/100m)	Plan curvature (R/100m)	Convergence
314513	4920658	0.027	0.0057	0
314759	4921082	-0.04	0.04	5
314437	4919675	-0.001	0.0005	-2
314923	4920124	-0.007	-0.001	2
313444	4921603	0.014	0.0002	0
313924	4921165	0.02	0.002	2
314239	4921014	-0.006	-0.003	-1
314631	4921063	0.04	-0.04	-7
313827	4921111	-0.006	-0.008	-7
313432	4921124	0.0002	0.002	2
313470	4920873	-0.016	-0.014	-40
313184	4921343	-0.004	-0.003	-1
313930	4919788	0.0008	-0.001	5
313718	4920726	-0.0002	-0.001	0
314704	4919439	0.002	-0.0058	0
313710	4919802	0.0004	-0.0029	-12
314088	4919450	-0.005	0.0009	-7
315471	4919987	-0.004	-0.08	0
314784	4920576	-0.0001	0.0004	0
314862	4920342	-0.006	-0.004	2
313483	4921663	-0.002	-0.002	2
313388	4921520	-0.006	-0.005	-7
313367	4920870	0.003	-0.01	-5
313801	4920757	0.0007	-0.024	0
315438	4919489	0.0006	0.067	10
315241	4919008	-0.008	-0.001	6
314389	4918959	0.0002	0.004	0
314800	4919545	-0.013	-0.01	-16
313310	4921620	0.012	-0.0007	-3
315609	4919430	-0.011	0.002	-19
314813	4919109	0.0001	-0.16	-4
314085	4921495	0.04	-0.003	-8
313442	4921929	0.025	0.035	16
313833	4922559	-0.009	0.034	0
313472	4922676	-0.018	0.009	-5
313666	4922920	0.01	-0.003	-4

UTM X (m)	UTM Y (m)	Wetness index	Overland flow distance to channel network (m)	Elevation(m)	LS
315120	4919300	6	21	1393	16
313833	4920867	9	11	1890	97
313729	4920638	7	28	1885	37
315014	4919407	7	20	1428	43
315115	4918970	6	0	1298	305
314861	4920020	6	24	1622	60
315146	4919761	8	26	1522	58
313717	4920109	6	19	1805	3
314675	4920035	6	13	1630	19
314465	4920370	7	0	1722	0
315130	4919300	6	19	1392	20
313722	4920558	8	0	1870	73
314945	4919239	6	0	1376	48
314350	4919739	10	0	1618	88
315024	4919407	6	0	1427	173
314497	4920512	6	40	1741	26
315107	4919049	6	18	1321	61
315080	4919349	10	28	1405	53
314423	4920312	5	10	1714	22
315227	4920440	5	15	1747	30
315224	4919193	10	17	1341	156
313935	4919684	7	0	1716	13
314243	4919058	5	28	1566	36
314871	4919923	7	33	1569	61
314921	4920416	11	0	1704	21
314362	4919969	7	0	1673	34
315019	4919111	7	0	1341	69
314513	4920658	6	28	1805	40
314759	4921082	7	27	1973	58
314437	4919675	8	13	1590	67
314923	4920124	6	19	1659	3
314513	4919658	8	20	1566	47
313444	4921603	6	0	2121	51
313924	4921165	9	28	1963	92
314239	4921014	9	19	1901	43
314631	4921063	9	0	1927	125
313827	4921111	9	17	1910	113
313432	4921124	7	0	2054	31
313470	4920873	10	0	1989	12
313184	4921343	7	13	2186	21
313930	4919788	8	0	1725	26
313718	4920726	9	0	1904	36

UTM X (m)	UTM Y (m)	Wetness index	Overland flow distance to channel network (m)	Elevation(m)	LS
314704	4919439	6	14	1476	20
313710	4919802	7	0	1749	29
314088	4919450	8	0	1653	65
315471	4919987	7	0	1593	80
314784	4920576	9	12	1757	82
314862	4920342	7	0	1686	13
313483	4921663	7	46	2113	83
313388	4921520	7	16	2120	58
313367	4920870	8	0	2013	40
313801	4920757	9	0	1890	34
315438	4919489	7	16	1454	53
315241	4919008	8	15	1282	12
314389	4918959	6	63	1525	29
314800	4919545	12	15	1443	251
313310	4921620	7	34	2173	64
315609	4919430	9	0	1342	190
314813	4919109	6	26	1443	62
314085	4921495	8	13	2201	137
313442	4921929	5	27	2236	38
313833	4922559	5	25	2539	39
313472	4922676	9	23	2611	85
313666	4922920	7	11	2736	134

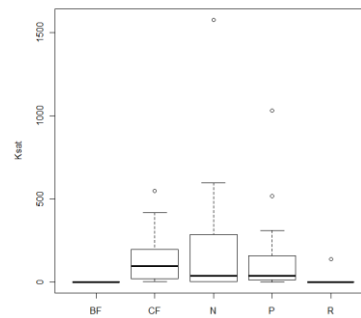
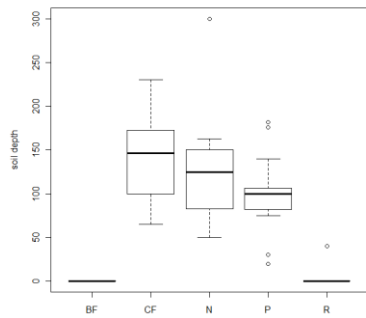
APPENDIX II: SCATTER PLOTS

The box plots and scatter plots of the soil depth (left) and K_s (right) against the environmental variables

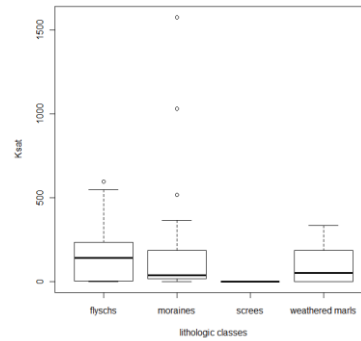
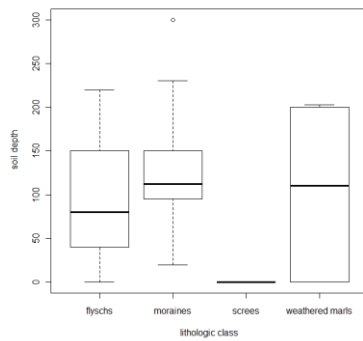
Note: the K_s is in (mm.hr⁻¹) and soil depth in (mm).

BF = broad-leaved forest; CF = Coniferous forest; N = Natural grassland; P = pastures; R = bare rock

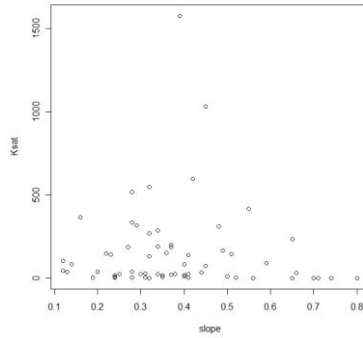
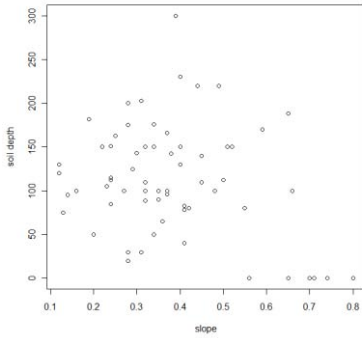
1. Land cover variable



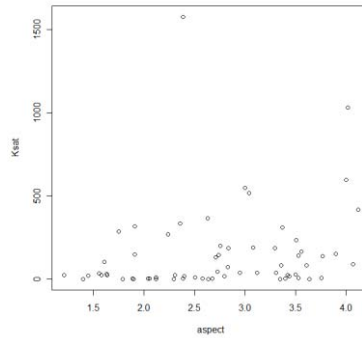
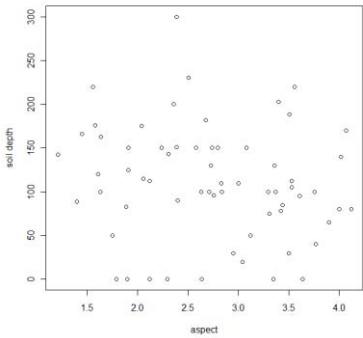
2. Lithologic variable



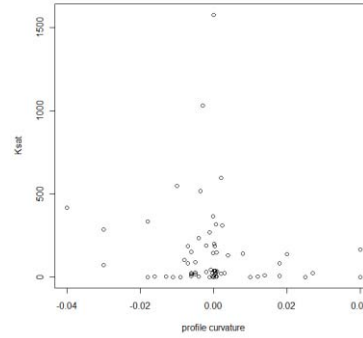
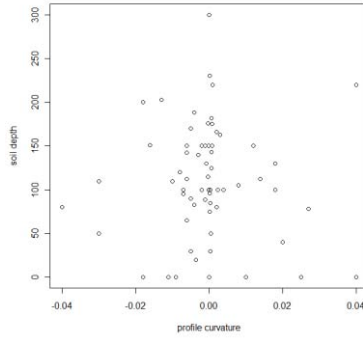
3. Slope variable



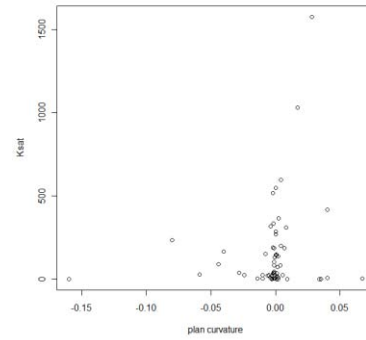
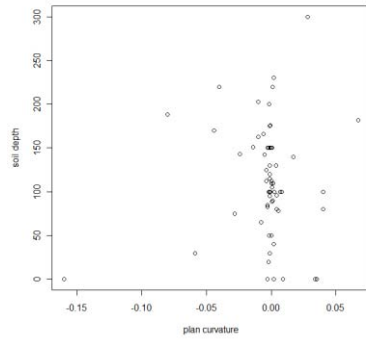
4. Aspect variable



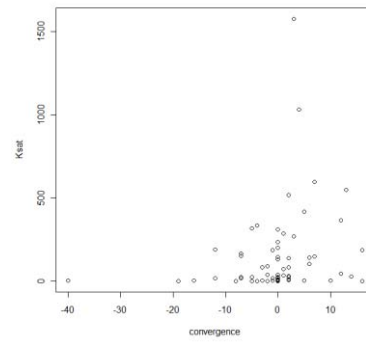
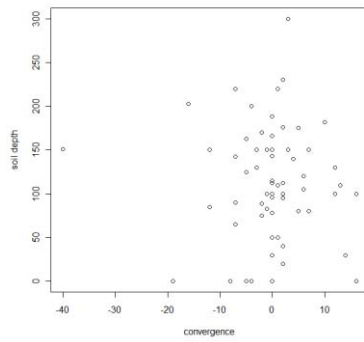
5. Profile curvature variable



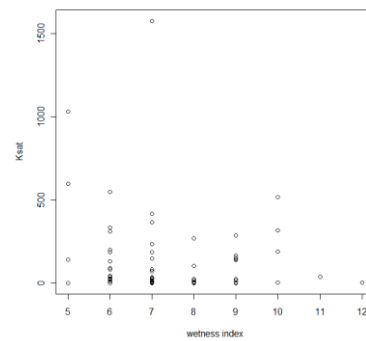
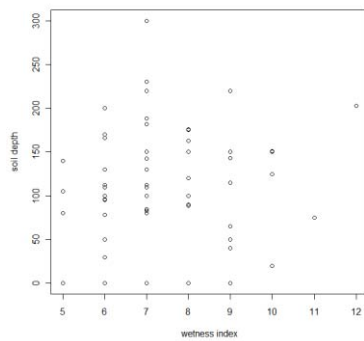
6. Plan curvature variable



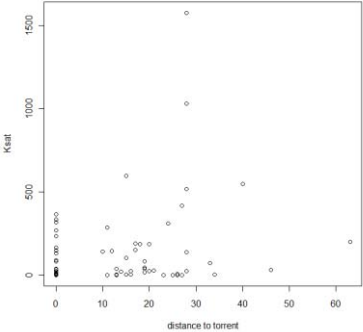
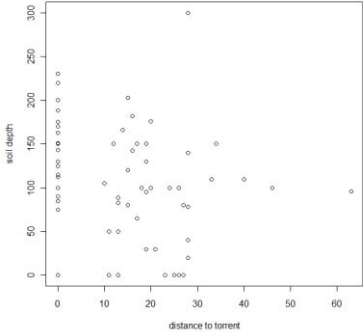
7. Convergence variable



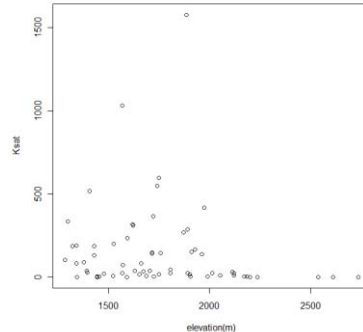
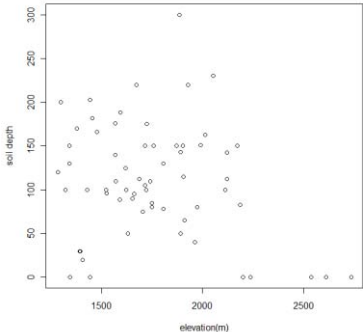
8. Wetness index variable



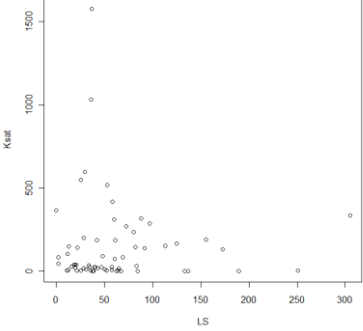
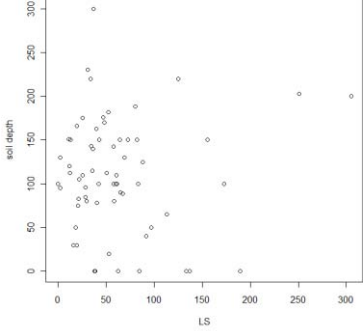
9. Variable of Overland flow distance to channel network



10. Elevation variable



11. LS factor variable



APPENDIX III : THE R SCRIPT

```
##### The R Script used for the thesis, University of Twente,
Enschede, The Netherlands #####
#####By: Pooyan Rahimy, Feb. 2011 #####
#####

K=Ks (mm/hr)
depth =soil thickness (mm)
landusel=land cover classes
lithologyl=lithologic classes
flowdistance = variable of overland flow distance to channel network

#####the Ks normal distribution scrutiny#####
require(foreign)
require(sp)
require(maptools)
require(Hmisc)
require(gstat)
require(rgdal)
require(lattice)
sol<-read.csv("fieldresults.csv")
str(sol)
coordinates(sol)=~X+Y
proj4string(sol)=CRS("+init=epsg:32632")
bbox(sol)
plot(coordinates(sol), asp = 1, pch = 20, col = "blue", main = "sampling
points distribution")
grid()
summary(sol$K)
hist(sol$K,xlab="Ksat (mm/hr)",ylab="frequency")
sk<-sol$K
s<-sol$depth
shapiro.test(sol$K)
summary(sk)
shapiro.test(sol$depth)
summary(sol$depth)
hist(sol$depth, xlab="soil depth",ylab="frequency")

##### Linear model by the predictors for Ks#####
Sol$landuse=as.factor(sol$landuse) ### defines the land cover classes as
factor class ###

klanduse<-lm(sk~sol$landuse)
summary(klanduse)
anova(klanduse)
plot(sk~sol$landuse, xlab="landuse classes",ylab="Ksat")
par(mfrow=c(2,2))
plot.lm(klanduse)
sol$lithology=as.factor(sol$lithology) ### defines the lithology as
factor class###

klithology<-lm(sk~sol$lithology)
summary(klithology)
plot(sk~sol$lithology,xlab="lithologic classes",ylab="Ksat" )
par(mfrow=c(2,2))
plot.lm(klithology)
kslope<-lm(sk~sol$slope)
summary(kslope)
plot(sk~sol$slope,xlab="slope",ylab="Ksat")
```

```

abline(kslope)
par(mfrow=c(2,2))
plot.lm(kslope)
kmodel<-lm(sk~coordinates(sol))
summary(kmodel)
par(mfrow=c(2,2))
plot.lm(kmodel)
kaspect<-lm(sk~sol$aspect)
summary(kaspect)
plot(sk~sol$aspect, xlab="aspect",ylab="Ksat")
abline(kaspect)
par(mfrow=c(2,2))
plot.lm(kaspect)
kprof<-lm(sk~sol$profile_curvature)
summary(kprof)
plot(sk~sol$profile_curvature, xlab="profile curvature",ylab="Ksat")
abline(kprof)
par(mfrow=c(2,2))
plot.lm(kprof)
kplan<-lm(sk~sol$plan_curvature)
summary(kplan)
plot(sk~sol$plan_curvature,xlab="plan curvature",ylab="Ksat")
abline(kplan)
par(mfrow=c(2,2))
plot.lm(kplan)
convk<-lm(sk~sol$convergence)
summary(convk)
plot(sk~sol$convergence,xlab="convergence",ylab="Ksat")
abline(convk)
par(mfrow=c(2,2))
plot.lm(convk)

kwet<-lm(sk~sol$wetness_index)
summary(kwet)
plot(sk~sol$wetness_index,xlab="wetness index",ylab="Ksat")
abline(kwet)
par(mfrow=c(2,2))
plot.lm(kwet)
kdis<-lm(sk~sol$dist)
summary(kdis)
plot(sk~sol$dist,xlab="distance to torrent",ylab="Ksat")
abline(kdis)
par(mfrow=c(2,2))
plot.lm(kdis)
kdem<-lm(sk~sol$elevation)
summary(kdem)
plot(sk~sol$elevation,xlab="elevation(m)", ylab="Ksat")
abline(kdem)
par(mfrow=c(2,2))
plot.lm(kdem)
kls<-lm(sk~sol$LS)
summary(kls)
plot(sk~sol$LS,xlab="LS",ylab="Ksat")
abline(kls)
par(mfrow=c(2,2))
plot.lm(kls)

#####predictors for Ks#####
y<-lm(sk~sol$landuse+sol$aspect)

```

```

summary(y)...> R2=0.044
par(mfrow=c(2,2))
plot.lm(y)
plot(sk~sol$landuse+sol$aspect)
abline(y)
y1<-lm(sk~sol$landuse+sol$aspect+sol$profile_curvature)
summary(y1)...>R2=0.042
par(mfrow=c(2,2))
plot.lm(y1)
plot(sk~sol$landuse+sol$aspect+sol$profile_curvature)
abline(y1)
y2<-lm(sk~sol$landuse+sol$aspect+sol$profile_curvature+sol$plan_curvature)
summary(y2)...>R2=0.057
par(mfrow=c(2,2))
plot.lm(y2)
plot(sk~sol$landuse+sol$aspect+sol$profile_curvature+sol$plan_curvature)
abline(y2)
y3 <-
lm(sk~sol$landuse+sol$aspect+sol$profile_curvature+sol$plan_curvature+sol$d
ist)
summary(y3)..>R2=0.09
par(mfrow=c(2,2))
plot.lm(y3)
plot(sk~sol$landuse+sol$aspect+sol$profile_curvature+sol$plan_curvature+sol
$dist)
abline(y3)
y4<-
lm(sk~sol$landuse+sol$aspect+sol$profile_curvature+sol$plan_curvature+sol$d
ist)
summary(y4)..>R2=0.09
yg<-
lm(sk~sol$landuse*sol$aspect*sol$profile_curvature*sol$plan_curvature*sol$d
ist)
summary(yg)
anova(yg)
par(mfrow=c(2,2))
plot.lm(yg)
#####soil physical characteristics predictors of ks
predictor<-read.csv("poro-k.csv")
pork=lm(predictor$K~predictor$porosity)
summary(pork)
par(mfrow=c(2,2))
plot.lm(pork)

#####
#
#####linear model by predictors for soil depth#####

dlanduse<-lm(s~sol$landuse)
summary(dlanduse)
plot(sk~sol$landuse, xlab="land use classes",ylab=" soil depth")
par(mfrow=c(2,2))
plot.lm(dlanduse)
dlithology<-lm(s~sol$lithology)
summary(dlithology)
plot(s~sol$lithology, xlab="lithologic class",ylab=" soil depth")
par(mfrow=c(2,2))
plot.lm(dlithology)
dslope<-lm(s~sol$slope)
summary(dslope)
plot(s~sol$slope,xlab="slope",ylab="soil depth")

```

```

abline(dslope)
par(mfrow=c(2,2))
plot.lm(dslope)
dmodel<-lm(s~coordinates(sol))
summary(dmodel)
par(mfrow=c(2,2))
plot.lm(dmodel)
daspect<-lm(s~sol$aspect)
summary(daspect)
plot(s~sol$aspect, xlab="aspect",ylab="soil depth")
abline(daspect)
par(mfrow=c(2,2))
plot.lm(daspect)
dprof<-lm(s~sol$profile_curvature)
summary(dprof)
plot(s~sol$profile_curvature,xlab="profile curvature",ylab="soil depth")
abline(dprof)
par(mfrow=c(2,2))
plot.lm(dprof)
dplan<-lm(s~sol$plan_curvature)
summary(dplan)
plot(s~sol$plan_curvature,xlab="plan curvature",ylab="soil depth")
abline(dplan)
par(mfrow=c(2,2))
plot.lm(dplan)
convd<-lm(s~sol$convergence)
summary(convd)
plot(s~sol$convergence,xlab="convergence",ylab="soil depth")
abline(convd)
par(mfrow=c(2,2))
plot.lm(convd)
dwet<-lm(s~sol$wetness_index)
summary(dwet)
plot(s~sol$wetness_index,xlab="wetness index",ylab="soil depth")
abline(dwet)
par(mfrow=c(2,2))
plot.lm(dwet)
ddis<-lm(s~sol$dist)
summary(ddis)
plot(s~sol$dist, xlab="distance to torrent", ylab="soil depth")
abline(ddis)
par(mfrow=c(2,2))
plot.lm(ddis)
ddem<-lm(s~sol$elevation)
summary(ddem)
plot(s~sol$elevation,xlab="elevation (m)",ylab="soil depth")
abline(ddem)
par(mfrow=c(2,2))
plot.lm(ddem)
dls<-lm(s~sol$LS)
summary(dls)
plot(s~sol$LS,xlab="LS",ylab="soil depth")
abline(dls)
par(mfrow=c(2,2))
plot.lm(ddem)
s
~sol$landuse+sol$lithology+sol$aspect+sol$profile_curvature+sol$plan_curvat
ure+sol$convergence+sol$valley_depth+sol$wetness_index
dmodell <- lm(s
~sol$landuse+sol$lithology+sol$slope+sol$aspect+sol$profile_curvature+sol$

```

```

lan_curvature+sol$convergence+sol$valley_depth+sol$wetness_index+sol$dist+s
ol$elevation+sol$LS)
summary(dmodel1)
plot(s
~sol$landuse+sol$lithology+sol$slope+sol$aspect+sol$profile_curvature+sol$p
lan_curvature+sol$convergence+sol$valley_depth+sol$wetness_index+sol$dist+s
ol$elevation+sol$LS)

par(mfrow=c(2,2))
plot.lm(dmodel1)
dmodel2 <- lm(s
~sol$landuse+sol$lithology+sol$slope+sol$aspect+sol$profile_curvature+sol$p
lan_curvature+sol$convergence+sol$valley_depth+sol$wetness_index+sol$dist+s
ol$elevation)
summary(dmodel2)
par(mfrow=c(2,2))
plot.lm(dmodel2)
dmodel3 <- lm(s
~sol$landuse+sol$lithology+sol$slope+sol$aspect+sol$profile_curvature+sol$p
lan_curvature+sol$convergence+sol$valley_depth+sol$wetness_index+sol$dist)
summary(dmodel3)
par(mfrow=c(2,2))
plot.lm(dmodel3)
hist(dmodel3$resid)

dmodel4 <- lm(s
~sol$landuse+sol$lithology+sol$aspect+sol$profile_curvature+sol$plan_curvat
ure+sol$convergence+sol$valley_depth+sol$wetness_index)
summary(dmodel4)
par(mfrow=c(2,2))
plot.lm(dmodel4)
dmodel5 <- lm(s
~sol$landuse+sol$lithology+sol$aspect+sol$profile_curvature+sol$convergence
+sol$valley_depth)
summary(dmodel5)
par(mfrow=c(2,2))
plot.lm(dmodel5)
dmodel6 <- lm(s
~sol$landuse+sol$lithology+sol$aspect+sol$profile_curvature)
summary(dmodel6)
par(mfrow=c(2,2))
plot.lm(dmodel6)
dmodel7 <- lm(s ~sol$landuse+sol$lithology+sol$aspect)
summary(dmodel7)
dmodel8 <- lm(s ~sol$landuse+sol$lithology)
summary(dmodel8)

l<-lm(s~sol$landuse+sol$dist)
summary(l)
anova(l)
hist(l$residuals)
par(mfrow=c(2,2))
plot.lm(l)
plot(s~sol$landuse+sol$dist)
abline(l)
f<-lm(s~sol$landuse*sol$dist)
summary(f)
anova(f)
hist(f$residuals)
par(mfrow=c(2,2))

```

```

plot.lm(f)
plot(s~sol$landuse*sol$dist)
abline(f)
anova(f)
w<-lm(s~(sol$landuse+sol$dist)+(sol$landuse*sol$dist))
summary(w)
par(mfrow=c(2,2))
plot.lm(w)
anova(w)
l2<-lm(s~sol$landuse+I(sol$dist^2)+sol$dist)
summary(l2)
#####
#####
####empirical variogram
#Emperical Variogram fitting for  ksat#####
str(sol)

vktest2<-variogram(sk~1,loc=sol,cutoff=1500,width=150) ### variogram of
ksat
print(plot(vktest2, pl = T, main = "Ksat empirical variogram"))

vkmodel2<-vgm(99000,"Exp",500,0) ##### defining the variogram model
parameters
vkmodel2
vktest2.f <- fit.variogram(vktest2, vkmodel2)
plot(vktest2, pl=T, model=vkmodel2, main="Ksat variogram")

#####
###
#####
###
##### empirical variogram for soil depth
vdtest <- variogram(sol$depth ~ 1, loc = sol,cutoff=1000,width=85)
print(plot(vdtest, main = "soil depth empirical variogram"))
vdmodel<-vgm(2000,"Cir",410,2000)
vdmodel
vdtest.f <- fit.variogram(vdtest, vdmodel)
plot(vdtest, pl=T, model=vdmodel, main=" soil depth variogram")

#####defining new grid for the Kriging#####

landcover <- read.asciigrid("landcover3.asc")#### reads the land cover as
the grid for kriging
gr2 <- as(landcover, "SpatialPointsDataFrame") #### makes land cover the
grid
str(gr2)
proj4string(gr2)=CRS("+init=epsg:32632")
gridded(gr2)<-TRUE
class(gr2)

#####
#####
#####
#####Ordinary Kriging for soil depth

okd<-krige(depth~1, loc=sol,newdata=gr2, model=vdmodel)
plotokd <- spplot(okd, zcol = "var1.pred",col.regions = terrain.colors(64),
main = "soil depth (mm)",scales = list(draw = T), xlab = "E", ylab = "N")

```

```

print(plotokd, more= T)
hist(okd$var1.pred, xlab="", ylab="", main="")
#####export the kriged map to ascii
write.asciigrid(okd[1], "soildepth_ok.asc")
#### ordinary kriging corss-validation

okd.cv<-krige.cv(depth~1,sol,model=vdmmodel)
# OK residuals histogram
hist(okd.cv$residual, xlab="soil depth")
# Mean Error (ME)
sum(okd.cv$residual) / length(okd.cv$residual)
# Root Mean Square Error (RMSE)
sqrt(sum(okd.cv$residual)^2) / 64)
#### Ok variance for soil depth
okdv <- spplot(okd, zcol = "var1.var", col.regions = terrain.colors(64),
main = " soil depth OK variance ", scales = list(draw = T))
plot(okdv, more=T)
#####
#####

#####soil depth RK#####

flowdistance<-read.asciigrid("flowdistance.asc")
proj4string(flowdistance)=CRS("+init=epsg:32632")
SpatialPoints(flowdistance)
str(flowdistance)

landcover.ov = overlay(landcover, sol) # create grid-points overlay
sol$landcover3.asc =landcover.ov$landcover3.asc # copy the landcover
values
distance.ov = overlay(flowdistance, sol) # create grid-points overlay
sol$flowdistance.asc =distance.ov$flowdistance.asc # copy the distance
values
str(sol)
## add distance to river to prediction grid
gr2$flowdistance.asc <- overlay(flowdistance, gr2)$flowdistance.asc
str(gr2)

#####Estimate the residuals and their
autocorrelation structure (variogram) for the soil depth:

vrkd <- variogram(depth~landcover3.asc+flowdistance.asc, loc=sol)

print(plot(vrkd, pl = T))

# recompute vgm with wider bins
vrkd <- variogram(depth~landcover3.asc+flowdistance.asc, loc=sol,
cutoff=1000, width=200)
plot(vrkd, pl=T)
vrkdmodel<-vgm(2000,"Cir",360,0)
vrkdmodel
vrkd.f <- fit.variogram(vrkd, vrkdmodel)
plot(vrkd, pl=T, model=vrkd.f)
vrkd.f
#####Run UK

sdepth_uk1 <- krige(depth~landcover3.asc+flowdistance.asc, locations=sol,
newdata=gr2, model=vrkdmodel)

```

```

spplot(as(sdepth_uk1,"SpatialPixelsDataFrame"), zcol="var1.pred",
col.regions=bpy.colors(64),scales = list(draw = T),xlab="UTM
X(m)",ylab="UTM Y(m)",main=" soil depth (mm) ")
print(spplot(sdepth_uk1, "var1.var", main="soil depth regression kriging
variance"), more=F)
hist(sdepth_uk1$var1.pred,xlab="",ylab="",main="")

#####export the kriged map to ascii
write.asciigrid(sdepth_uk1[1], "soildepth_rk.asc")

##### soil depth kriging cross validation
sdepth_uk_cv <- krige.cv(depth~landcover3.asc+flowdistance.asc,
locations=sol, model=vrkmodel)
# Mean Error (ME)
sum(sdepth_uk_cv$residual) / length(sdepth_uk_cv$residual)
# Root Mean Square Error (RMSE)
sqrt(sum((sdepth_uk_cv$residual)^2) / 64)
### Histogram of the kriging residuals
hist(sdepth_uk_cv$residual, xlab=" residuals", main=" the RK residuals")
summary(sdepth_uk_cv$residual)
##### export the kriged map to ascii
write.asciigrid(sdepth_uk1[1], "depth_uk.asc")

#####conditional simulation for soil depth (OK)###

osd<-krige(depth~1, loc=sol,newdata=gr2, model=vdmodel, nsim=30,nmax=64)
hist(osd$sim1,xlab="",ylab="",main="")
### showing the 4th simulated field
spplot(osd,zcol="sim4",col.regions=bpy.colors(64),main="4th realization of
soil depth(mm)")
##### export the simulated fields for soil depth
write.asciigrid(osd[1], "depth_ok1.asc")

##### conditional simulation for the soil depth resulted from the
RK###
srd <- krige(depth~landcover3.asc+flowdistance.asc, locations=sol,
newdata=gr2, model=vrkmodel,nsim=30,nmax=64)
hist(srd$sim1,xlab="",ylab="",main="")
###showing the 4th simulated field of the soil depth produced by the
Regression Kriging
spplot(srd,zcol="sim4",col.regions=bpy.colors(64),main="4th realization of
soil depth(mm)")
##### export the 4th simulated fields of soil depth
write.asciigrid(srd[4], "depth_rk4.asc")

##### mapping other soil properties #####

por<-read.csv("porosity2.csv")
str(por)
coordinates(por)=~x+y
proj4string(por)=CRS("+init=epsg:32632")
### porosity
hist(por$porosity, xlab="porosity", main="")
###empirical variogram
vpor<-variogram(porosity~1,loc=por,cutoff=10000,width=400)
print(plot(vpor, pl = T, main = "soil porosity empirical variogram"))

```

```

vporm<-vgm(0.015,"Exp",2500,0.08) ##### defining the variogram model
parameters
vporm
vpor.f <- fit.variogram(vpor, vporm)
plot(vpor, pl=T, model=vpor.f)
### defining the grid
landcover <- read.asciigrid("landcover3.asc")#### reads the land cover as
the grid for kriging
gr2 <- as(landcover, "SpatialPointsDataFrame") #### makes land cover the
grid
proj4string(gr2)=CRS("+init=epsg:32632")
gridded(gr2)<-TRUE
class(gr2)
##### ordinary kriging of soil porosity
okp<-krige(porosity~1, loc=por,newdata=gr2, model=vporm)
plotokp <- spplot(okp, zcol = "var1.pred",col.regions =
terrain.colors(64),scales = list(draw = T), xlab = "E", ylab = "N")
print(plotokp, more = T)
##### export the kriged map as asci
write.asciigrid(okp[1], "porosity.asc")
#####stoniness map
summary(por$stoniness)
hist(por$stoniness)
vston<-variogram(stoniness~1,loc=por, cutoff=10000,width=400)
print(plot(vston, pl = T, main = "stoniness emrpical variogram"))
vstonm<-vgm(0.1,"Sph",400,0)
vston.f <- fit.variogram(vston, vstonm)
plot(vston, pl=T, model=vstonm, main="Ssurface stoniness variogram")

##### stoniness mapping
oks<-krige(stoniness~1, loc=por,newdata=gr2, model=vstonm)
plotoks <- spplot(oks, zcol = "var1.pred",col.regions = terrain.colors(64),
main = " surface stoniness map ",scales = list(draw = T), xlab = "E", ylab
= "N")
print(plotoks, more = T)
##### export the kriged map as asci
write.asciigrid(oks[1], "stoniness.asc")

#####
#####
initial moisture mapping # Note: the Field Capacity (FC) was used instead
fc<-read.csv("fc.csv")
str(fc)
coordinates(fc)=~x+y
proj4string(fc)=CRS("+init=epsg:32632")
moisture<-fc$F.C.
hist(moisture)
#####variogram of FC
vfc<-variogram(moisture~1,loc=fc, cutoff=5000,width=400)
print(plot(vfc, pl = T, main = "Field capacity emrpical variogram"))
vfcm<-vgm(0.015,"Cir",1500,0.08)
vfcm
vfcm.f <- fit.variogram(vfc, vfcm)
plot(vfc, pl=T, model=vfcm.f, main="")
#####kriging for FC mapping
okfc<-krige(moisture~1, loc=fc,newdata=gr2, model=vfcm)
plotokfc <- spplot(okfc, zcol = "var1.pred",col.regions =
terrain.colors(64),scales = list(draw = T), xlab = "E", ylab = "N")
print(plotokfc, more = T)
##### export the kriged map as asci
write.asciigrid(okfc[1], "fc.asc")

```

```

#####
Bulk density mapping
#####
bd<- por$BD
hist(bd)
####variogram of Bukl density
vbd<-variogram(bd~1,loc=por, cutoff=5000,width=400)
print(plot(vbd, pl = T, main = "Bulk Density emrpical variogram"))
vbdm<-vgm(0.15,"Cir",2500,0.06)
vbdm
vbdm.f <- fit.variogram(vbd, vbdm)
plot(vbd, pl=T, model=vbdm)
##### bulk density mapping
okb<-krige(bd~1, loc=por,newdata=gr2, model=vbdm)
plotokb <- spplot(okb, zcol = "var1.pred",col.regions = terrain.colors(64),
main = " Soil Bulk density (g/cm3) ",scales = list(draw = T), xlab = "E",
ylab = "N")
print(plotokb, more = T)
##### export the kriged map as asci
write.asciigrd(okb[1], "bd.asc")
#####

##### matric potential map
psi<-read.csv("psi.csv")
coordinates(psi)~x+y
proj4string(psi)=CRS("+init=epsg:32632")
vpsi<-variogram(c~1,loc=psi, cutoff=3000)
print(plot(vpsi, pl = T))
vpsim<-vgm(150000,"Nug",0,0) ##### defining the variogram model parameters
vpsim
vpsi.f <- fit.variogram(vpsi, vpsim)
plot(vpsi, pl=T, model=vpsi.f)
okpsi<-krige(c~1, loc=psi,newdata=gr2, model=vpsim)
plotokpsi <- spplot(okpsi, zcol = "var1.pred",col.regions =
terrain.colors(64),scales = list(draw = T), xlab = "E", ylab = "N",
main="soil matric potential (cm)")
print(plotokpsi, more = T)
#####export to asci
write.asciigrd(okpsi[1], "psi.asc")

```

APPENDIX IV: THE PCRASTER SCRIPT

Script used for PCRaster maps:

LDD map:

```
Pcr calc ldd.map=lddcreate (dem.map,1e9,1e9,1e9,1e9)
Pcr calc -- lddin ldd.map=lddcreate(dem.map,1e9,1e9,1e9,1e9)
```

AREA map:

```
Pcr calc area.map=catchment(ldd.map,pit(ldd.map))
```

Generation of contributing cells draining towards a given point:

```
Pcr calc ups.map=accuflux(ldd.map,1)
```

GRAD map:

```
Pcr calc grad.map=slope(dem.map)
Pcr calc grad.map=sin(atan(max(0.001,grad.map)))
```

ID map:

```
Pcr calc id.map=nominal(spreadzone(gauge.map,0,1))
```

OUTLET map:

```
Pcr calc pit.map=pit(ldd.map)
Pcr calc outlet.map=pit(ldd.map)
```

Sub-basins map:

```
Pcr calc ws.map=catchment(ldd.map,outlet.map)
```

MASK map:

```
Pcr calc mask.map=scalar(if(ws.map eq 34,1)) ##### 34 refers to the number of the produced sub basin#####
```

NOMINAL MASK map:

```
pcr calc masknom.map=nominal(mask.map)
```

ROADWIDTH map:

```
pcr calc roadwidt.map=scalar(if(roads.map eq 1,2,0)) ### 2 refers to the width of the roads which is 2 meters####
```

all other scalar maps were multiplied by the scalar mask map and the nominal maps by the nominal mask, using scripts like the following:

```
pcr calc per2.map=mask.map * per.map ##### in which per.map is the ground cover map#####
```

CHANNEL MASK map:

```
Pcr calc chanmask.map=if(accuflux(ldd.map,1) gt 1000,1)
```

CHANNEL LDD map:

```
Pcr calc -- lddin lddchan.map=lddcreate(dem.map*chanmask.map,1e9,1e9,1e9,1e9)
```

CHANNEL SIDE map:

```
Pcr calc chanside.map=0*chanmask.map ### the channel was assumed rectangular###
```

CHANNEL WIDTH map:

```
Pcr calc channelwidt.map=if(ups.map gt 1000,ups.map/2040)
```

the denominator 2040 was to adjust the width of the channel##

For other soil and channel parameters that no data were available, a mask with 0 value was made#

APPENDIX V: THE LISEM PART

A. The run file used for the LISEM (one of the scenarios)

[LISEM for WINDOWS run file v3]

[LISEM main type]

LISEM Type=0

[Work Directory]

WorkDir=G:\litem\data-ilwis\run

[Input]

Map Directory=G:\litem\data-ilwis\

Table Directory=G:\litem\data-ilwis\

Rainfall Directory=G:\litem\data-ilwis\

Rainfall file=rain-calib.txt

Incude Snowmelt=0

Snowmelt Directory=0

Snowmelt file=0

[Output]

Result Directory=G:\litem\data-ilwis\results

Main results file=res.csv

Filename point output=pointoutput.txt

Report point output separate=0

Report point output for SOBEK=0

SOBEK date string= / /

Erosion map=0

Deposition map=0

Soilloss map=0

[Simulation times]

Begin time=0

End time=550

Timestep=10

[General options]

No Erosion simulation=1

Include main channels=0

Include channel infil=0

Include channel baseflow=0

All water and sediment to outlet=0

Include snowmelt=0

No erosion at outlet=0

Alternative flow detachment=0

Simple depression storage=0

Hard Surfaces=0

[Interception]

Use canopy storage map=0

Canopy storage equation=1

Stemflow fraction=0.054

[Conservation]
Include grass strips=0
Grassstrip Mannings n=0.3
Include buffers=0
Sediment bulk density=1800
Include Sediment traps=0

[Calibration]
Ksat calibration=1
N calibration=1
Channel Ksat calibration=1
Channel N calibration=1
Splash Delivery Ratio=0.1

[Gully options]
Fcrit relation=0
Threshold gradient=
QW relation=0
QW param A=
QW param B=
Gully infiltration=0
Use initial gully dimensions=0

[Infiltration]
Infil Method=3
Include wheeltracks=0
Include crusts=0
Impermeable sublayer=0
Subsoil drainage=0
SWATRE internal minimum timestep=0
Matric head files=0
Geometric mean Ksat=0

[Output maps]
Runoff maps in l/s/m=1
Timeseries as PCRaster=1
Timeplot as PCRaster=1
Regular runoff output=1
Erosion map units (0/1/2)=2
Output interval=0
User defined output=1
Output times=
CheckOutputMaps=1,0,1,0,0,0,0,0,0,0,0
CheckOutputMapsNUT=0,0,0,0,0,0,0,0,0,0,0,0,0,0,0,0
CheckOutputMapsMC=0,0,0,0,0,0,0
CheckOutputMapsGUL=0,0,0,0,0

[Texture classes]
ClassMu=2,16,32,53,75,105

[map names]

[OutputBASIC]
OUTRUNOFF=G:\lisem\data-ilwis\results\ro
OUTCONC=G:\lisem\data-ilwis\results\conc
OUTWH=G:\lisem\data-ilwis\results\wh

OUTRWH=G:\litem\data-ilwis\results\whc
OUTTC=G:\litem\data-ilwis\results\tc
OUTEROS=G:\litem\data-ilwis\results\det
OUTDEPO=G:\litem\data-ilwis\results\depo
OUTVELO=G:\litem\data-ilwis\results\velo
OUTINF=G:\litem\data-ilwis\results\inf
OUTSS=G:\litem\data-ilwis\results\sstor
OUTCHVOL=G:\litem\data-ilwis\results\chanvol

[OutputMC]

OUTMU0=G:\litem\data-ilwis\results\smu0
OUTMU1=G:\litem\data-ilwis\results\smu1
OUTMU2=G:\litem\data-ilwis\results\smu2
OUTMU3=G:\litem\data-ilwis\results\smu3
OUTMU4=G:\litem\data-ilwis\results\smu4
OUTMU5=G:\litem\data-ilwis\results\smu5
OUTD50SUSP=G:\litem\data-ilwis\results\D50s

[OutputNut]

OUTPSOLUT=G:\litem\data-ilwis\results\NPsol
OUTPSUS=G:\litem\data-ilwis\results\NPsus
OUTPINF=G:\litem\data-ilwis\results\NPinf
OUTNH4SOLUT=G:\litem\data-ilwis\results\NNH4sol
OUTNH4SUS=G:\litem\data-ilwis\results\NNH4sus
OUTNH4INF=G:\litem\data-ilwis\results\NNH4inf
OUTNO3SOLUT=G:\litem\data-ilwis\results\NNO3sol
OUTNO3SUS=G:\litem\data-ilwis\results\NNO3sus
OUTNO3INF=G:\litem\data-ilwis\results\NNO3inf

[OutputNutErosDep]

OUTPDEP=G:\litem\data-ilwis\results\NPdep.map
OUTNH4DEP=G:\litem\data-ilwis\results\NNH4dep.map
OUTNO3DEP=G:\litem\data-ilwis\results\NNO3dep.map
OUTPDET=G:\litem\data-ilwis\results\NPdet.map
OUTNH4DET=G:\litem\data-ilwis\results\NNH4det.map
OUTNO3DET=G:\litem\data-ilwis\results\NNO3det.map

[OutputGul]

OUTGULD=G:\litem\data-ilwis\results\guld
OUTGULW=G:\litem\data-ilwis\results\gulw
OUTGULA=G:\litem\data-ilwis\results\gula
OUTGULF=G:\litem\data-ilwis\results\gulf
OUTGULDEM=G:\litem\data-ilwis\results\guldem

[Catchment]

grad=G:\litem\data-ilwis\grad.map
ldd=G:\litem\data-ilwis\ldd.map
outlet=G:\litem\data-ilwis\outlet.map
ID=G:\litem\data-ilwis\id.map
outpoint=G:\litem\data-ilwis\out1.map

[Landuse]

cover=G:\litem\data-ilwis\per.map
lai=G:\litem\data-ilwis\lai.map
ch=G:\litem\data-ilwis\ch.map
smax=G:\litem\data-ilwis\hardsurf.map
road=G:\litem\data-ilwis\roadwidt.map

grasswidth=G:\litem\data-ilwis\hardsurf.map

[Buffers]

bufferID=G:\litem\data-ilwis\hardsurf.map

bufferVolume=G:\litem\data-ilwis\hardsurf.map

[Snowmelt]

SnowID=G:\litem\data-ilwis\hardsurf.map

[Erosion]

coh=G:\litem\data-ilwis\hardsurf.map

cohadd=G:\litem\data-ilwis\hardsurf.map

aggrstab=G:\litem\data-ilwis\hardsurf.map

d50=G:\litem\data-ilwis\hardsurf.map

[Surface]

rr=G:\litem\data-ilwis\rr.map

manning=G:\litem\data-ilwis\manning.map

crustfrc=G:\litem\data-ilwis\crust.map

compfrc=G:\litem\data-ilwis\compac.map

stonefrc=G:\litem\data-ilwis\stoniness.map

hardsurf=G:\litem\data-ilwis\hardsurf.map

[InfilHoltan]

A=G:\litem\data-ilwis\A

FP=G:\litem\data-ilwis\FP

P=G:\litem\data-ilwis\P

[InfilExtra]

ksatcrst=G:\litem\data-ilwis\hardsurf.map

ksatcomp=G:\litem\data-ilwis\hardsurf.map

ksatgras=G:\litem\data-ilwis\hardsurf.map

[InfilGA2]

ksat2=G:\litem\data-ilwis\k_ok.map

psi2=G:\litem\data-ilwis\psi.map

thetas2=G:\litem\data-ilwis\porosity.map

thetai2=G:\litem\data-ilwis\fieldcapacity.map

soildep2=G:\litem\data-ilwis\soildepth-ok.map

[InfilGA1]

ksat1=G:\litem\data-ilwis\k_ok.map

psi1=G:\litem\data-ilwis\psi.map

thetas1=G:\litem\data-ilwis\porosity.map

thetai1=G:\litem\data-ilwis\fieldcapacity.map

soildep1=G:\litem\data-ilwis\soildepth-ok.map

[InfilSmith]

ksat1=G:\litem\data-ilwis\k_ok.map

psi1=G:\litem\data-ilwis\psi.map

thetas1=G:\litem\data-ilwis\porosity.map

thetai1=G:\litem\data-ilwis\fieldcapacity.map

soildep1=G:\litem\data-ilwis\soildepth-ok.map

[InfilMorel]

ksat1=G:\litem\data-ilwis\k_ok.map

psi1=G:\litem\data-ilwis\psi.map

thetas1=G:\litem\data-ilwis\porosity.map
thetai1=G:\litem\data-ilwis\fieldcapacity.map
soildep1=G:\litem\data-ilwis\soildepth-ok.map

[InfilSwatre]

profinp=G:\litem\data-ilwis\hardsurf.map
profmap=G:\litem\data-ilwis\hardsurf.map
profcrst=G:\litem\data-ilwis\hardsurf.map
profwltr=G:\litem\data-ilwis\hardsurf.map
profgras=G:\litem\data-ilwis\hardsurf.map
inithead=G:\litem\data-ilwis\hardsurf.map
headout=G:\litem\data-ilwis\hardsurf.map

[InfilDrainage]

drfactor=G:\litem\data-ilwis\hardsurf.map

[InfilKsat]

ksat1=G:\litem\data-ilwis\k_ok.map

[Channelinfil]

chanksat=G:\litem\data-ilwis\hardsurf.map

[Channels]

liddchan=G:\litem\data-ilwis\liddchan.map
chanwidth=G:\litem\data-ilwis\chanwidt.map
chanside=G:\litem\data-ilwis\chanside.map
changrad=G:\litem\data-ilwis\changrad.map
chanman=G:\litem\data-ilwis\hardsurf.map
chancoh=G:\litem\data-ilwis\hardsurf.map

[ChannelBaseflow]

chanbaseflux=G:\litem\data-ilwis\hardsurf.map
chanincrease=G:\litem\data-ilwis\hardsurf.map
chanvolini=G:\litem\data-ilwis\hardsurf.map

[Macropore]

[Wheeltrack]

liddwheel=G:\litem\data-ilwis\hardsurf.map
wheelnbr=G:\litem\data-ilwis\hardsurf.map
wheelwidth=G:\litem\data-ilwis\hardsurf.map
wheeldepth=G:\litem\data-ilwis\hardsurf.map
wheelgradient=G:\litem\data-ilwis\hardsurf.map
wheelman=G:\litem\data-ilwis\hardsurf.map
wheelcohesion=G:\litem\data-ilwis\hardsurf.map
ksatwt=G:\litem\data-ilwis\hardsurf.map

[Texture]

fractionmu0=G:\litem\data-ilwis\hardsurf.map
fractionmu1=G:\litem\data-ilwis\hardsurf.map
fractionmu2=G:\litem\data-ilwis\hardsurf.map
fractionmu3=G:\litem\data-ilwis\hardsurf.map
fractionmu4=G:\litem\data-ilwis\hardsurf.map
fractionmu5=G:\litem\data-ilwis\hardsurf.map

[NutsP]

pcont=G:\litem\data-ilwis\hardsurf.map

psolute=G:\litem\data-ilwis\hardsurf.map
pefficiency=G:\litem\data-ilwis\hardsurf.map
psorp=G:\litem\data-ilwis\hardsurf.map
pconv=G:\litem\data-ilwis\hardsurf.map

[NutsNO3]

no3cont=G:\litem\data-ilwis\hardsurf.map
no3solute=G:\litem\data-ilwis\hardsurf.map
no3efficiency=G:\litem\data-ilwis\hardsurf.map
no3sorp=G:\litem\data-ilwis\hardsurf.map
no3conv=G:\litem\data-ilwis\hardsurf.map

[NutsNH4]

nh4cont=G:\litem\data-ilwis\hardsurf.map
nh4solute=G:\litem\data-ilwis\hardsurf.map
nh4efficiency=G:\litem\data-ilwis\hardsurf.map
nh4sorp=G:\litem\data-ilwis\hardsurf.map
nh4conv=G:\litem\data-ilwis\hardsurf.map

[NutsBD]

bulk=G:\litem\data-ilwis\hardsurf.map

[Gully]

dem=G:\litem\data-ilwis\hardsurf.map
gullyn=G:\litem\data-ilwis\hardsurf.map
bulkdens1=G:\litem\data-ilwis\bulkdensity.map
gulksat1=G:\litem\data-ilwis\hardsurf.map
gullydep=G:\litem\data-ilwis\hardsurf.map
gullycoh=G:\litem\data-ilwis\hardsurf.map
bulkdens2=G:\litem\data-ilwis\hardsurf.map
gulksat2=G:\litem\data-ilwis\hardsurf.map
nonfcrit=G:\litem\data-ilwis\hardsurf.map

[GullyInit]

gulwinit=G:\litem\data-ilwis\hardsurf.map
guldinit=G:\litem\data-ilwis\hardsurf.map

B. One of the rainfall scenarios in the text file used for the LISEM

Note: the first column denotes cumulative time in minute and the second column denotes the rainfall intensity in (mm/hr)

RUU CSF TIMSERIE INTENSITY NORMAL 1

station_1

000.00	000.00
060.00	030.00
200.00	000.00

C. An example of the LISEM display window after Runoff simulation

